THESIS FOR THE DEGREE OF DOCTOR OF PHILOSOPHY (PHD)

Molecular alterations associated with a BRAF inhibitor and an ER stress inducer

Present and possible future therapies of cutaneous melanoma

by István Szász

Supervisor: Margit Balázs, PhD, DSc

UNIVERSITY OF DEBRECEN

DOCTORAL SCHOOL OF HEALTH SCIENCES

DEBRECEN, 2021

TABLE OF CONTENT

TABLE OF CONTENT

Abbreviations

aCGH: array comparative genomic hybridization

AKT: v-akt murine thymoma viral oncogene

ANGPLT4: angiopoietin like 4

ASR: age-standardized rate

ATF6: activating transcription factor 6

BiP/GRP78/HSPA5: binding-immunoglobulin protein/ glucose- regulated protein 78/ heat shock protein A5

BRAF: v-raf murine sarcoma viral oncogene homolog B1

BRAFi BRAF inhibitor

CCND1: cyclin D1

CDK4: cyclin dependent kinase 4

CDKN2A: cyclin dependent kinase inhibitor 2A

CHOP/DDIT3: DNA damage inducible transcript 3

COT/ MAP3K8: mitogen activated protein kinase kinase kinase 8

DMSO: dimethyl sulfoxide

DRAM1: DNA damage regulated autophagy modulator 1

ECM: extracellular matrix

EGFR: epidermal growth factor receptor

EPHA2: EPH receptor A2

ER: endoplasmic reticulum

ERAD: ER associated degradation

EXT1: exostosin glycosyltransferase 1

FBS: fetal bovine serum

FDR: false discovery rate

FGF2: fibroblast growth factor 2

FISH: fluorescence in situ hybridization

Grb2: growth factor receptor bound protein 2

IGF-1R: insulin-like growth factor 1 receptor

IL-2: interleukin-2

ABBREVIATIONS

IRE1: inositol-requiring enzyme 1

LOXL1: lysyl oxidase like 1

MAPK: mitogen-activated protein kinase

mTOR: mechanistic target of rapamycin

NF1: neurofibromin 1

NGS: next generation sequencing

OPN/SPP1: osteopontin/ secreted phosphoprotein 1

PBS: phosphate-buffered saline

PERK/EIF2AK3: eukaryotic translation initiation factor 2 alpha kinase 3

PI3K: phosphoinositide-3-kinase

PMEL: premelanosome protein

PTBs: phosphotyrosine binding domain- containing proteins

PTEN: phosphatase and tensin homolog

RAF: rapidly accelerated fibrosarcoma

RIN: RNA integrity number

RIPA: radioimmunoprecipitation assay

RTKs: receptor tyrosine kinases

SAMD12: sterile alpha motif domain containing 12

SERPINE1: serpin family E member 1

SH2: src homology 2

SSM: superficial spreading melanoma

TNF: tumor necrosis factor

TZBs: thiazole benzensulfonamides

UPR: unfolded protein response

UVB: ultraviolet-B

VCAM-1: vascular cell adhesion molecule 1

VEGF: vascular endothelial growth factor

WNT5A: wnt family member 5A

WST-1: water soluble tetrazolium (salt)-1

XBP1: x-box binding protein 1

Introduction

Cutaneous malignant melanoma is the most serious type of skin cancer, and represent a high public health problem in different part of the world. Unfortunately the incidence of the disease has increased continuously during the last decades [1]. It accounts for over 132,000 cases each year worldwide. The highest incidence rates were reported from Australia and New Zealand in 2020 (ASR incidence: 26.7-1-32.0). Incidence rates within European countries show relatively high variation, the highest rate have been reported from North and West Europe (ASR incidence: 2.4-1-27.6), while the lowest incidence rates were found in the Mediterranean and Eastern countries (ARS incidence 5.3-10.7) (**Figure 1**).

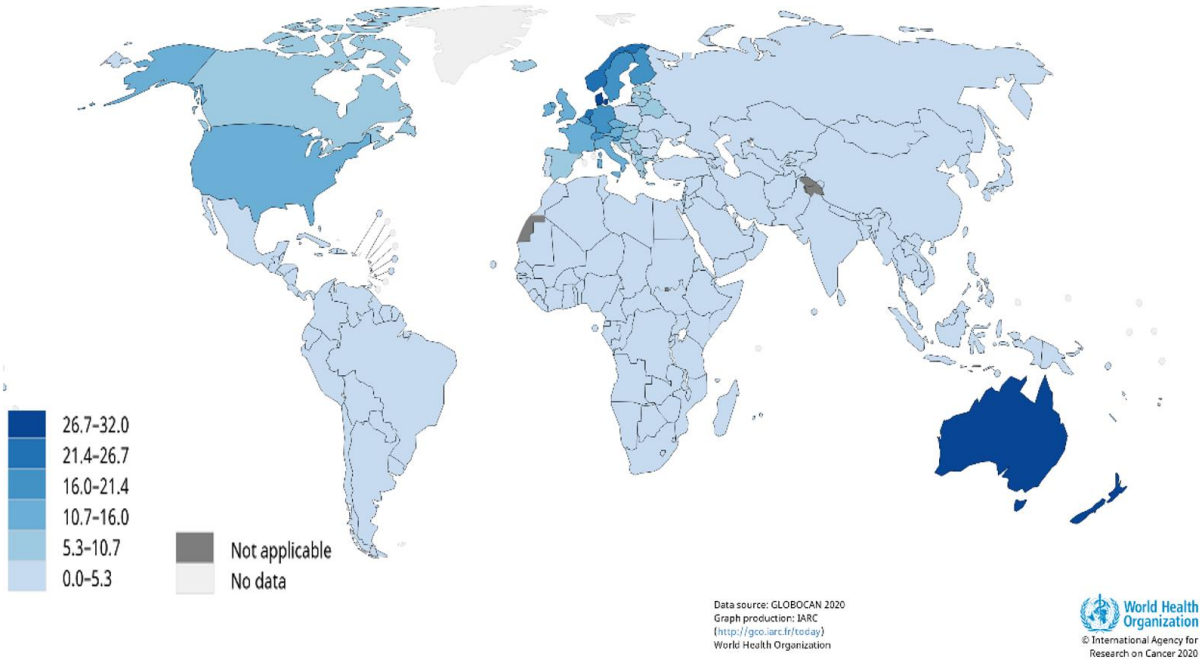

Figure 1. Estimated age-standardized incidence rate of melanoma of the skin (World), both sexes, age 0-74. *Data source: GLOBOCAN 2020; Graph production: IARC 2021.*

Individual risk factors for cutaneous malignant melanoma include: light skin colour, freckles, eye- and hair colour, large number and certain types of moles, family and/or personal history of skin cancer and age [1]. In addition, the relationship between ultraviolet-B (UVB) radiation, as well as sunburns in childhood and melanoma development is well known [2,3]. Although melanoma represents only 5% of cutaneous cancers, it is responsible for almost 75% of all skin cancer deaths [4].

Globally, the estimated age-standardized mortality rates from cutaneous malignant melanoma were the highest in New Zealand (ASR: 3.5) and in Norway (ASR: 2.4) in 2020. In Hungary, the age-standardized mortality rate of cutaneous melanoma was 1.3 (**Figure 2**).

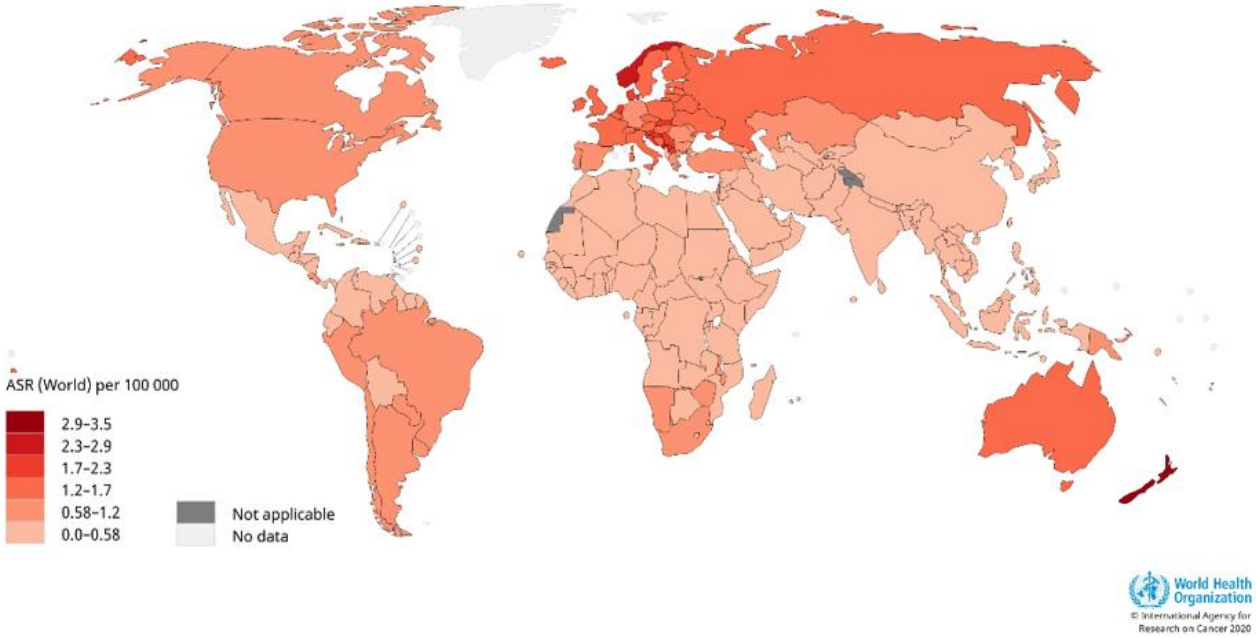

Figure 2. Estimated age-standardized mortality rates (World) in 2020, melanoma of the skin, both sexes, ages 0-74. *Data source: GLOBOCAN 2020; Graph production: IARC 2021.*

Unfortunately, patient survival with melanoma is still very poor, especially for patients with metastatic lesions. Tumour stage significantly determines the overall survival (OS), as the 5-years OS is estimated to be 94-100% for stage I melanoma, while only 9-28% for stage IV tumour.

During the last decade, the treatment possibilities has been highly increased for the disease, but the survival of patients with malignant melanoma is still poor, especially if the patients have advanced or metastatic tumour [5,6]. Activating mutations in the *BRAF* oncogene are the most widespread genetic alterations observed in melanoma, with up to a 45-60 % incidence, the most frequent mutation consist of a single amino acid substitution of valine by glutamic acid at the 600-position ($BRAF^{V600E}$). This hotspot mutation leads to a ~500-fold increase in kinase activity, which constitutively activates the mitogen-activated protein kinase (MAPK) pathway. Currently, targeted inhibition of the mutant $BRAF^{V600E}$ gene is one of the most promising therapeutic approaches for patients with unresectable or metastatic melanoma [7]. Beside

BRAF inhibitors, other successful treatment possibilities include immune check point blockade therapies like anti-PD-1 and anti-CTLA-4 alone or in combination [7-11]. These advances in melanoma treatment have led to an increased median overall survival of patients with metastatic disease from ~ 9 months to over 2 years and, in some cases, have resulted in long-term remission [12].

Even these new therapeutic approaches have significantly improved patient survival, resistance to the BRAF inhibitors and the frequent side-effects of immunotherapies remain unsolved problems. It is urgently needed to discover the molecular background of drug resistance and find new therapeutic targets to improve the success of patient's survival.

The aims of our study were to investigate the growth inhibitory effect of a BRAF inhibitor (PLX4720 a tool compound of vemurafenib) on melanoma cell line pairs (primary tumour and metastasis-derived melanoma cell lines originating from the same patients), develop PLX4720-resistant cell lines and determine what kind of genomic alterations, proteins expression are associated with acquired BRAF inhibitor resistance. In parallel with these experiments we have chosen a recently synthesized and characterized drug, named HA15, which was announced by the authors (Cerezo et al.) as an anti-melanoma drug [13]. The authors described that HA15 induces selective death of all melanoma cells, independently of the cells mutational status, and no resistance are developed against the drug in the applied melanoma cell lines [13]. During our experiments we noticed that HA15 treatment conditions applied by Cerezo et al. was far from the optimal cell culture conditions, therefore we aimed to investigate the effect of HA15 on the viability/proliferation, gene expression on $BRAF^{V600E}$-mutant melanoma cells using different cell culture conditions. In addition we successfully developed HA15 resistant cell lines that Cerezo et al failed. In addition we were able to characterize gene expression differences between the HA15 sensitive and resistant cell lines.

Background

Genetic landscape of human malignant melanoma

Melanoma malignum is an extremely complex disease and has the highest mutational burden among all tumours. The disease is caused by a combination of environmental (UV radiation) and inherited genetic factors. Both somatic and familial mutations are associated with high risk for the development of disease. Approximately 1% of primary melanoma cases occur within families. The most frequently mutated gene in inherited tumours is the *CDKN2A* tumorsuppressor gene, in addition approximately 10 genes with high penetrance are have been also identified. However, these mutations explain only ~22% of the familial melanoma cases [14]. A systematic review on the impact of genetic testing on familial melanoma was just recently published [15].

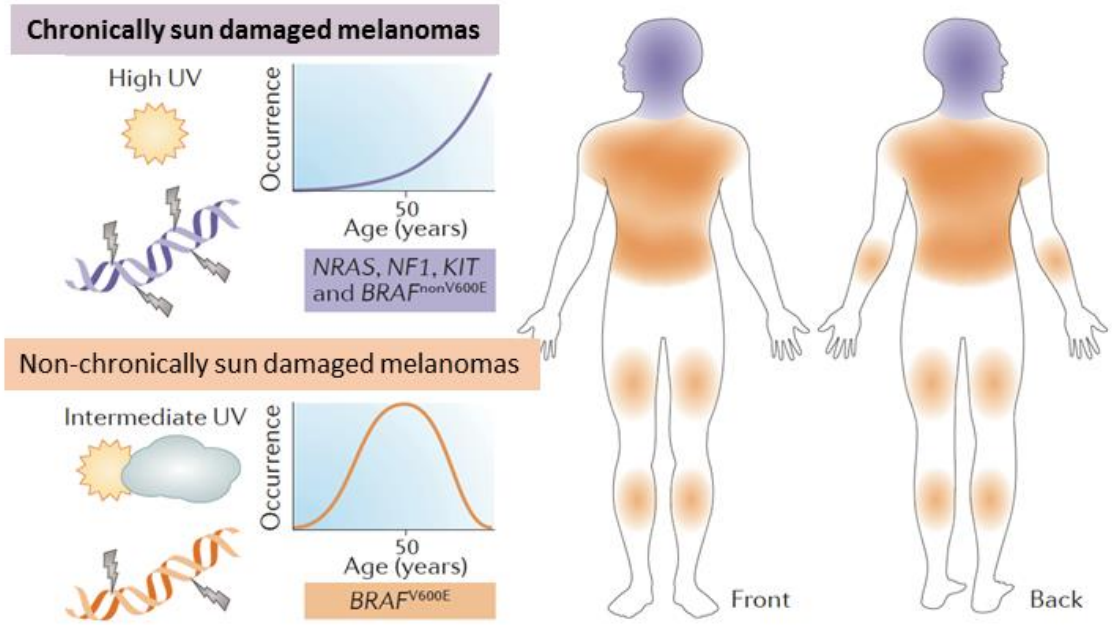

Figure 3. Distinct types of chronically sun damaged and non-chronically sun damaged melanomas. *Adopted from Shain and Bastian [16]*

The timing and pattern of sun exposure is important for the development of cutaneous melanomas (**Figure 3**). During the last two decades different molecular genetic methods, including fluorescence in situ hybridization (FISH), array comparative genomic hybridization

(aCGH), different next generation sequencing (NGS) approaches were performed to define genetic/genomic alterations underlying melanoma development and progression [16].

Genetic alterations leading to the malignant phenotype includes somatic point mutations, structural alterations, chromosome rearrangements and copy number alterations. Different melanoma subtypes have different evolutionary routes associated with genetic different alterations [16] [17]. Chronically sun damaged melanomas arise most frequently from melanoma in situ and associated with mutations of the *NRAS*, *NF1*, *KIT* and *BRAF* (other than the *V600E* mutation) genes, while the non-chronically sun damaged lesions commonly arise from dysplastic or benign naevi and the characteristic mutation is $BRAF^{V600E}$. Curtin et al hypothesized that the high clinical heterogeneity in malignant melanoma can be explained by genetically distinct types of melanomas [18]. Based on their results, cutaneous melanomas with and without chronically sun-damaged skin and mucosal surfaces can be classified into multiple subtypes: (i) chronically-, (ii) intermittent-, (iii) minimal- sun exposure and (iv) protected from sun **(Figure 4)**.

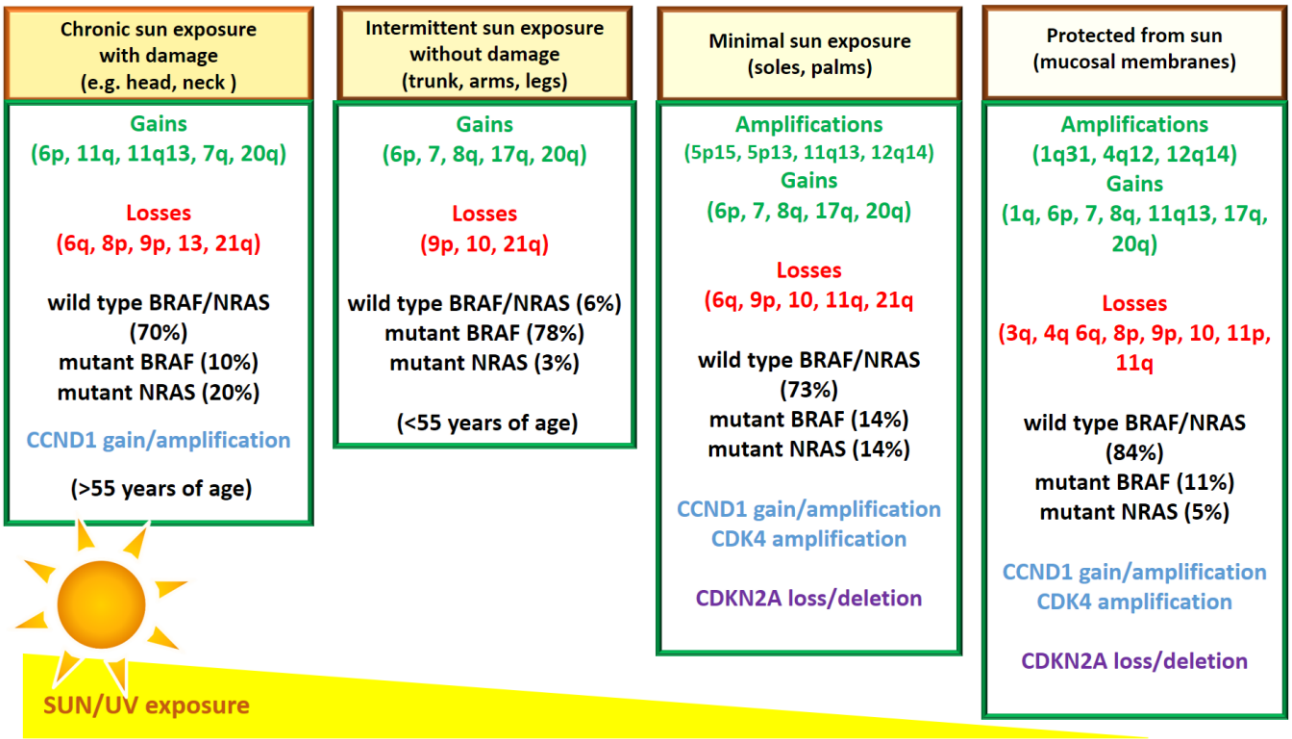

Figure 4. Classification of cutaneous melanomas into four groups on the basis of the changes in the number of copies of genomic DNA. *Edited on the basis of Curtin et al. results [18].*

Large-scale sequencing approaches have led to the further classification of cutaneous melanoma into four major subtypes: (i) *BRAF* mutant melanomas (~50-60% of melanomas), (ii) *RAS* mutant melanomas (~25% of melanomas), (iii) *NF1* mutant melanomas (~15% of melanomas), and (iv) *BRAF/NRAS/NF1* triple wild-type melanomas (~10% of melanomas) [19]. The pathways that trigger melanoma development are the BRAF associated nevus prone pathway (initiated by early sun exposure and promoted by intermittent sun exposure), usually associated with young age and the tumour arise on non-sun-exposed skin. These lesions develop on the trunk, arms and legs and the subtype is SSM. Chronic sun exposure related pathway is mainly associated with either *RAS* mutations (*NRAS:* principally at codon *Q61*, *KRAS* or *HRAS*) without any association with the number of nevus [20]. Intermittent sun exposure is associated with mainly *BRAF* mutations, and more common in young age. *NRAS* mutations are present in older patients with the disease and the histological subtype is mainly nodular melanoma [21].

A systematic survey to identify driver mutations in melanoma were published by Hodis et al., their results offer a comprehensive view of the landscape of driver coding mutations in human melanoma, these data are summarized on **Figure 5**. [22].

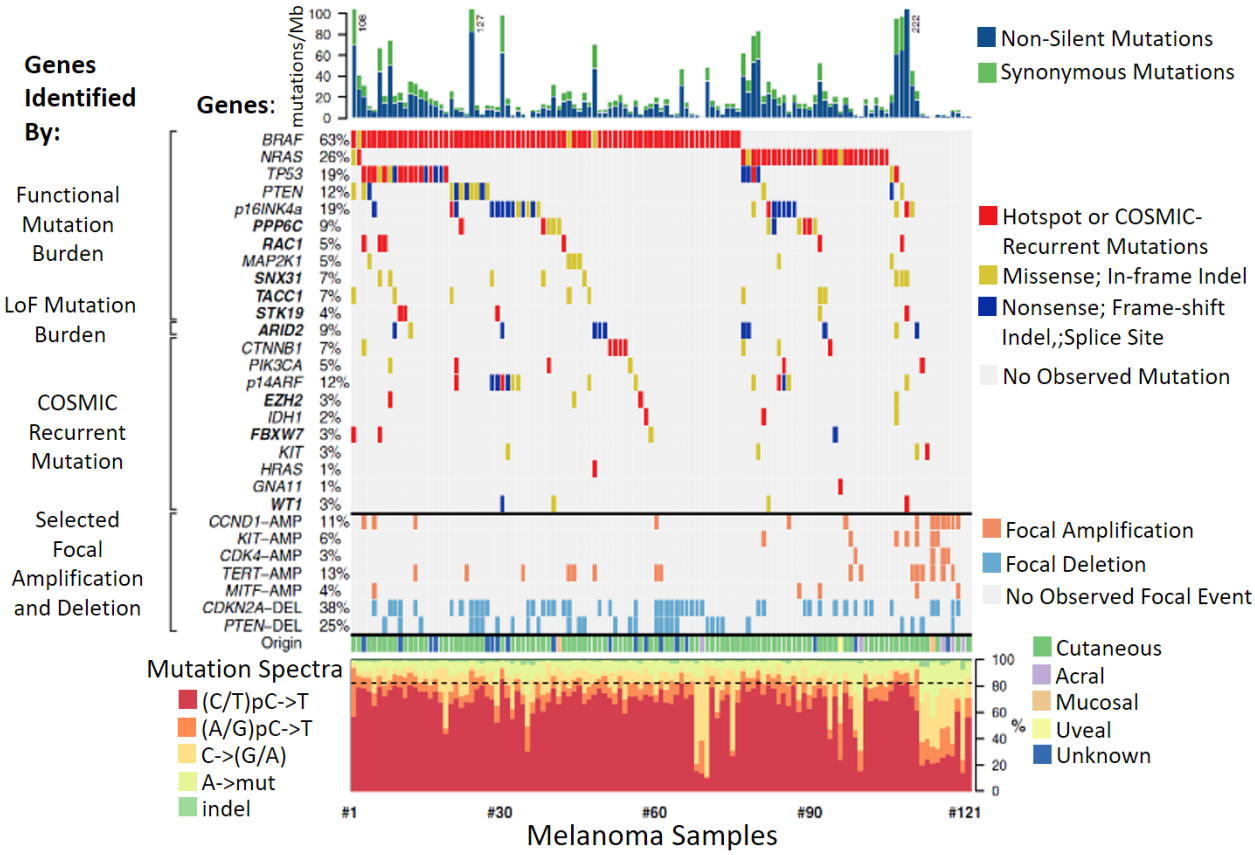

Figure 5. Landscape of driver mutations in malignant melanoma. *Adapted form Hodis et al.* [22]

Hodis et al. used whole-exome sequencing data from 121 melanoma tumour/normal tissue pairs, employed a statistical approach that infers positive selection at each gene locus based on exon/intron mutational distributions, as well as the predicted functional impact of each mutation. Based on the data they were able to discover not only new cancer related genes with functionally consequential, but the analysis allowed the identification of numerous driver mutations directly attributable to UV mutagenesis [22]. These included six well-known cancer genes (*BRAF, NRAS, PTEN, TP53, p16INK4a* [transcript of the *CDKN2A* gene locus], and *MAP2K1*) and five new candidate genes (*PPP6C, RAC1, SNX31, TACC1*, and *STK19*). Functional mutations with high frequency included the following genes: *BRAF* (63%), *NRAS* (23%), *P53* (19%), *PTEN* (12%), *p16INK4a* (19%). *BRAF* and *NRAS* mutation were not present in the same sample. Mutations of these genes frequently associated with gene amplifications (*TERT, MITF, KIT, CCND1 and CDK4*) and/or deletions. Deletion in the *CDKN2A* was 38% and the *PTEN* tumorsuppressor gene was deleted in 25% of cases. These results are in a very good aggrement with Curtin et al. data [18].

The identified mutations are potential therapeutic targettable mutation. Most of the commonly altered genes are member of the mitogen-activated protein kinase pathway, including mutations in *BRAF, EGFR, KIT, RAS, MEK*, and *ERK* oncogenes.

Mitogen-activated protein kinase pathway

The mitogen-activated protein kinase (MAPK) pathway (also known as the Ras/Raf/MEK/ERK pathway) is one of the most important signalling cascade in eukaryotic cells [23]. The pathway regulates molecular processes including cell proliferation, cell differentiation, apoptosis, cell survival, cancer cell dissemination, and resistance to different types of drug therapy. The activation of the pathway is triggered by binding growth factors (e.g.EGFR) to their transmembrane receptor tyrosine kinases (RTKs) located on the cell surface in non-malignant cells. This binding will lead to the dimerization and auto-phosphorylation of these receptors. The subsequent phosphorylation of RTKs on the C termini serve as binding sites for Src homology 2 (SH2) and phosphotyrosine binding (PTB) domain- containing proteins, like Grb2 which localizes SOS (a guanine nucleotide exchange factor) to the plasma membrane, which catalyses the activation of RAS by exchanging GDP for GTP. The RAS proteins (N-RAS, K-RAS, H-RAS) act as a molecular switches; recruits, binds and activate multiple effectors from the RAF (Rapidly Accelerated Fibrosarcoma) serine-threonine kinases (ARAF, BRAF, and

CRAF). RAFs phosphorylate and activate the dual specificity kinases MEKs at key serine residues, S218 and S222 (Rushworth et al. 2006). Activated MEKs phosphorylate and activate ERK1/2. ERK1/2 phosphorylate a variety of cytoplasmic translocate to the nucleus to control transcription of genes involved in cell proliferation [24]. Phosphorylation and activation of the ERK1 and ERK2 MAPKs, they will be able to translocate to the nucleus. (**Figure 6**).

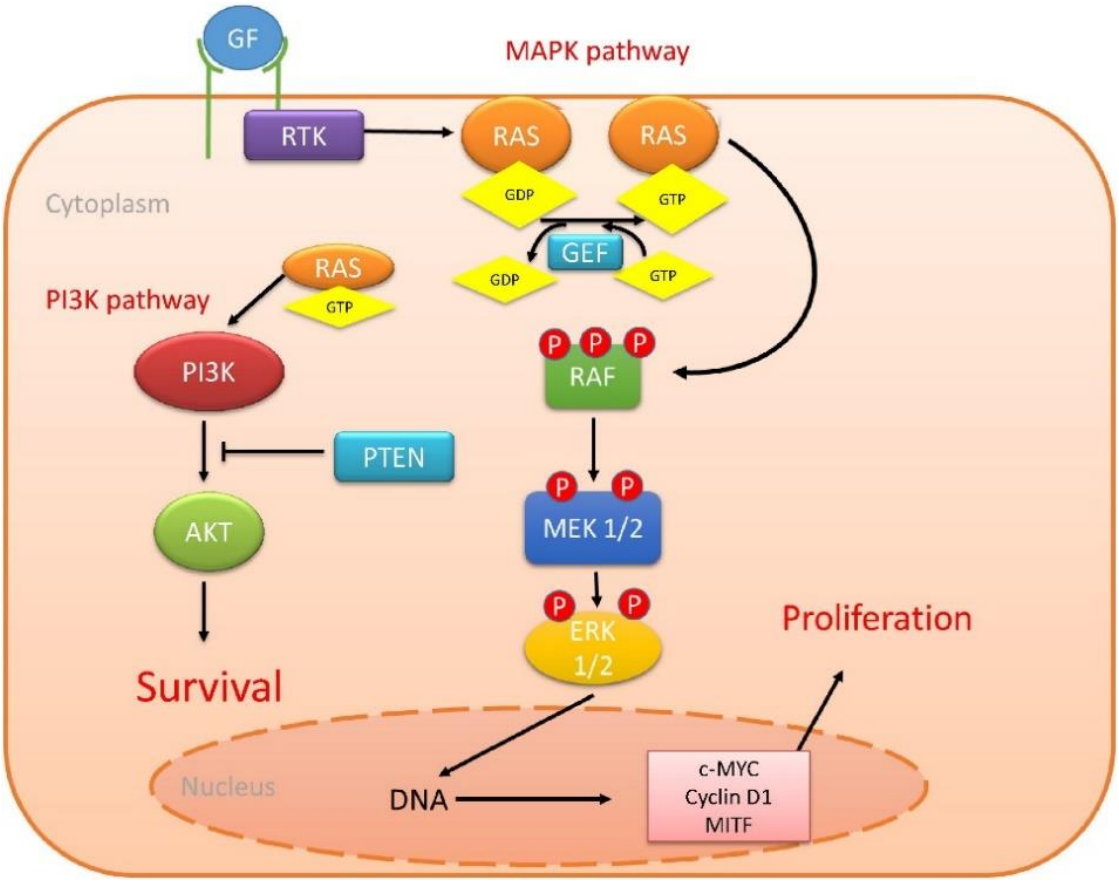

Figure 6. Shematic illustration of the cellular events during MAPK signalling. *Activated RAS will phosphorylate RAF, leading to its activation, then RAF can phosphorylate and activate MEK1 and MEK2 and subsequently activate ERK1/2, resulting in the translocation and regulation of several transcription factors in the nucleus [23].*

After this process several transcription factors will be regulated resulting in gene expression changes of *c-MYC* and *MITF* and other transcription factors. In addition, MAPK signalling can lead to the increased expression of CCND1. Besides initiation of MAPK signalling, RAS-GDP is also able to promote survival through the PI3K signalling pathway, by activating AKT.

Important mutation of the MAPK pathways components

The *BRAF* oncogene mutations are the most common alterations in cutaneous melanoma, approximately 45-60 % of all melanomas harbour this activating mutation [25]. Mutations of *NRAS* (at the *Q61* loci and a few percent at *G12, G13* locus) shows the second highest mutational frequency in the disese (15-20%). The *HRAS* and *KRAS* mutation rate is infrequent, account about ~1 %. *NF1* gene, encoding a large protein neurofibromin 1 is also frequently mutated (12-30%) [26]. The middle of the *NF1* gene contains the GAP (GTPase-activating protein) domain. These enzymes turns off RAS by stimulating the GTPase activity, loss- of-function mutation of the *NF1* gene resulting in the activated RAS and MAPK pathway [27].
The $BRAF^{V600E}$ alteration induces a conformational change within the activation loop of the BRAF protein and leads to constitutive increase in kinase activity, and RAS-independent activation of BRAF and downstream MEK-ERK1/2 signalling. Other codon 600 substitutions are also found, with lysine (*V600K*), aspartate (*V600D*), and arginine (*V600R*) being the most frequent. As a group these codon 600 lesions have been called class 1 mutations.

Approximately 80% of all *BRAF* mutations in any cancer are *class 1 mutations*, and in cutaneous melanoma, this type comprise about 90% of *BRAF* mutations. $BRAF^{V600E}$ mutations are more commonly associated with overall low mutation burden and with younger age versus $BRAF^{V600K}$ mutations [28]. Conversely, *V600K* mutations are more commonly associated with higher mutational rate in tumour suppressor genes including *PTEN*, *CDKN2A*, and *p53*. Other codon mutations belonging to *class 2 mutations* are mutations in codons 464, 469, 597, and 601 [29].These mutations cause constitutive dimerization of RAF, resulting in enhanced kinase activity. Recently, the increased number of sequenced melanoma samples shed light on fusions of dimerization domains to RAF kinase domains (usually but not always BRAF) and recognized as melanoma oncogenes. The mutations in codons 466, 581, and 594 (class 3 mutations) typically cause reduced kinase activity, a phenomenon that was initially confusing [30,31]. Interestingly, subsequent analysis revealed that these mutations co-occur with RAS mutations or other events that cause upstream activation of the pathway. Therefore, these class 3 mutations stabilize a dimeric RAF enzyme (BRAF protomer can dimerize with CRAF and lead to an activated heterodimer) in the presence of RAS GTP. Inhibition of class 3 mutations with RAF inhibitors will be challenging due to the co-occurrence of RAS pathway activation. Last but not least, the *ARAF* and the *CRAF* could be mutated, but at very low frequency (~1-3 %). These

findings have ramifications for differential therapeutic vulnerability by *BRAF* mutation type and even within the V600 population. On the other hand, it is important to understand not only the $BRAF^{V600E}$ mutation but the other classes of *BRAF* mutations since they significantly highlight the biology of BRAF and will likely be important in resistance to targeted therapies. Since the discovery the high frequency of $BRAF^{V600E}$ mutation in malignant melanoma, extensive research were performed, to develop effective targeted therapy to inhibit the activation of the mutant protein.

BRAF inhibitors

At the beginning of the development of drugs that inhibit the RAF pathway, the direct effector of RAS, drug discovery efforts led to CRAF kinase inhibitors. Several compounds were discovered, like ZM336372, L-779,450, and GW5074, but only sorafenib made it to clinical development [32,33]. Sorafenib was initially developed by Bayer Pharmaceuticals as BAY 43-9006 in 2001 [34]. First studies showed efficacy in renal cell carcinoma, hepatocellular carcinoma, and thyroid cancer, but further studies revealed it is primarily due to inhibition of VEGF receptors (VEGFRs), and despite initial optimism, sorafenib failed to show efficacy in large phase III clinical trials for BRAF mutated melanoma [35]. Deeper analysis suggests that sorafenib, more selective for CRAF than BRAF and if it binds to the BRAF protein, it will bind to the inactive form not to the hyperactive kinase activity presented by the $BRAF^{V600E}$ allele that predominates in melanoma tumours and therefore is a very poor inhibitor of the oncoprotein. Structural characterization revealed at least two different binding mechanisms of the kinase inhibitors: type I and type II. Type I inhibitors bind to the activated form of kinases in the activation loop bearing amino acids Asp-Phe-Gly (DFG) (also known as DFG-in), while type II inhibitors bind to inactive (DFG-out) forms that block activation but not the constitutively active kinases (**Figure 7**).

After the costly failure of sorafenib and the discovery of the *BRAF* mutation in 2002 the drug finding efforts focused on type I kinase inhibitors. Numerous compounds were discovered, but only three of them achieved clinical efficacy in melanoma: vemurafenib, dabrafenib, and encorafenib.

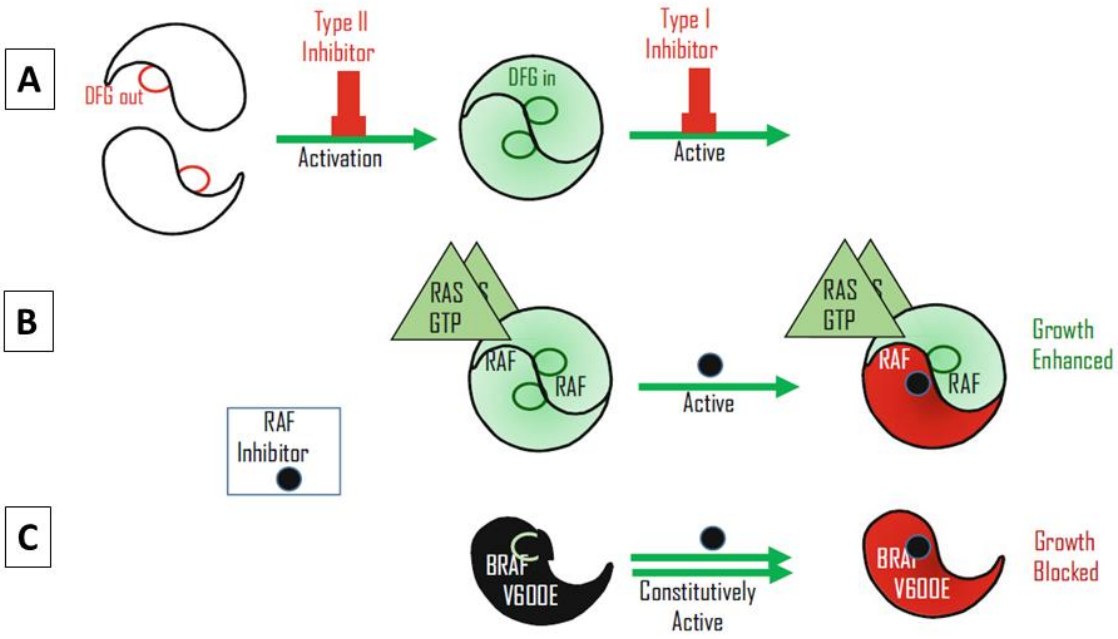

Figure 7. Illustration of biochemical mechanisms that can be altered through targeted therapies. ***A.)*** *Illustration of typical activation mechanism of protein kinases - e.g. through ligand binding to a receptor kinase or phosphorylation by an upstream kinase – causes the DFG loop to switch to the "in" conformation that enables ATP binding.* ***B.)*** *Paradoxical activation by RAF inhibitors which occurs since RAS induces formation of an asymmetric RAF dimer.* ***C.)*** *$BRAF^{V600E}$ signals as an active monomer which is effectively blocked by type I RAF inhibitors.*

The first type I inhibitor which enters to the clinical trials was vemurafenib. The development started at Plexxikon with a structure-guided drug identification and continued with the discovery of PLX4720 the tool compound of vemurafenib (**Figure 8**). The most important empirical discovery entailed elaboration of a phenyl-sulfonamide at the 3-position of the azaindole. Fluorine substitution of the phenyl group was key in order to impart acidity to the sulfonamide nitrogen: this makes key interactions with a newly revealed specificity sub-pocket. Finally the 5-chloro azaindole substituent was replaced by a 5-p-chloro-phenyl moiety yielding vemurafenib (PLX4032, RG7420, Zelboraf).

At the same time another project led to the discovery of dabrafenib (GSK2118436, Tafinlar) which has a different structure to bind to the mutated BRAF protein but also utilizes the fluoro-phenyl sulfonamide to engage the specificity sub-pocket [36]. The last in line type I inhibitor is encorafenib (LGX818), an important properties of this compound compared to the others is having differential binding affinities for each protomer of asymmetric BRAF dimers and a very

slow off-rate from the BRAF enzyme [29]. Currently, numerous "pan-RAF" inhibitors have entered the clinic include (e.g. LXH254, TAK-632, MLN2480, CEP-32496 etc) [29] which have broader activity on the RAF isoforms, in part through blocking dimeric RAF proteins [37]. However, these compounds are all relatively early in clinical development. Further studies require to determine their efficacy, safety and their clinical applicability.

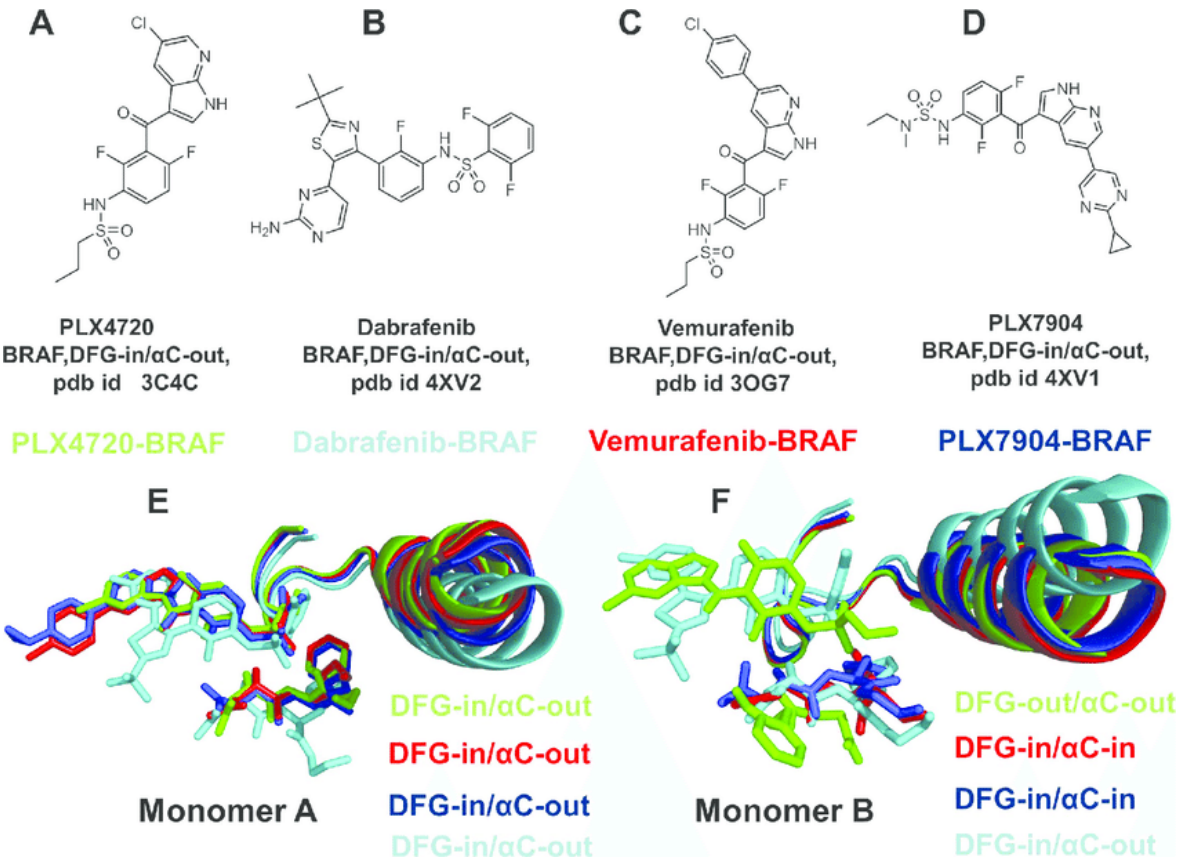

Figure 8. Chemical Structures and Structural Binding Modes of the BRAF Inhibitors. (A) *PLX4720,* ***(B)*** *Dabrafenib,* ***(C)*** *Vemurafenib and* ***(D)*** *PLX7904.* ***(E)*** *The binding modes of the BRAF inhibitors in the first binding site (monomer A). PLX4720 (in green), Vemurafenib (in red), PLX7904 (in blue), and Dabrafenib (in cyan).* ***(F)*** *The binding modes of the BRAF inhibitors in the second binding sites (monomer B). Among studied inhibitors, only PLX4720 (in green) and Dabrafenib (in cyan) bind to the second monomer. Note structural similarity of the inhibitor binding mode and DFG-in/αC-out kinase conformation in the first monomer, while alternative inhibitor binding modes and conformational variability in the second. Adapted from Amanda Tse [38]*

Last, but not least, we have to notice one important phenomenon in connection with RAF inhibitors, which is the "RAF inhibitor paradox" [39]. The researchers came to a surprising discovery at the beginning of using RAF inhibitors using sorafenib or vemurafenib. They found increased incidence of cutaneous squamous cell carcinoma (cSCC) and the related malignancy keratoacanthoma [40]. Although, this tumour easily controlled by routine dermatological methods, the prevalence was worrisome. Intense scientific scrutiny led to the identification of a surprising etiology: RAF inhibition could lead to paradoxical activation of the MAPK pathway. The cSCC/keratoacanthomas arise within a few weeks, so de novo development is highly unlikely. Deeper research has made it obvious, these lesions had been initiated by RAS mutation. RAS mutations or alternative upstream activation of the RAS pathway suffer MAPK pathway activation in response to RAF inhibitors. Treatment of these cells with RAF inhibitors has relatively modest effects on growth properties, but when growth is affected, increased proliferation and downstream signalling of the pathway is observed. Hence the paradoxon: MAPK pathway blocking can lead to MAPK pathway activation. While the details of the mechanism under investigation, it seems that binding of RAF inhibitor to one protomer of a RAF dimer induces enhanced ATP binding to the neighbouring protomer. This is similar with the role of RAS in stimulating RAF dimer formation at the membrane. The *BRAFV600* mutated proteins active as monomers, without dimerization, hence, the inhibitor effectively bind them and suppress signalling. The MAPK pathway is essential for BRAF mutant tumours this is the reason why these agent has huge therapeutical efficacy. There is only one exception in the literature where there is no paradox RAF activation. PLX8394 now is in early clinical development, but seems to binds to the active site of BRAF, without stimulating the neighbouring protomer, and actually destabilizes the dimer [41]. Finally, we have to note that, these first generation RAF inhibitors are ineffective in case of cells bearing the very rare, structurally different class 2 or class 3 mutation.

Resistance to BRAF inhibitors

Despite the significant response using selective BRAF mutant inhibitors most patients develop resistance and tumour regrowth. There are three chronologically distinct phases of resistance: (i) within a day, changing in cellular signalling leads to a new homeostasis; (ii) within a month, epigenetic, immuno-, and micro-environmental adaptation leads to tolerance; and (iii) after months (to years), genetic mutations result in outgrowth of resistant clones. Normally, ERK

activation leads to pathway attenuation through DUSP and Sprouty proteins. BRAF inhibition direct consequence is the ERK dependent negative feedback cannot be achieved [42], but as the tumour cells adapt to the presence of the inhibitor, and a new "steady state" is achieved. Within a few weeks some "tolerant" cells persist and can seed recurrence of the tumour due to the above mentioned epigenetic and microenvironmental factors induce adaptation and tolerance [43,44]. Finally, after months, a new tumour population develops with high intratumoral heterogeneity and often with distinct resistance mechanism [45]. If we look at the mechanisms not as a function of time but as a basis for molecular changes, then non-ERK dependent and ERK dependent groups can be created, this group includes one of the earliest discovered mechanism which play a crucial role in overcoming the toxicity of BRAFi; the upregulation of receptor tyrosine kinases (RTK) (**Figure 9A**) [46-48].

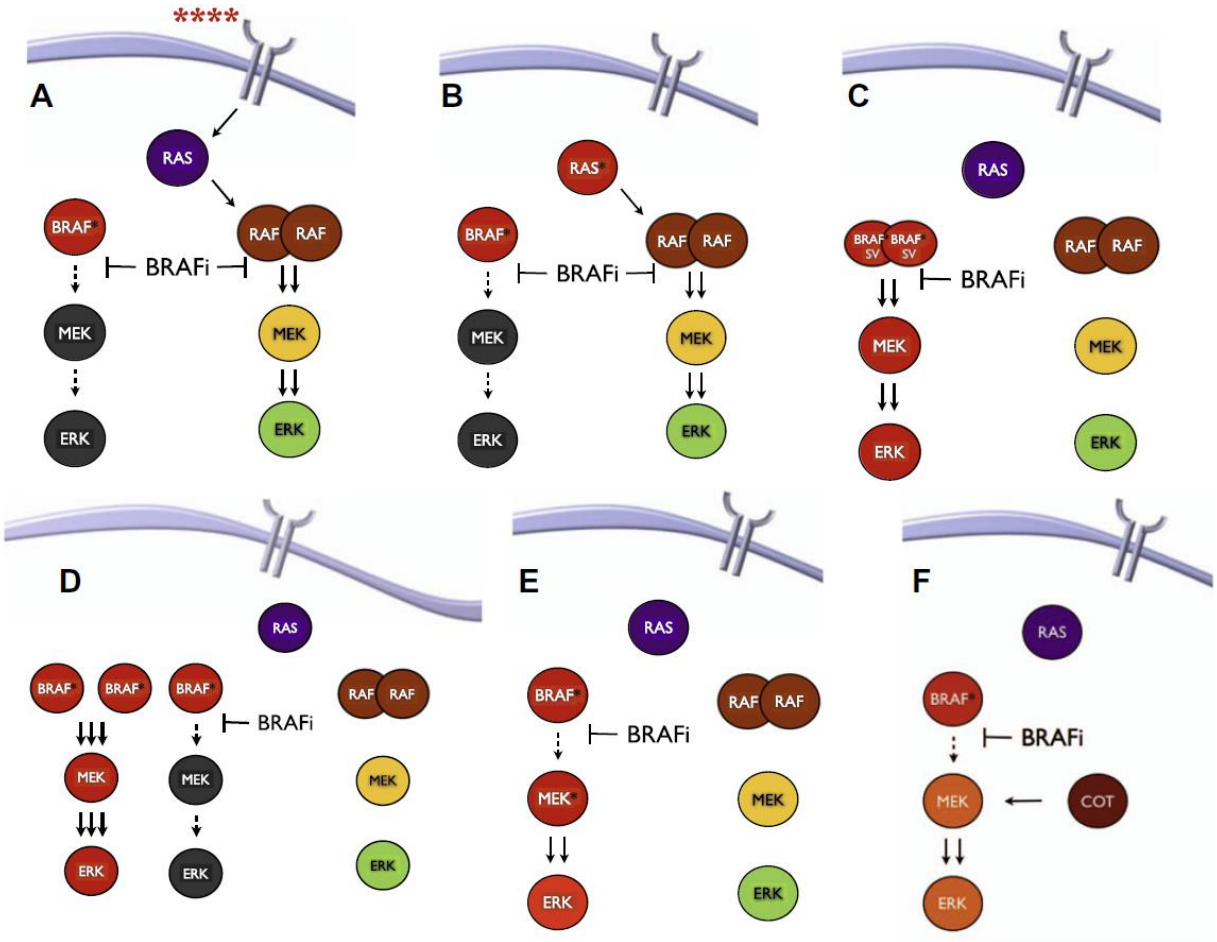

Figure 9. Different mechanism of acquired resistance against BRAF inhibitors (asterisk indicates mutated protein). *Adapted from Ryan J [49].*

Furthermore, several studies and biopsy samples from resistant tumours shows activation of PI3K, mTOR, AKT pathways, due to platelet derived growth factor receptor beta (PDGFRβ) and insulin-like growth factor 1 receptor (IGF-1R) activation and overexpression. However, dual inhibition of the MAPK pathway (MEKi) and mediators of the PI3K pathway (PI3K, mTOR, AKT) appears to be an effective strategy at overcoming this type of resistance [50].

ERK dependent mechanisms includes cells which harbour 'gate-keeper' mutations which lead to conformational changes in the binding site that alters the binding affinity of a molecule to the target. The above mentioned BRAF inhibitor paradox is another way of resistance. In this case the BRAF inhibitors facilitate RAF signalling in non-mutant cells [51,52]. Emergence of cells harbouring additional genetic events including concomitant BRAF and NRAS mutations (**Figure 9B**) and splice versions of BRAF (**Figure 9C**)[46,53,54]. In case of alternative splice variation of the *BRAF* gene, the truncated BRAF isoform maintains the mutation at the 600 position (i.e. *V600E*) but dimerises in the presence of a BRAF inhibitor thereby hyperactivating the MAPK pathway [54]. Other ERK dependent mechanism is the overexpression of the mutant BRAF which overcome the inhibition and can be bypass, by increasing the dose of the BRAF inhibitor (**Figure 9D**) [55]. Another way to reactivate the MAPK pathway is the downstream activation of MEK or ERK, which has been described by upregulation of alternative MAPK, such as COT, and through secondary mutations in MEK (**Figure 9E and F**)[47,56,57]. In spite of the extensive research of the resistant mechanisms, about 40% of resistant tumours does not shown these typical changes, and the real cause of resistance remains hidden.

Landscape of melanoma therapies- FDA Approval Overview

Pioneering research at the cancer biological and immunological fields during the last two decades has led to the discovery and expansion of novel therapeutics, including the immune checkpoint inhibitors and molecular targeted therapies, all of those have revolutionized the clinical management of patients with advanced primary and metastatic melanoma. Recent data from the largest clinical trials continue to support the use of these new treatment opportunities, both in the metastatic and in adjuvant settings. However, with increasing evidence that neoadjuvant therapy is also associated with high rates of recurrence-free survival, the question about whether patients should receive adjuvant or neoadjuvant treatment raises new questions about therapeutic possibilities. Finally, management after the development of resistance and

intervention with novel immunotherapies are newer challenges, particularly in the field of non-cutaneous melanoma [58].

The first FDA approved drug for advanced and metastatic melanoma was dacarbazine in 1975 [59]. The first trials of interferon for resectable melanoma started at 1984, when it was demonstrated that interleukin-2 (IL-2)-dependent T cells could be trained to recognize and attack malignant melanoma [60]. Rosenberg and his team was the first to use immunotherapy, based on autologous tumour-infiltrating lymphocytes and IL-2 in case of a patient with metastatic melanoma, but the treatment was approved just in 1996 after a multicenter, randomized, controlled phase III study [61,62]. After a long gap, in 2011, the FDA approved three drugs: pegylated interferon (Sylatron™), vemurafenib (Zelboraf®, PLX4032), and ipilimumab (Yervoy®) for melanoma treatmen [63]. At the end of 2014 (phase Ib of clinical trials) Mario Sznol and his team reported one- and two-year survival rates in advanced melanoma patients (unresectable or metastatic melanoma; success rate 94% and 88%, respectively) using the combination of monoclonal antibodies (nivolumab and ipilimumab), [64].

After this discovery, the FDA approved the combination therapy for these two drugs. Combination of small molecule inhibitors (dabrafenib (Tafinlar®) and trametinib (Mekinist®)) were approved in 2014 and a combination of combimetinib (Cotellic®) and vemurafenib in 2015, both for patients with unresectable or metastatic melanoma with $BRAF^{V600E}$ or $BRAF^{V600K}$ mutations. In 2017, the FDA approved a combination of dabrafenib and trametinib for those patients and nivolumab (Opdivo®) for the adjuvant treatment. Both therapies are dedicated to patients with involvement of lymph nodes or who have complete resection. In 2018, the FDA approved a combination of encorafenib (Braftovi®) and binimetinib (Mektovi®) for unresectable or metastatic melanoma with $BRAF^{V600E}$ or $BRAF^{V600K}$ mutations. In 2015, the FDA announced the first in class oncolytic virus therapy for advanced melanoma called talimogene laherparepvec (Imlygic™, Amgen)[63].

Table 1. FDA approved melanoma drugs, drugs combinations and oncolytic virus

Drug Name	Brand	Type	Biological Classification	Target	First FDA Approval
Monotherapies					
dacarbazine	DTIC-Dome® Bayer	small-molecule	antineoplastic agent	DNA	November 1975
IL-2 (aldesleukin)	Proleukin® Nestle	protein	interleukin	agonist/modulator of IL-2 receptor subunit alpha/beta, agonist of cytokine receptor common subunit gamma	January 1998
ipilimumab	Yervoy® Bristol Mayer Squibb	antibody immune therapy	monoclonal antibody (mAb)	antagonist of CTLA-4	March 2011
peginterferon alfa-IIb	Peginton® Merck&Co	small-molecule	interferons	agonist of interferon alpha/beta receptor 1 and 2	March 2011
vemurafenib	Zelboraf® Roche/Genetech	small-molecule signaling antagonist	kinase inhibitor	mutant BRAF	August 2011
dabrafenib	Tafinlar® Novartis Pharmaceuticals Corp.	small-molecule signaling antagonist	kinase inhibitor	mutant BRAF	May 2013
trametinib	Mekinist® Novartis Pharmaceuticals Corp.	small-molecule signaling antagonist	kinase inhibitor	MEK	May 2013
pembrolizumab	Keytruda® Merck&Co	antibody-immune therapy	monoclonal antibody (mAb)	antagonist of PD-1	September 2014
nivolumab	Opdivo® Bristol Mayer Squibb	antibody-immune therapy	monoclonal antibody (mAb)	antagonist of PD-1	December 2014
taumogene laherparepvec	Imlygic® Amgen	oncolytic virus	virus	DNA polymerase catalytic subunit, heparan sulfate	October 2015

Drugs Combination	Brand	Type	First FDA Approval
trametinib (Mekinist®) + dabrafenib (Tafinlar®)	Novartis	small-molecule targeted therapy	January 2014
nivolumab (Opdivo®) + ipilimumab (Yervoy®)	Bristol Mayer Squibb	antibody-immune therapy	September 2015
vemurafenib (Zelboraf®) + cobimetinib (Cotellic®)	Roche/Genetech	small-molecule targeted therapy	November 2015
encorafenib (Braftovi®) + binimetinib (Mektovi®)	Array BioPharma	small-molecule targeted therapy	June 2018

Endoplasmic reticulum stress as a novel therapeutic target in cancer

In eukaryotic cells endoplasmic reticulum (ER) is responsible for calcium homeostasis, lipid biosynthesis, protein folding and quality control as the first compartment of secretory pathway. However, similarly to any system, errors can occur in ER, and numerous proteins fails ER quality control criteria due to misfolding. The improperly folded proteins addressed to the ER associated degradation (ERAD) system which targets them for ubiquitinylation and

proteosomal degradation [65-67]. Under homeostatic conditions protein folding, export and degradation are not saturated, the ER can cope with the protein folding demand. However, some certain physiological and pathological conditions can disrupt ER homeostasis and impose stress to the ER, leading to accumulation of unfolded or misfolded proteins in the ER. The ER to cope with the increased stress evolves highly specific signalling pathways collectively called "unfolded protein response" (UPR) to restore normal ER homeostasis [68].

The role of the UPR is (i) inhibit misfolded protein accumulation by attenuating protein translation, (ii) support ER folding capacity by increasing the amount of chaperones, (iii) enhancing the unfolded protein degradation [69,70]. **Figure 10** summarizes the UPR pathway. During ER stress BiP dissociates from the three sensors ATF6, IRE1, PERK and allow their

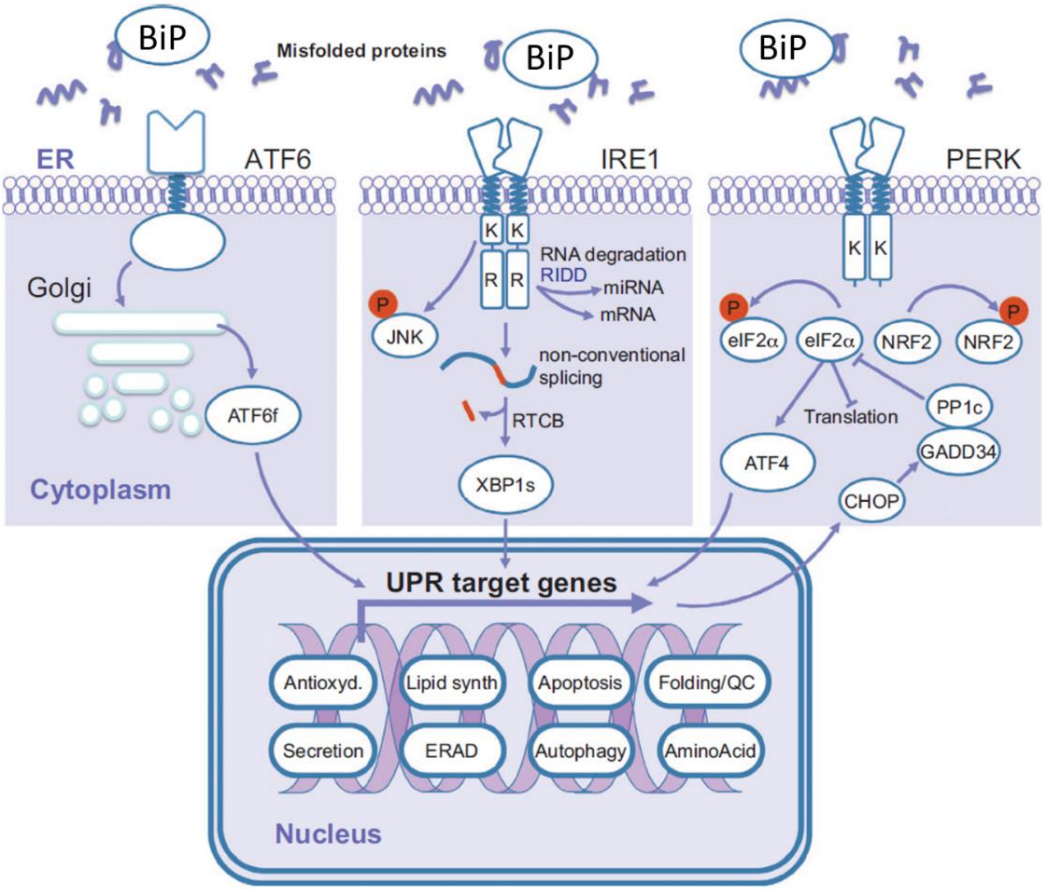

Figure 10*. *Unfolded protein response pathway. *Abbreviations: antioxid: antioxidant response; Lipid synth, lipid synthesis; QC, quality control Adapted from Avril et al [71].*

Dimerisation or export to the Golgi apparatus. ATF6 will enter to the Golgi apparatus where proteases cleaved it into an active transcription factor. The active ATF6 moves to the nucleus and induces transcription of genes involved in protein folding (*BiP*, *XBP1*, *CHOP*, etc.) and

ERAD. At the IRE1 arm, BiP dissociation activate IRE1, which cleaves a 26 nucleotide intron from the XBP1 mRNA and that induces expression of genes involved protein folding, secretion, ERAD and lipid synthesis. PERK activation leads to phosphorylation of NRF2 and eIF2α. Phosphorylation of eIF2α induces global translation attenuation and prompts that of AFT4. ATF4 and NRF2 induce expression of genes involved in antioxidant response, protein folding, mino-acid metabolism, autophagy and apoptosis. [71].

If the homeostasis cannot be re-established due to prolonged or intense stress, the UPR also triggers signals that will destine cells to die via apoptosis in order to protect the organism by removing cells that produce malfunctioning proteins [72]. During cancer development, a significant amount of protein is required to support the cancer cells in proliferation, migration and differentiation [67]. However, the higher rate of proliferation of cancer cells results a microenvironment with limited oxygen, and nutrients due to inadequate vascularization. Therefore, cancer cells have to cope with hypoxia, pH variation and nutrient deprivation that leads to higher cellular stress compared to normal cells [69,73,74].

Targeting ER stress in melanoma

Melanoma cells using numerous survival strategies, including induction of the unfolded protein response, which mediates resistance to endoplasmic reticulum (ER) stress induced apoptosis. These mechanism can occur in many way, like activation of oncogene which suppress ER stress induced apoptosis and/or upregulation of ER chaperone which increase the protein folding capacity of the cell. Both of them helps to avoid apoptosis for melanoma cells [75]. Therefore, modulation of UPR could be a possible target in melanoma treatment and could be exploited in two ways (**Figure 11**). On one hand, blocking UPR components makes it impossible for the cell to restore its normal state. The other option is to overload the already active UPR pathway. Both strategies drive the tumour cells to apoptosis [76]

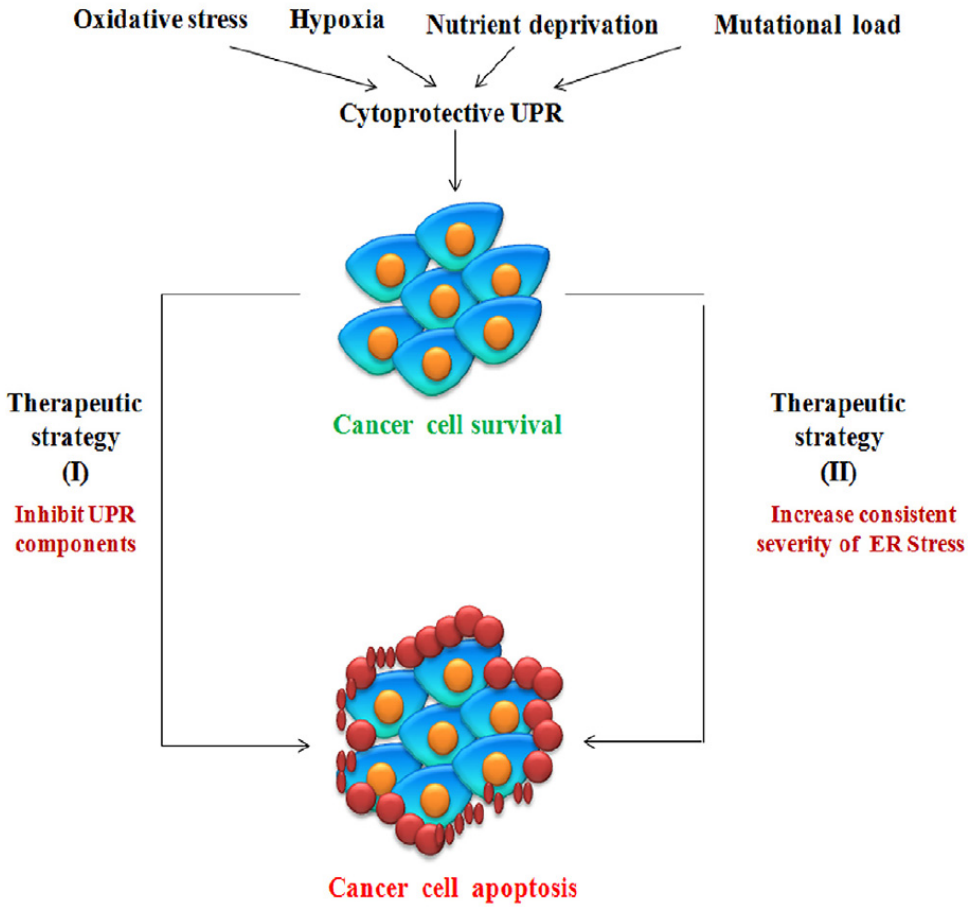

Figure 11. Two ways exploiting UPR for purposes of drug development. *One way is to inhibit UPR components, so the cells can not cope with the increased stress and it will lead to apoptosis. The second way is, to further increase the ER stress in the tumour cell, where the UPR is already activated. In this case the overloaded UPR unable to resolve the stress and drive the cell to death. Adapted from Ojha et al. [76].*

In melanoma both BRAF and NRAS driver mutation induce cytoprotective UPR pathway in order to actively inhibit ER stress induced apoptosis and promote tumour progression [77], this theory is also supported by a research where inhibition of $BRAF^{V600E}$ by vemurafenib results in ER stress induced apoptosis of the $BRAF^{V600E}$ mutant melanoma cells [78]. Further studies suggest the MAPK pathway involvement for the response to ER stress, and its activation in melanoma likely maintain prosurvival UPR signalling while supressing ER stress induced apoptosis [79]. Hence, in case of melanoma the most useful strategy for exploiting ER stress the

combination of agents that inhibit cytoprotective function of UPR arms along with those that actively induce ER stress [75].

Other important properties of melanomas the “chaperone addiction”. This phenomenon means cells become dependent upon continual chaperone expression for survival. Therefore, inhibiting chaperone proteins expression is a potential new way for the treatment of melanoma [80,81]. Accordingly, it is not surprising that, as a key molecule, BiP is overexpressed in many tumors, including melanoma, and is associated with higher tumor grades and reduced patient survival [82-86]. Several studies show that, inhibition of BiP/GRP78 with E. coli subtilase, green tea polyphenol epigallocatechingallate or Magnolia grandiflora derivative honokiol, both of them are potent inducers of ER stress, resulting in the apoptosis of melanoma cells [80,87,88].

Most recently Cerezo et al. synthesized and characterized a new molecule family, thiazole benzensulfonamides (TZBs), which have anti-cancer properties [89]. Based on their results, Cerezo et al. focused on one molecule of the family, named HA15, which was identified as the lead compound that induces elevated endoplasmic reticulum (ER) stress specifically in cancer cells without any adverse effects in normal cells [89]. Cerezo et al. showed that the drug induces the death of all melanoma cells independently of the cell mutational status. Similar observations were reported for freshly isolated melanoma cells, independent of whether patients were sensitive or resistant to BRAF inhibitors [89]. Cerezo et al. also identified the ER protein BiP/GRP78/HSPA5 as being a specific target of HA15, describing the fact that interaction between the compound and BiP enhances ER stress and leads to cell death via the concomitant induction of autophagy and apoptotic mechanisms in prostate, breast, colon, pancreas, glioma, cervical, and melanoma cells regardless of driver mutations or BRAF inhibitor resistance [89].

Objectives

The major focus of our study were to investigate the effect of two drugs targeting melanoma cells, with different molecular mechanisms. First we characterized the molecular background of a BRAF inhibitor: PLX4720 which is a vemurafenib analogue targeting the *BRAF*^{V600E} mutated melanomas. We aimed to investigate effect of a recently synthesized anti-melanoma drug, named HA15, which (as was reported by Cerezo et al) displays anti-cancer activity not only against melanoma cells but also other liquid and solid tumours [89].

In details, during our study we aimed to

I.

- investigate the effect of a BRAF inhibitor (PLX4720) on melanoma cell lines
- generate PLX4720-resistant cell lines using melanoma cell line pairs (primary tumour and metastasis-derived melanoma cell lines originated from the same patients),
- determine which genetic alterations, gene and protein expressions are associated with the development of BRAFi resistance,
- compare the invasive properties of the parental and resistant cell lines
- examine the effect of drug withdrawal on cell proliferation in the resistant cell lines,

II.

- investigate the effect of the recently synthesized anti-melanoma drug (HA15) on the viability/proliferation of BRAF^{V600E}-mutant and resistant melanoma cells using different cell culture conditions,
- determine the gene expression differences of ER stress and autophagy markers under different cell culture conditions,
- generate HA15 resistant cell lines,
- compare the gene expression pattern of HA15 sensitive and resistant cell lines using RNA-seq analysis.

Materials and methods

Cell cultures and development of BRAF inhibitor and HA15 resistant cell lines

Our study included 10 melanoma cell lines, the characteristics of the cell lines are summarized in **Table 2**. All cell lines carried the $BRAF^{V600E}$ mutation and were wild type for NRAS. Five cell lines ($WM983A^{p1}$/$WM983B^{m1}$; $WM278^{p2}$/$WM1617^{m2}$ and A375) were obtained from the Coriell Institute for Medical Research (Camden, NJ, USA). All cell lines were cultured in RPMI-1640 medium (Lonza Group Ltd., Basel, Switzerland) supplemented with 10% foetal bovine serum (FBS, Gibco, CA, USA), 2 mmol/L glutamine, and 50 mg/mL gentamycin sulfate at 37°C. The BRAF inhibitor (PLX4720) and HA15 resistant cell lines were developed in our laboratory [90]. Shortly, the four BRAFi (PLX4720) sensitive cell lines (WM983A, WM983B, WM278 and WM1617) were seeded at low densities in T25 flasks until the cells reached 80% confluence. Then, the cells were switched to a medium containing 5 μM PLX4720 and cultured. The surviving cells were given medium containing PLX4720 every 3 days, the cells reached the required confluence (80%) after10 weeks, after we were able to grow the cells in the presence of 5 μM PLX4720 continuously. These resistant cell lines were designated as: $WM983A^{RES}$, $WM983B^{RES}$, $WM278^{RES}$, and $WM1617^{RES}$.

To develop HA15 resistant melanoma cell lines we used the WM983B melanoma cell line, because this was the most sensitive to the drug treatment, the treatment method was similar to the generation of BRAFi resistant cell lines. The only difference was that we had to use increasing HA15 concentration (10 μM, 20 μM and 30 μM) during this experiment. The WM983B cell line was seeded at a low density in T25 flasks until the cells reached 80% confluence. The medium was then switched to medium containing 10 μM HA15, and during cell culture the concentration of the drug was increased up to 30 μM HA15. The surviving cells were treated with 30 μM HA15 every 3 days. The cells reached 80% confluence after ~8 weeks. The resistant cell line was designated $WM983B^{HA15RES}$. Melanocytes plate at 30×10^4 cells per T25 flask and cultured in RPMI-1640 supplemented with 10% FBS, 200 nM 12-O-tetradecanoylphorbol 13-acetate (TPA), 100 pM cholera toxin (CT), 10 nM endothelin 1 (ET1), and 10 ng/ml human stem cell factor (SCF) and place the culture in a humidified, 37°C, 5%

CO2 incubator. HA15 and PLX4720 were purchased from Selleck Chemicals, TX, USA, and MedChemExpress LLC, NJ, USA.

Table 2. Characteristics of human melanoma cell lines

Cell line	Origin[a]	Growth Phase[b]	Histologic Type[c]	BRAF mutation status[d]	NRAS mutation status[e]
WM983A^{p1}	primary	VGP	n.d.	V600E	wt
WM983A^{PLX4720RES}	primary	VGP	n.d.	V600E	wt
WM983B^{m1}	metastasis inguinal node	-	-	V600E	wt
WM983B^{PLX4720RES}	metastasis	-	-	V600E	wt
WM278^{p2}	primary	VGP	NM	V600E	wt
WM278^{PLX4720RES}	primary	VGP	NM	V600E	wt
WM1617^{m2}	metastasis axillary lymph node	-	-	V600E	wt
WM1617^{PLX4720RES}	metastasis	-	-	V600E	wt
WM983B^{HA15RES}	metastasis	-	-	V600E	wt
A375	primary	-	-	V600E	wt

[a]tumor type of melanomas which the cell lines were derived from; [b]VGP: vertical growth phase; [c]NM: nodular melanoma, n.d.: no data; [d]V: valine, E: glutamic acid; [e]wt: wild-type; $^{p1, p2}$primary tumor derived cell line with metastatic pair from the same patient; $^{m1, m2}$metastatic pair of primary derived cell line

Cell proliferation assay

To define the viability of cells, the WST-1 (2-(4-iodophenyl)-3-(4-nitrophenyl)-5-(2,4-disulfophenyl)-2H-tetrazolium) (Sigma-Aldrich Inc., St Louis, Missouri, USA) cell proliferation reagent was applied according to the manufacturer's guidelines. Briefly, melanoma cells were seeded in 96-well plates (0.5×10^4 cells/well/100 µL medium) and treated either with increasing concentrations of PLX4720 (5-5000 nM) for 72 hours (each concentration was tested in triplicate); or with different concentrations (10 µM, 20 µM and 30 µM) of HA15 in triplicate; DMSO (0.5%) was used as a control during both study. In another experimental setup, the cells were starved without FBS for 14 hours before drug stimulation, than the medium was changed

complete medium containing the HA15 drug. In the third experimental setup, the starved cells were maintained without FBS during HA15 treatment (starvation condition). Then, generally 10 µL WST-1 was added into each well, and the cells were incubated for 3 hours at 37°C. Absorbance was measured at 440 nm using an Epoch™ Microplate Spectrophotometer (BioTek Instruments, Winooski, VT, USA). The reference absorbance was set at 700 nm. Cell viability was calculated by dividing the absorbance of the treated cells by that of the vehicle-treated (DMSO (0.5%)) control cells (considered 100%).

BRAFi and HA15 withdrawal from the resistant cell lines

Cells ($5x10^4$ cells/500 µl) from each of the resistant cell lines were seeded in a 24-well plate (in triplicate) and cultured in RPMI 1640 medium supplemented with 5 µM PLX4720 or 30 µM HA15 until cell attachment. Then, half of the cells from each cell line were switched from the drug-supplemented medium to vehicle control (DMSO (0.5%), the solvent of drugs)-supplemented medium, while the other half of the cells remained in drug-supplemented medium for 72 hours. WST-1 reagent was added (50 µl/well) to the cell culture, and cells were incubated for 120 minutes at 37°C. Absorbance was measured as previously described. The absorbance of the cells cultured with the solvent (DMSO (0.5%)) of the drugs was considered 100%.

Matrigel in vitro invasion assay of the BRAFi sensitive and resistant cell lines

The invasive potential of melanoma cell lines was determined using BD BioCoat Matrigel Invasion Chambers (pore size: 8 µm, 24-well; BD Biosciences, Bedford, MA, USA) as described by Koroknai et al. [91]. For the parental cell lines, the upper chamber of the insert was filled with 500 µl of cell suspension in serum-free medium ($5x10^4$ cells/well). In the lower chamber 10% FBS containing medium was applied to as a chemoattractant. For the resistant cell lines, the upper chamber of the insert was filled with 500 µl of cell suspension in a FBS free medium containing 5 µM PLX4720 ($5x10^4$ cells/well). The lower chamber contained medium with 10% FBS and 5 µM PLX4720 as a chemoattractant. After a 24-hour incubation at 37°C, the cells in the lower chamber were fixed with methanol and stained with haematoxylin-eosin. The invaded cells were counted under a light microscope in 7 different visual fields at 200X magnification, and the data are presented as the mean ± SD of three independent experiments.

Flow cytometry

The effects of HA15 on WM983A cells were analysed by flow cytometry using Alexa Fluor 488 Annexin V/Dead Cell Apoptosis Kit (Invitrogen, Camarillo, CA, USA). Cells were treated with DMSO (control (0.5%)) and various concentrations of HA15 (10, 50, and 100 μM) for 48 hours. Before drug treatment, we used starvation conditions (FBS was removed from the medium) for 14 hours, then the cells were harvested and washed with cold PBS. After centrifugation, the supernatant was discarded, and the cell pellets were resuspended in 1× Annexin-binding buffer to a final concentration of 1×10^6 cells/mL. After adding 1 μL of Alexa Fluor 488 Annexin V and 1 μL of 100 μg/mL propidium iodide (PI) working solution to each 100-μL cell suspension, cells were incubated at room temperature for 15 min. After incubation, 400 μL of 1 × Annexin-binding buffer was added, and the stained cells were detected by flow cytometry measuring fluorescence emission at 530 and 575 nm.

Nucleic acid extraction, quality control

RNeasy Mini Kit (Qiagen GmbH, Hilden, Germany) was used to isolate total RNA from the melanoma cell lines. The RNA was quantified using a NanoDrop ND-1000 UV-Vis spectrophotometer, and only samples with 260/280 nm ratio greater than 1.8 were included in the analysis. All sample quality was evaluated using an Agilent 2100 Bioanalyzer (Agilent Technologies Inc., Santa Clara, CA, USA). The RNA integrity was determined using the RNA Integrity Number (RIN), and only samples with value greater than 7.5 were considered in the hybridization to the Affymetrix Human Gene 1.0 microarrays (Affymetrix~~,~~ Inc., Santa Clara, CA, USA).

RNA based microarray experiments

The labelling, hybridization and imaging setup were performed by UD-GenoMed Medical Genomic Technologies Ltd. (University of Debrecen, Debrecen, Hungary). The microarray data have been published in the Gene Expression Omnibus (GEO) repository under accession number GSE114443. Filtering and normalization were performed as previously described [92].

DNA-based microarray experiments

A G-spin™ Genomic DNA Extraction Kit (iNtRON Biotechnology, Korea) was used to isolate DNA from the melanoma cell lines. The DNA was quantified using a NanoDrop ND-1000 UV-Vis spectrophotometer, and only samples with 260/280 nm a ratios greater than 1.8 were included in the analysis. The sample quality was evaluated using 1% agarose gel electrophoresis. The sample labelling, hybridization to Affymetrix CytoScan 750K microarrays (Affymetrix Inc., Santa Clara, CA, USA) and imaging setup were performed by UD-GenoMed Medical Genomic Technologies Ltd. using 400 ng of tumour DNA. The microarray data have been published in the GEO repository under accession number GSE114488.

DNA-based microarray experiments

DNA microarray data were analysed using Nexus Copy Number 6.1 software (BioDiscovery, Inc., Hawthorne, California, USA). To adjust the sensitivity of the segmentation algorithm, we used a significance threshold of 10^{-6} and specified 1000 kbp as the maximum spacing between adjacent probes. To eliminate small copy number alterations (CNAs), the minimum number of probes per segment was set to 5. To detect the DNA copy number (CN) gains and losses, the following $\log_2$ ratio thresholds were set: ± 0.3 for gains and losses, 0.6 for high CN-gains and -1.0 for homozygous deletions. Significantly different CN events between the parental and resistant melanoma cell lines were identified using a two-sided Fisher's exact test. A False Discovery Rate (FDR) adjustment was performed to correct for multiple testing using the Nexus Copy Number 6.1 Comparison feature. To avoid sex bias, all probes on chromosomes X and Y were discarded.

RNA sequencing (RNA-Seq)

Total RNA sample quality was determined using an Agilent BioAnalyzer with a Eukaryotic Total RNA Nano Kit according to the manufacturer's protocol. Samples with an RNA integrity number (RIN) were accepted for library preparation. cDNA li-braries for RNA-Seq analyses were prepared from 1 μg total RNA using an Ultra II RNA Sample Prep kit (New England BioLabs Inc., USA) according to the manufactur-er's protocol. Briefly, poly-A RNAs were captured by oligo-dT conjugated magnetic beads, and the mRNAs were eluted and fragmented at 94°C. First-strand cDNA was generated by random priming reverse transcription, and after the second strand syn-thesis step, double-stranded cDNA was produced. After repairing the

ends and A-tailing and adapter ligation steps, adapter-ligated fragments were amplified by en-richment PCR; sequencing libraries were thus obtained. Sequencing runs were exe-cuted using an Illumina NextSeq500 instrument with single-end 75-cycle sequencing. Library preparations and sequencing were performed at the Genomic Medicine and Bioinformatics Core Facility of University of Debrecen.

RNS-Seq data analysis

The RNA-Seq raw data have been deposited into the Sequence Read Archive da-tabase: (https://www.ncbi.nlm.nih.gov/geo/query/acc.cgi?acc=GSE164261) under accession number GSE164261. The raw sequencing data (fastq) were aligned to human reference genome version GRCh38 using the HISAT2 algorithm, and BAM files were generated. Down-stream analysis was performed using StrandNGS software (www.strand-ngs.com). The BAM files were imported into the software DESeq1 algorithm was used for normalization.

Pathway analysis

To gain mechanistic insight into gene lists generated from the RNA-Seq and microarray data, functional enrichment analysis was used to identify biological pathways more enriched in a gene list than would be expected by chance. The ToppFun tool ToppGene suite (https://toppgene.cchmc.org/) was used to detect functional enrichment of genes (which showed at least a 2-fold change difference between the treated and control groups) based on Gene On-tology (GO) pathways. The tool was used with default settings and a p-value cutoff of 0.05. For visualization of the molecular functional gene networks, we used the ClueGo (v. 2.3.5) tool kit of Cytoscape (www.cytoscape.org) software (v. 3.5.1) (10) with default settings and a p-value cutoff of 0.05. For Gene Set Enrichment analysis (GSEA), we used Molecular Signatures Database (MSigDB) hallmark gene sets, which summarize and represent specific well-defined biological states or processes and dis-play coherent expression (www.gsea-msigdb.org).

Quantitative real -time PCR

The relative expression levels of the selected genes were determined by performing quantitative real-time PCR (qRT-PCR) using a LightCycler 480 Real-Time PCR System (Roche Diagnostics GmbH, Mannheim, Germany). Reverse transcription of the total RNA (600 ng) was performed using a High- Capacity cDNA Archive Kit (Applied Biosystems, Foster City,

CA, USA). To perform qRT-PCR, SYBR Premix Ex Taq (Takara Holding Inc., Kyoto, Japan) master mix was used. The primer sequences of the candidate genes are listed in Supplementary Table 1. The qRT-PCR data were analysed using the Livak method (2DDCt), and glyceraldehyde-3-phosphate dehydrogenase (Hs9999 9905_m1) served as the reference gene.

Protein expression analysis using Proteome Profiler Human XL Oncology Array Kit

Cells were cultured to approximately 80% confluence in T25 flasks and gently washed twice with 10 ml of ice-cold PBS. After adding 1 ml of RIPA Lysis and Extraction Buffer (Thermo Fisher Scientific Inc. Waltham, MA, USA) containing 20 µl of Halt™ Protease and Phosphatase Inhibitor Cocktail (Thermo Fisher Scientific Inc. Waltham, MA, USA) to each plate, a cell scraper was used to scrape the cells. Then, the cell lysates were transferred to a new microtubes, incubated on a rocking shaker for 30 minutes at 4°C, and centrifuged at 13,000 rpm for 30 minutes at 4°C. The supernatant was collected (avoiding the pellet) into new microtubes. The protein concentration was determined with a Quick Start™ Bradford Protein Assay (Bio-Rad Hungary Ltd., Budapest, Hungary) following the manufacturer's protocol.

A Proteome Profiler Human XL Oncology Array Kit (enable to analysis of the relative expression of 84 cancer-related proteins) was purchased from R&D Systems (Cat. ARY026, USA). The experiment was performed according to the manufacturer's protocol. Briefly, 200 µg of cell lysate was incubated with each array overnight at 4°C on a rocking platform shaker. On the following day, the cell lysates were removed, and the membranes were washed 3 times with wash buffer. After the arrays were incubated with a detection antibody cocktail for 1 hour at room temperature on a rocking platform shaker, the membranes were again washed 3 times with wash buffer. Then, 2 ml of streptavidin-HRP mix was added to each membrane, and the membranes were incubated for 30 minutes and washed 3 times. The labelled protein spots were visualized using Chemi Reagent Mix. The density of each duplicated spot was assessed using the ImageJ program (1.51a, NIH, Bethesda, MD, USA) and evaluated by subtracting the background. The density of the positive control was considered 100%.

Statistical analyses

SPSS 19.0 (SPSS Inc., Chicago, IL, USA) was used for statistical analysis. The Shapiro-Wilk test was used to evaluate the normality of the data. Spearman's correlation coefficient was calculated to correlate the array comparative genomic hybridization (aCGH) and qRT-PCR

data. To identify differentially expressed genes between conditions (parental-resistant, starved-not starved), we used the moderated t-test with the Benjamini-Hochberg FDR for multiple testing correction. A p-value less than 0.05 was considered statistically significant.

Results

Growth inhibitory effect of PLX4720 on BRAF^{V600E} mutant melanoma cell lines

To define the growth inhibitory effect of a BRAFi (PLX4720: a vemurafenib analogue), we treated two pairs of BRAF^{V600E} mutant cell lines (WM983A^{p1} and WM983B^{m1}, WM278^{p2} and WM1617^{m2}) with the drug at various concentrations (0, 5, 50, 500, 1000, 2000 and 5000 nM). A significant ($p < 0.001$) decrease in cell viability was observed following above 500 nM PLX4720 in all cells (**Figure 12**).

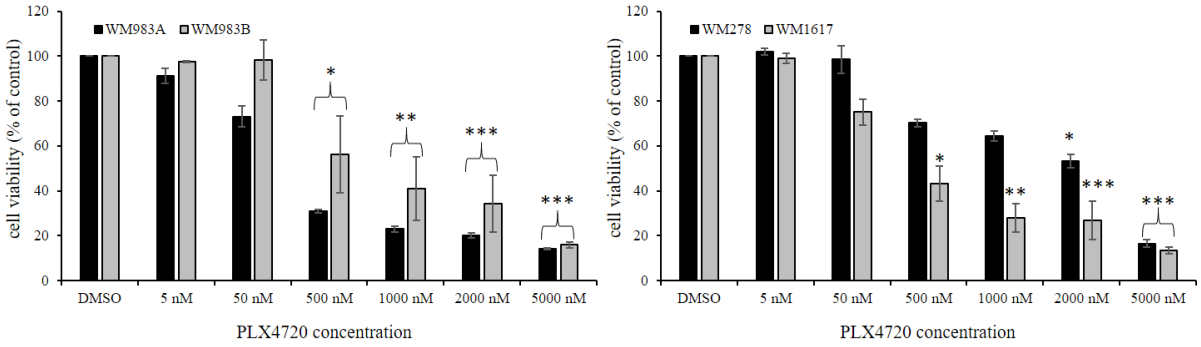

Figure 12. PLX4720 inhibits proliferation of melanoma cells in a dose-dependent manner. *Average viability of four BRAF^{V600E} mutant cell lines in response to PLX4720 treatment after 72 hours. Cell survival was measured using the WST1 assay. The data are presented as the mean ± SD of three independent experiment. Significant differences ($p \leq 0.05$*; $p \leq 0.01$**;$p \leq 0.001$***) were indicated by asterisks.*

Development and characterization of BRAF inhibitor resistant melanoma cell lines

To establish resistant cell line variants, cells were continuously treated with 5 μM PLX4720 for ~10 weeks and cultured until the surviving cells reached confluency. The morphology of the resistant cells differed from that of the original cells (**Figure 13)**. Three of the resistant cell lines exhibited elongated, fibroblast-like shape, only WM1617^{RES} was similar to the parental cell line. Through gene expression analyses, we observed upregulation of α5β1 integrin, snail, and miR21 and downregulation of E-cadherin, desmoplakin, and laminin α1 in the resistant cell lines, supporting the hypothesis that BRAFi resistance is associated with the epithelial-to-mesenchymal transition (EMT) phenotype [93] and increases the invasive potential of resistant melanoma cells [94], what we also found in our experiments.

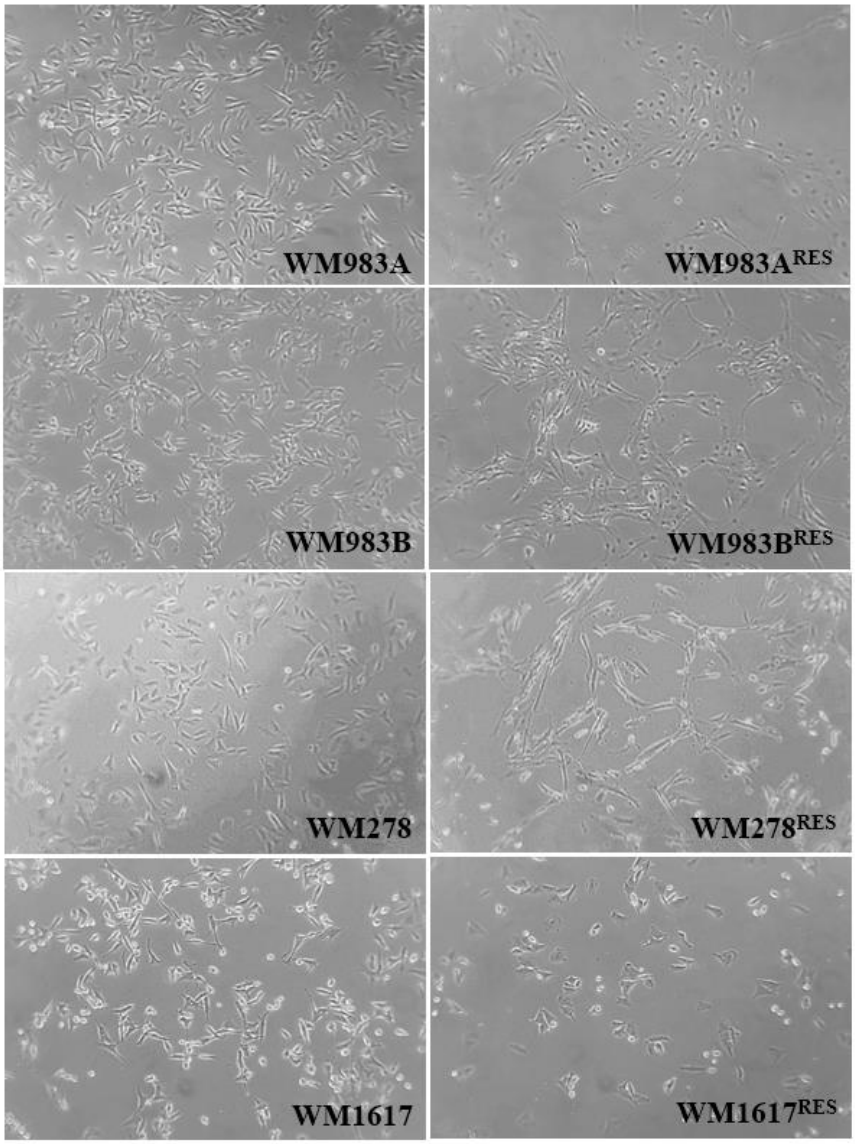

***Figure 13. Photomicrographs of the PLX4720 sensitive and resistant melanoma cell lines (100X magnification*).**

Effect of BRAFi withdrawal on the cellular growth of the resistant cell lines

The BRAFi resistant cell lines were cultured in the presence of 5 μM PLX4720 or the same volume of the solvent (DMSO (0.5%)). Withdrawal of PLX4720 from the cell cultures reduced cell proliferation in 3 resistant cell lines ($WM983A^{RES}$, $WM983B^{RES}$ and $WM1617^{RES}$), this observation is consistent with the hypothesis that resistant cells can develop drug dependency [20]. Intermittent dosing could take advantage of this phenomenon by both reducing side effects of the drug and prolonging progression-free survival in patients with advanced melanoma.

Interestingly, WM278^{RES} cells exhibited growth promotion after drug withdrawal when compared to the continuously PLX4720 treated cells (**Figure 14**).

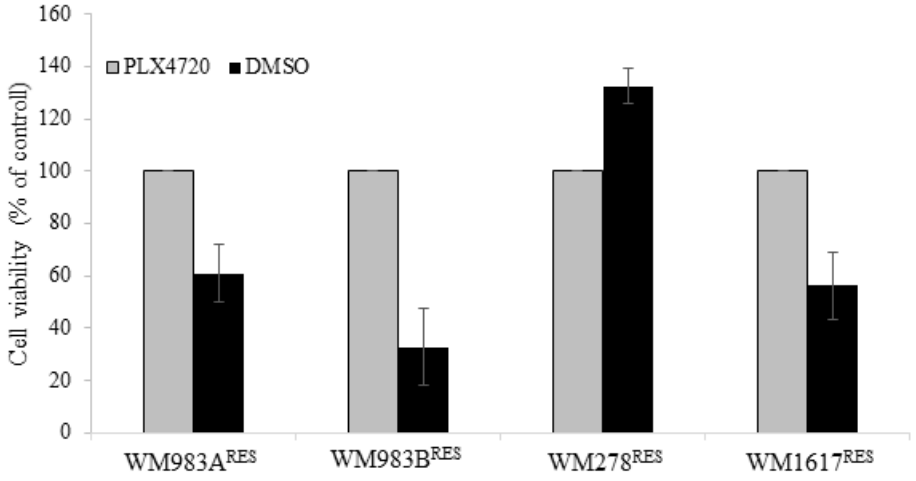

***Figure 14*. Effect of PLX4720 withdrawal on the resistant melanoma cell lines.** *The viability resistant cell lines after drug withdrawal (black columns) was compared to the cells grown in the presence of PLX4720 (grey columns). WM983A^{RES}, WM983B^{RES} and WM1617^{RES} cell lines showed decreased cell proliferation, while drug cessation resulted in increased cell proliferation in the WM278^{RES} cell line. The data are presented as the mean ± SD of three independent experiments.*

Invasive characteristics of the resistant cell line

To compare the invasive potential of the BRAFi sensitive and resistant cell lines, we performed a Matrigel invasion assay. The invasive properties of the sensitive cell lines were limited, the average number of invaded cells were between 0-1.8 (three independent experiments). In contrast, 3 of the four resistant cell lines (WM983A^{RES} WM983B^{RES} WM278^{RES}) the average number of the invaded cells were between 2.5-29,3. Neither the WM1617 nor the resistant pair of this cell lines (WM1617^{RES}) were invasive based on the Matrigel assay (**Table 3**). Notably, the WM1617^{RES} cell line did not exhibit the elongated, fibroblast-shaped phenotype observed in the other three invasive resistant cell lines. To further confirm that PLX4720 resistance is associated with melanoma cell phenotype switching behaviour, we determined the expression of two β-catenin co-factors (LEF1 and TCF4), both of which are phenotype specific. The β-catenin/LEF1 complex (high β-catenin expressing cells) is regulated by Wnt signalling and is preferentially expressed by cells with a proliferative phenotype, while TCF4 (low β-catenin expressing cells) is preferentially expressed by cells

with an invasive phenotype [95]. We found significant correlation between well-known invasion/proliferation markers (*TCF4* and *LEF1* genes) using qRT-PCR (R=0.854; p=0.007) [95].

Table 3. Single-cell invasiveness of melanoma cells by Matrigel invasion assay

Pair no.	Cell line	Avg. no. of invasive cells[1]	±SD[2]
1	WM983A	0.7	0.4
	WM983A^{RES}	29.3	14.6
2	WM983B	1.8	2.2
	WM983B^{RES}	2.5	2.6
3	WM278	0	0
	WM278^{RES}	7.1	7.9
4	WM1617	0	0
	WM1617^{RES}	0	0

[1]average of three independent experiments; [2]standard deviation

Copy number alterations in the BRAFi sensitive and resistant melanoma cell lines

Development of resistance is frequently associated with copy number alterations of different genes. In our study we performed array CGH analyses to define copy number changes during the development of BRAFi (PLX4720) resistance using Affymetrix CytoScan 750K array. We compared copy number alterations of the original and resistant cell lines. In overall, we found more CN in the resistant cell lines.

Copy number difference between the sensitive and resistant cell lines detected in all cell lines resistant to PLX4720 was found on a small part on chromosome 8q (**Figure 15**). This sequence contain the *EXT1* (8q24.11), *SAMD12* (8q24.12) and *REXO1L2P* (8q21.2) genes (**Figure 15A**). The copy numbers of the *EXT1* and *SAMD12* genes were elevated in all resistant cell lines (**Figure 15B**). In addition, we found increased copy number by aCGH on the 7q34 region in the WM1617^{RES} cell line, this sequence harbour the BRAF oncogene (**Figure 16**). All 8 cell lines contain *BRAF*^{V600E} mutation, but we have to note that this mutation is not detectable by aCGH. The EXT1 gene (exostosin glycosyltransferase 1) encodes a glycosyltransferase involved in heparan sulphate biosynthesis and has already been shown to play a role in cancer

progression [96-99]. The amplification of EXT1 has been reported to be associated with the aggressive behaviour of bone tumours [100]. More importantly, Manandhar et al. found that EXT1 regulates cancer cell stemness in doxorubicin-resistant breast cancer cells and promotes EMT-like behaviour, validating the gene as a tumour promoter and proposing its possible involvement in chemoresistance [101]. Both the increased CN and elevated mRNA level of the gene in all of our resistant cell lines strongly support the hypothesis that this gene plays an important role in BRAFi resistance in melanoma. Another CNA found in a resistant cell line ($WM1617^{RES}$) was the high-level amplification of the *BRAF* gene, which was associated with the increased mRNA level. *BRAF* amplification has already been shown to contribute to BRAF inhibitor resistance [55,102].

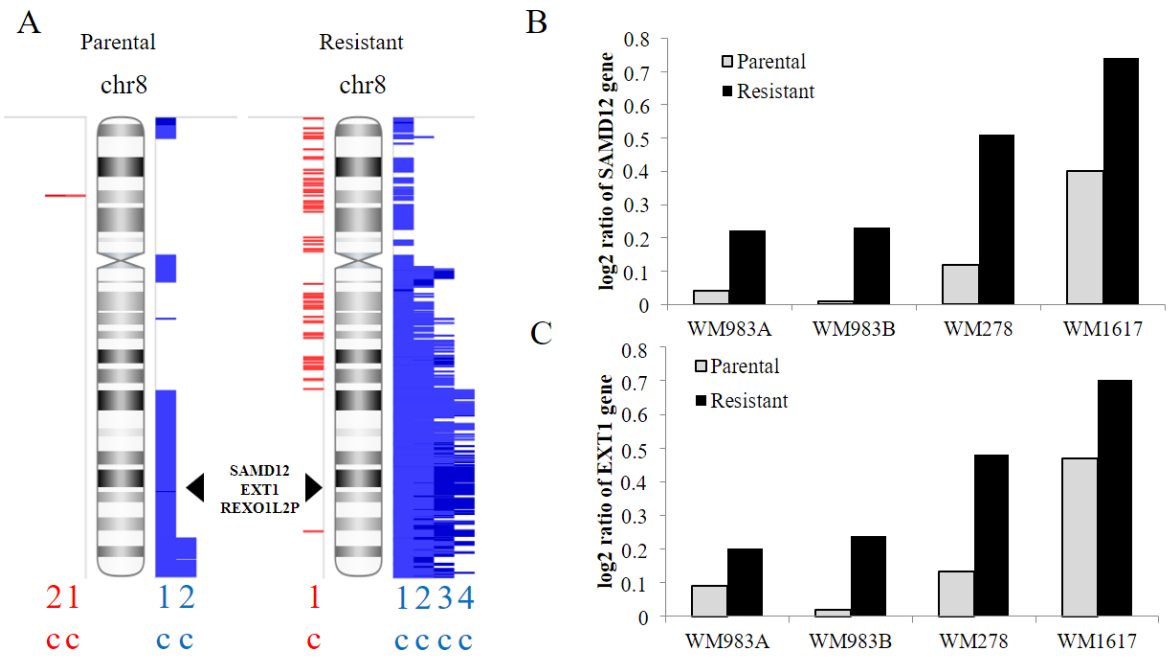

Figure 15. Copy number alterations on chromosome 8 in melanoma cell lines. *(A) Copy number changes uniquely detected in the resistant cell lines: columns 1–4 (indicated by "c") represent the pairs of parental cell lines (i.e. WM983A, WM983B, WM278 and WM1617) and the corresponding resistant cell lines. Red indicates CN losses and blue represents CN-gains. (B) Log2 ratio of the expression of the SAMD12 and(C) EXT1 genes in the parental cell lines and their PLX4720-resistant pairs.*

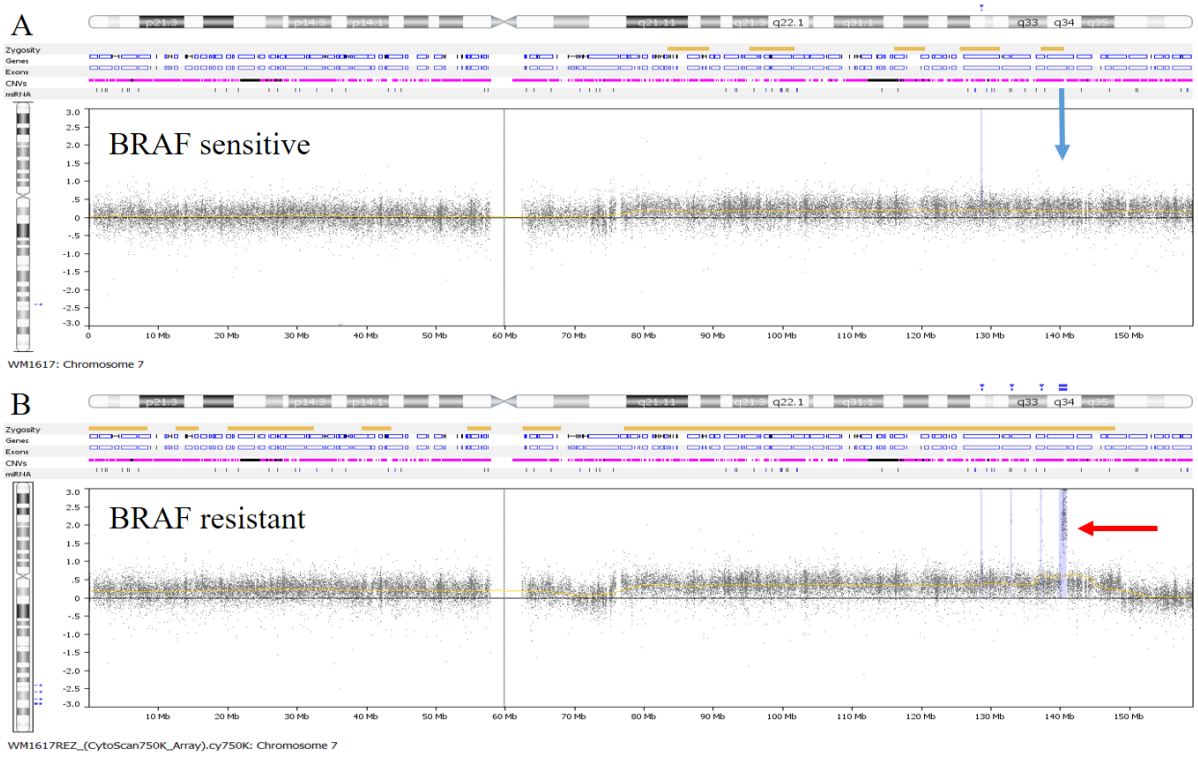

Figure 16. Copy number changes of chromosome 7 in WM167 melanoma cell lines. *(A) Sensitive and (B) the PLX4720 resistant WM1617^{RES} cell line. Red arrow indicates the localization of the amplified BRAF gene in the resistant WM1617 cell line. No alterations was observed in the sensitive cell line at this position (blue arrow) (Affymetrix CytoScan 750K microarray)*

Gene expression patterns of BRAFi sensitive and resistant cell lines

The gene expression patterns in the resistant cell lines were compared to the sensitive cells (Affymetrix Human Gene 1.0 microarrays). Using volcano plot filtering we found 1,903 differentially expressed genes in the established resistant cell lines (**Figure 17A**). Unsupervised hierarchical clustering of the differentially expressed genes could distinguish between the resistant and sensitive cell lines (**Figure 17B**). The number of unique genes with a > 2 fold change was 437, among these genes, 204 genes were upregulated and 233 downregulated in the resistant cell lines.

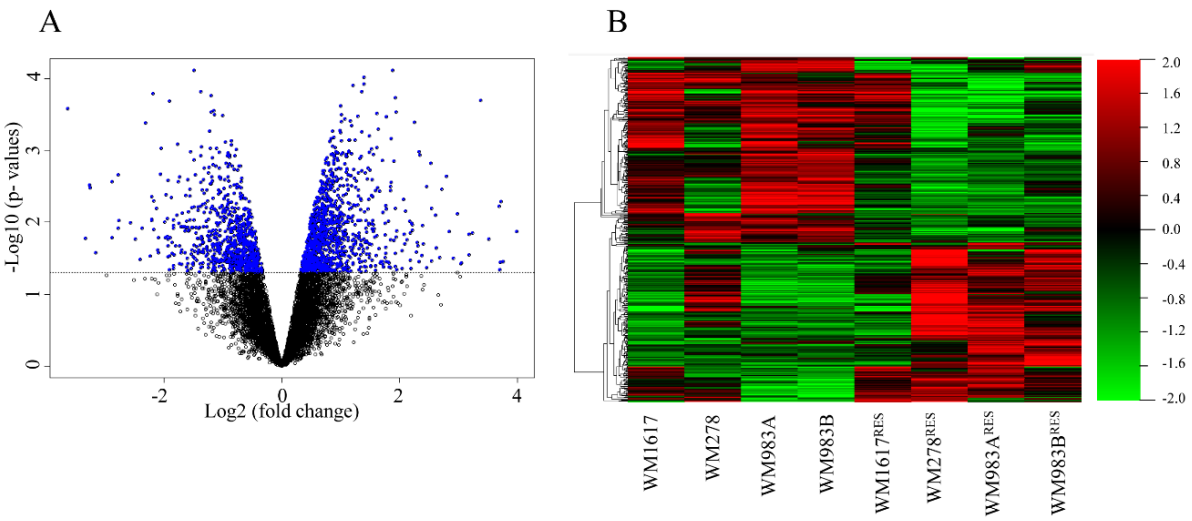

Figure 17. Gene expression patterns in the sensitive and resistant melanoma cell line pairs. *(A) Volcano plot analysis of 9,652 filtered unique genes. The blue dots represent significantly (paired t-test, p≤0.05) altered genes (1,903). (B) Unsupervised hierarchical clustering of 1,903 genes. The cell lines are displayed in columns, and genes are displayed in rows. The colour of each cell represents the median-adjusted expression value of each gene. Red indicates increased expression and green represents decreased expression relative to the median.*

Molecular functional characterization of the overexpressed genes are listed in **Table 4.** The overexpressed genes are associated with growth factors, growth factor receptors, the extra cellular matrix (ECM), integrins and cell adhesion molecules (**Figure 18**). These genes play important roles in 151 biological processes based on Gene Ontology (GO) classification, including angiogenesis, blood vessel development, cell migration and wound healing (**Supplementary Table 2)**.

Table 4. Significantly upregulated genes in resistant cell lines grouped by molecular function

ID	Name	P-value	Bonferroni	Genes included
GO:0008083	growth factor activity	2.02E-07	0.000161	*IL34, NRG1, INHB, BDNF, FGF2, FGF5, PDGFC, VEGFC, TGFB1, CSF2 DKK1, IL6*
GO:0005102	receptor binding	6.27E-07	0.000499	*IL34, NRG1, PDGFRB, INHBA, HLA-F ITGA5, BDNF, SLIT2, FAP, SRPX2, FBN1, CADM1, GRK3, FGF2, FGF5, C3, CCL5, PDGFC, VCAM1, VEGFC, RARB, WNT5A, LAMA3, ESM1, CAV1, AR, EDN1, TGFB1, THBS1, CSF2, DKK1, CYR61, STC2, SLIT3, SERPINE1, LRP1, LYN, ENG, IL6*
GO:0050840	extracellular matrix binding	1.97E-06	0.001565	*SLIT2, ADAMTS15, OLFML2B, NTN4, THBS1, CYR61, BCAM*
GO:0019838	growth factor binding	2.72E-06	0.002163	*CRIM1, PDGFRB, SRPX2, COL6A1, ESM1, TRIM16, THBS1, CYR61, OSMR, ENG*
GO:0070851	growth factor receptor binding	2.9E-06	0.002304	*PDGFRB, ITGA5, FGF2, FGF5, PDGFC, VEGFC, ESM1, CSF2, LYN, IL6*
GO:0005178	integrin binding	5.53E-06	0.004405	*NRG1, ITGA5, FAP, FBN1, VCAM1, ESM1, THBS1, CYR61, LYN*
GO:0050839	cell adhesion molecule binding	1.36E-05	0.01082	*NRG1, ITGA5, FAP, FBN1,CADM1, VCAM1,VCL, ESM1, THBS1, CYR61, LYN*

The significantly altered pathways involved at least 5 genes in the selected gene subset including the following: genes encoding the ECM and ECM-associated proteins; genes involved in the ECM organization; genes encoding ECM-associated proteins, including ECM-affiliated proteins, ECM regulators and secreted factors; genes involved in focal adhesion; genes encoding the core ECM, including ECM glycoproteins, collagens and proteoglycans; genes involved in non-integrin membrane ECM interactions; genes encoding secreted soluble factors; and genes involved in the TNF signalling pathway (**Figure 19,** see **details in Table S1**).

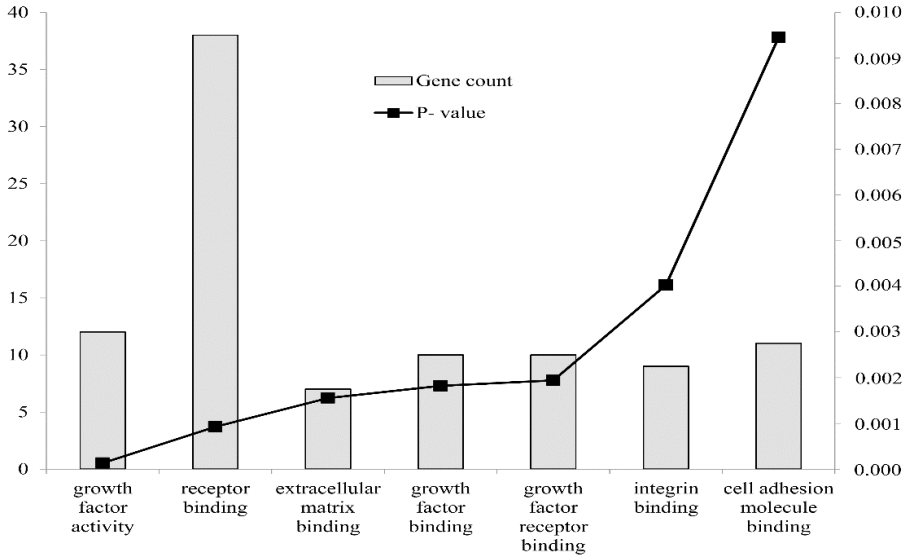

Figure 18. Molecular functional characterization of the significantly overexpressed genes (n=204) in the resistant cell lines compared to the sensitive cell lines based on GO classification*. Bonferroni correction was applied with a $p \leq 0.01$. Altered molecular pathways with at least 5 observations are displayed for the selected gene subset.*

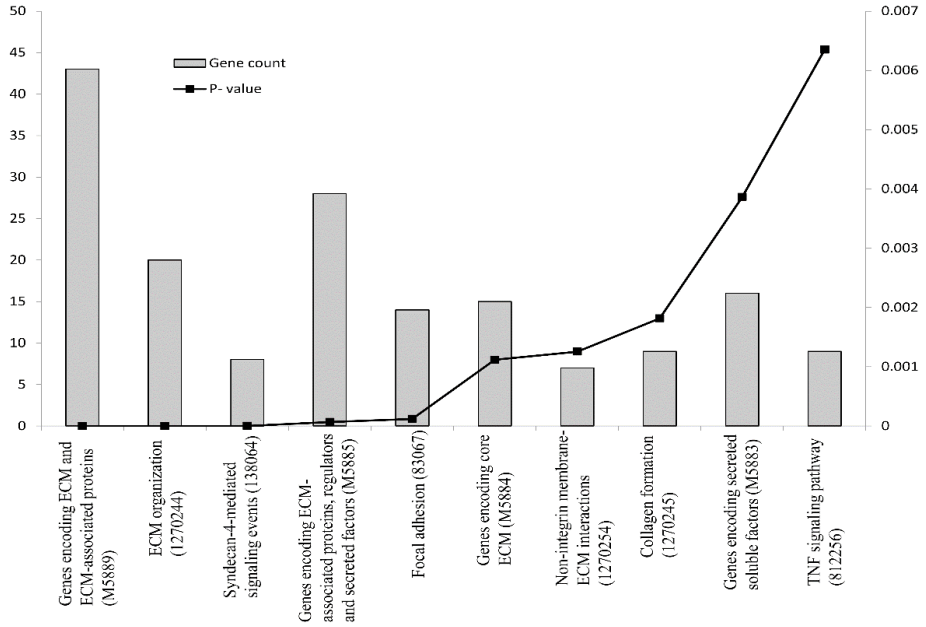

Figure 19. Pathway analysis of the significantly upregulated genes in the resistant cell lines. *Bonferroni correction was applied with a $p \leq 0.01$. Altered molecular pathways with at least 5 observations are displayed for the selected gene subset.*

Interestingly, the downregulated genes were not involved in any pathways or molecular functions, except for biological processes including developmental pigmentation, pigmentation, cellular lipid metabolic processes, melanocyte differentiation and lipid metabolic processes (**Table 5**). We performed qRT-PCR analysis to validate the relative gene expression level of five candidate genes (*PMEL*, *LOXL1*, *SERPINE1*, *EPHA2*, and *WNT5A*) and strong agreement was found between the microarray and qRT-PCR expression data, demonstrating high correlation among our datasets ($0.786 \leq R \geq 0.976$; $p \leq 0.05$).

Table 5. Significantly downregulated genes in resistant cell lines grouped by cellular processes

ID	Name	P-value	Bonferroni	Genes included (at least 5)
GO:0048066	developmental pigmentation	1.05E-08	3.69E-05	*MYO5A, TYRP1, HPS4, RAB27A, PMEL, MREG, SLC45A2, LRMDA, LEF1*
GO:0043473	pigmentation	3.46E-07	0.001221	*MYO5A, TYRP1, HPS4, RAB27A, RAB17, PMEL, MREG, SLC45A2, LRMDA, LEF1*
GO:0044255	cellular lipid metabolic process	6.29E-07	0.002219	*ERBB3, MBOAT1, MYO5A, BDH2, PLPPR5, GHR, ACSL3, TYRP1, FASN, GK, ST8SIA6, ST3GAL6, ST3GAL5, PLA1A, SMPDL3A, SCD, HPGD, RAB7A, PLA2G6, ALDH1A1, PIP4P2, PLSCR1, GPD2, PIK3R3, APOC1, APOD, IDI1, ST6GALNAC2, RLBP1, ASAH1, SDC3, PC*
GO:0030318	melanocyte differentiation	6.73E-07	0.002373	*MYO5A. TYRP1, HPS4, RAB27A, MREG, LRMDA*
GO:0006629	lipid metabolic process	1.17E-06	0.004112	*ERBB3, PDE3B, MBOAT1, MYO5A, ACAT2, BDH2, PLPPR5, GHR, ACSL3, TYRP1, FASN, GK, ST8SIA6, ST3GAL6, ST3GAL5, PLA1A, SMPDL3A, SCD, HPGD, RAB7A, PLA2G6, ALDH1A1, PIP4P2, PLSCR1, PNLIPRP3, GPD2, HSD17B7, PIK3R3, APOC1, APOD, IDI1, ST6GALNAC2, RLBP1, ASAH1, SDC3, PC, CYB5R2*

Protein array analysis of the BRAFi sensitive and resistant melanoma cell lines

To determine differences in the protein expression between the parental and resistant cell lines, we used a Proteome Profiler Human XL Oncology Array that includes 84 cancer-related proteins (**Figure 20**).

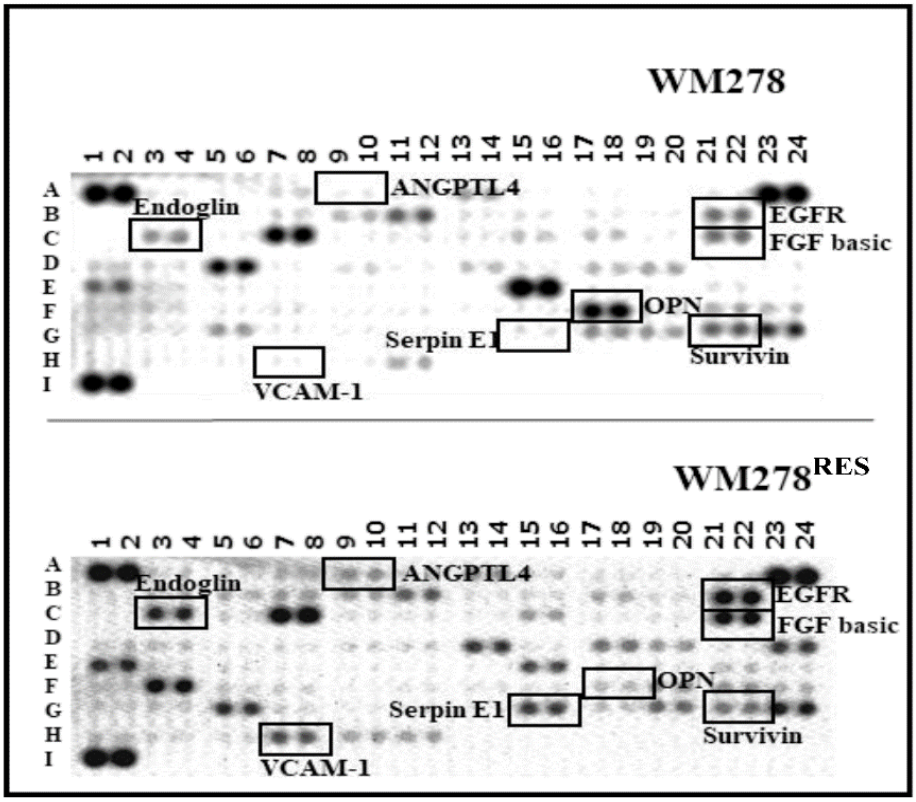

Figure 20. The Proteome Profiler Human XL Oncology Array membrane image. *The image is shown as an example for the WM278 and WM278RES cell lines. Black squared dots indicate the localisation and expression of the eight proteins which expressions changed universally in every resistant cell lines*

The list of the proteins are summarized in **Supplementary Table 3**. Numerous differentially expressed proteins were observed in the resistant cell lines compared to their sensitive counterparts. **Supplementary Figure 1** summarizes the proteins that were altered in the resistant cell lines. Importantly, the increased expression of six proteins (ANGPLT4, EGFR, Endoglin, FGF2, Serpin E1, and VCAM-1) and decreased expression of two proteins (OPN and Survivin) were consistently detected in all resistant cell lines (**Figure 21**).

ANGPTL4 (angiopoietin-like 4) plays a role in the development of chemoresistance and promotes tissue-specific metastasis to the brain in melanoma [103]. Recently, Liao and co-

workers demonstrated that EGFR overexpression can promote ANGPTL4-induced resistance and cancer cell migration and invasion in head and neck carcinoma [104]. Similar to our findings, simultaneously increased expression of SERPINE1, VCAM-1, and PDGFRβ has also been observed in a high EGFR subpopulation of melanoma cells [105,106]. The overexpression of these genes and proteins further elucidates that the migration behaviour of resistant cells is mediated by a syndecan-4-dependent mechanism, a pathway that is significantly altered in our resistant cell lines [107]. Additionally, our study is the first to reveal the increased expression of the VCAM-1 protein in PLX4720 resistant cells; furthermore, we found two proteins (Survivin and OPN) whose expression was significantly decreased in all four resistant cell lines. Similarly, Ji Z et al. found that melanoma cells treated with a BRAFi exhibited a dramatic reductions in the levels of Survivin (a major anti-apoptotic protein) [108].

One of the interesting findings of our study was that the expression of the OPN protein was decreased in all resistant cell lines. OPN has recently emerged as a potentially valuable biomarker for diagnosing and treating cancers [109]. This protein is involved in different physiological processes. It is overexpressed in several cancer types and has been clearly correlated with cell proliferation, migration, invasion and metastatic potential. Our findings are the first to suggest that decreased expression of OPN is clearly associated with acquired BRAFi resistance. We and others have previously described that increased levels of OPN are associated with malignant transformation and metastatic potential [110-112]. The unique role of OPN in resistance in leukaemia and breast cancer was also recently described [113]. The mRNA levels of the OPN isoforms are downregulated in leukaemic stem cells and these isoforms are thus assumed to be unique and useful molecular biomarkers associated with stem cell chemoresistance [114]. Other researchers have revealed that the expression of OPN can predict poor prognosis and cisplatin resistance in patients with advanced non-small cell lung cancer [114], and enhanced OPN expression has been observed in association with sorafenib resistance in human hepatoma cell lines [113]. Downregulation of OPN enhances the sensitivity of glioma U251 cells to temozolomide and cisplatin by targeting the NF-κB/Bcl-2 pathway [115]. On the other hand, it has recently been suggested that OPN may serve as a target to expand the number of patients who respond to immune checkpoint inhibitor therapy [116]. These data clearly show that OPN plays many different roles in cancer. The therapeutic potential of OPN targeting is still under intensive investigation, and future research is needed to elucidate the role of OPN in malignancies. No agents have yet advanced to the clinic. Based on our data, we propose that

decreased expression of OPN, which was detected in all resistant melanoma cell lines, may be unique, early marker of BRAFi resistance.

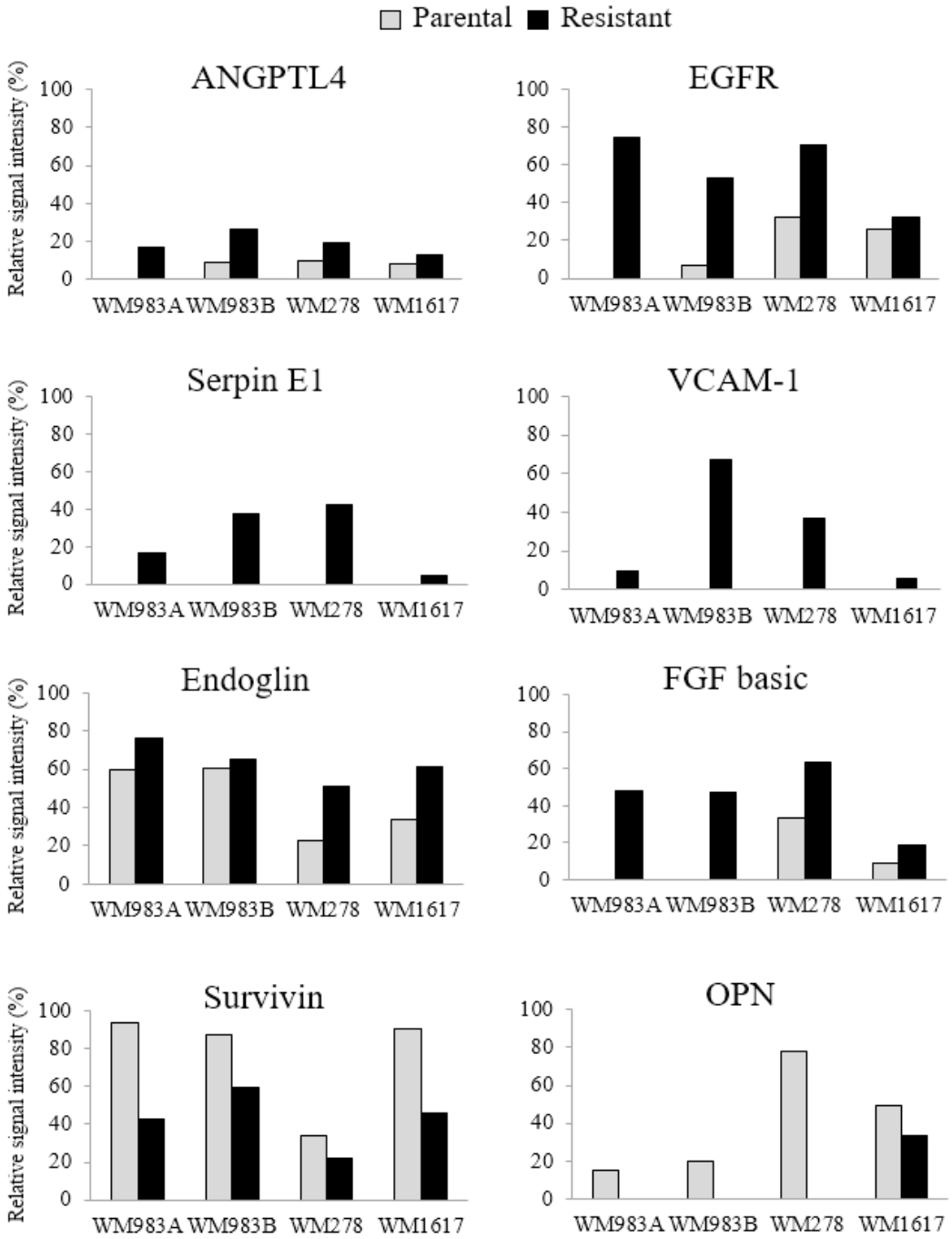

Figure 21. Relative e expression of proteins exclusively altered in all resistant cell lines. *The graph summarize the relative signal intensity of the indicated proteins. Increased expression of 6-(ANGPTL4, EGFR, SERPINE1, VCAM-1, ENDOGLIN, FGF2) and decreased expression of two proteins (Survivin and OPN) were detected in all resistant cell lines.*

Investigation the effect of HA15 (a new anti-melanoma drug) on BRAF^{V600E} mutated BRAFi sensitive and resistant melanoma cell lines

Control experiment: Effect of HA15 treatment on the viability of normal melanocytes

We first determined the effect of HA15 on normal human melanocytes using normal cell culture condition i.e. cells were cultured in the presence of 10% FBS. We used different concentrations of the drug and determined the viability of melanocytes using the WST-1 assay, viability of DMSO (solvent of the drug) treated cells were considered as 100% (**Figure 22**).

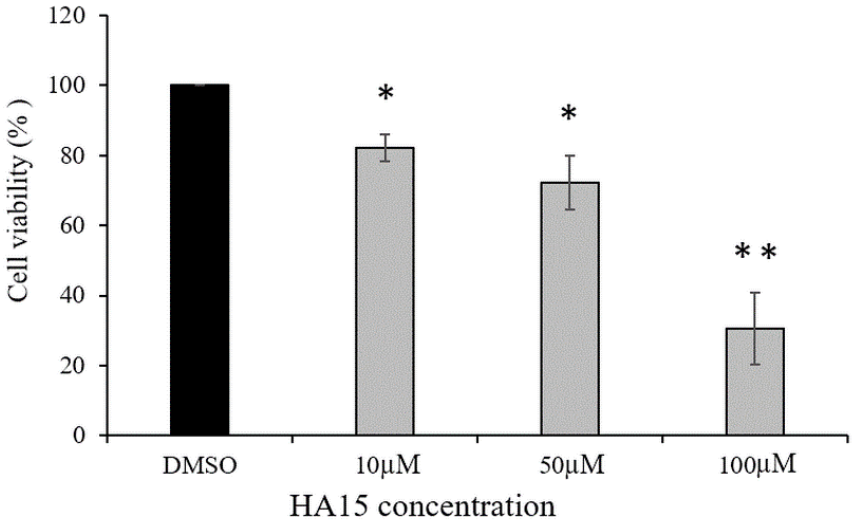

Figure 22. Viability of normal human melanocytes in response to increasing HA15 concentration under normal culture conditions after 48 hours of treatment. *DMSO (0.5%) is the solvent for HA15. The viability of cells was detected using the WST-1 assay. The data are presented as the mean ± SD of three independent experiments. Asterisks represent significant differences (* $p \leq 0.05$; ** $p \leq 0.01$).*

Our results clearly show that the viability of melanocytes decreased significantly ($p \leq 0.05$) even after low-dose HA15 (10 µM) treatment, and increasing the drug concentration up to 100 µM the cell viability further decreased under normal cell culture conditions ($p \leq 0.05$ and $p \leq 0.01$).

To simulate the cell culture conditions that were used by Cerezo et al. [13], melanocytes were cultured without FBS (altogether for 62 hours). After 14 hours starvation 10 µM HA15 was added and melanocytes were incubated for 48 hours (**Figure 23.** grey columns). Control cells were first starved for 14 hours and then cultured in the presence of 10% FBS and treated with

10 μM HA15 for 48 hours (**Figure 23.** black columns). In contrast to normal cell culture conditions, the viability of the starved melanocytes decreased below 60% without any drug, and adding 10 μM HA15 the cell viability decreased below 45% (**Figure 23**).

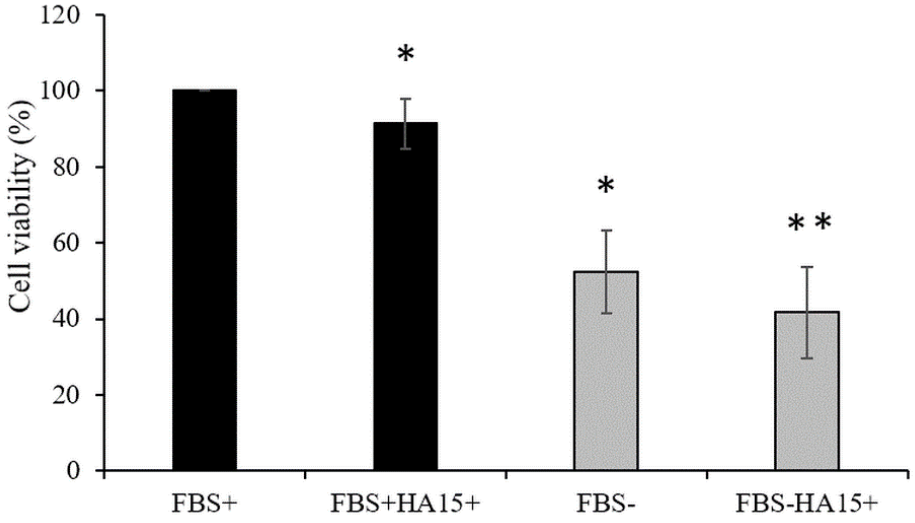

Figure 23. Viability of normal human melanocytes in response to 10 μM HA15 treatment. *First, cells were starved for 14 hours and then cultured under normal culture conditions (black columns: FBS+) or cultured without FBS (grey columns: FBS-) or treated with 10 μM HA15 (FBS+ HA15+ and FBS- HA15+) for 48 hours. Data are presented as the mean ± SD of three independent experiments. Asterisks represent significant differences (*p ≤ 0.05; ** p ≤ 0.01).*

Effect of HA15 treatment on the viability of melanoma cells

To investigate the effect of HA15 on *BRAF*^{V600E} mutant melanoma cell lines we used eight cell lines: four were sensitive for the PLX4720 BRAF inhibitor (WM983A and WM278 and originated from primary melanoma lesions and WM983B and WM1617 were developed from the metastases of the same patients, four – developed by us – were resistant for the BRAF inhibitor (WM983A^{BRAFiRES}, WM983B^{BRAFiRES}, WM278^{BRAFiRES}, WM1617^{BRAFiRES}). Similarly to Cerezo et al. published conditions, we also included the A375 melanoma cell line to compare our results to the published data [13].

During this experiment we cultured all melanoma cell lines under normal cell culture conditions and treated them with 10 μM HA15. The viability of the cell lines (WST-1 assay) was similar; however, the viability of two melanoma metastasis-originating cell lines (WM983B and WM1617) decreased below 70%. Interestingly, the viability of all four BRAF inhibitor-resistant cell lines was close to that of the control cells, at the same time the viability of the A375 cell line did not change at all (**Figure 24**).

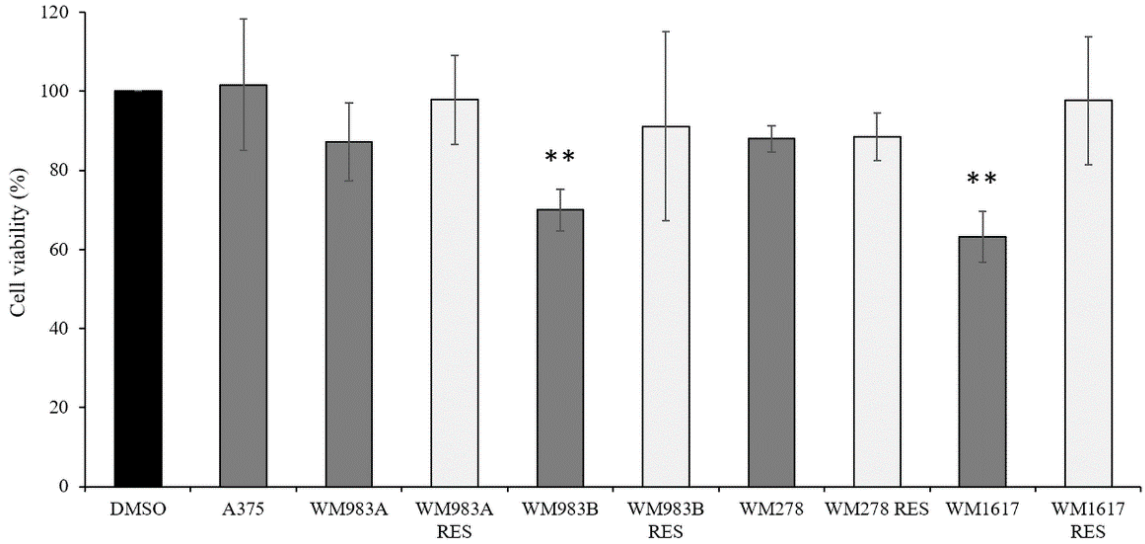

Figure 24. Cell viability of melanoma cell lines) and their BRAFi-resistant counterparts *(WM983A^{BRAFiRES}, WM983B^{BRAFiRES}, WM278^{BRAFiRES}, WM1617^{BRAFiRES}). All cell lines were treated with 10 µM HA15 for 48 hours in complete medium. Data represent the mean viability of three independent experiments (± SD). Significant differences are indicated by asterisks (**p ≤ 0.01.*

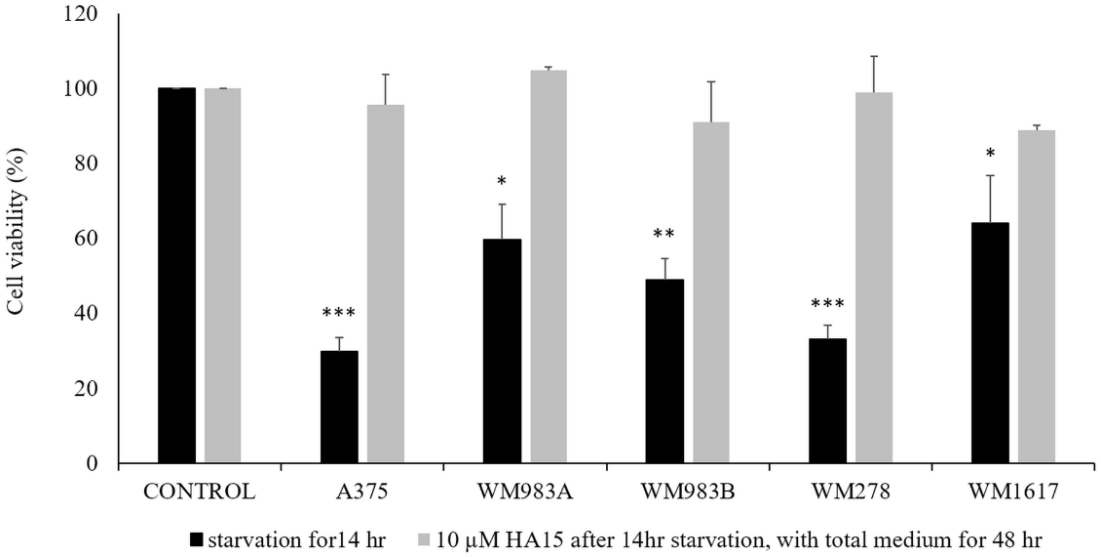

Figure 25. Cell viability of BRAF^{V600E}-mutant melanoma cell lines

*Cell lines were treated with 10 µM HA15 for 48 hours. Before drug treatment, the cells were starved for 14 hours (black columns); the medium was then replaced with complete medium containing 10 µM HA15, and cell viability was measured after 48 hours (grey columns) using the WST-1 assay. Data represent the mean viability of three independent experiments ± SD. Significant differences (*p ≤ 0.05; **p ≤ 0.01; ***p ≤ 0.001) are indicated by asterisk.*

In the second experimental arrangement, cell lines were starved for 14 hours before drug treatment. This condition resulted in a significant decrease in cell viability in all melanoma cell lines (**Figure**

25, black columns. however, if we replaced the medium with complete medium containing 10 µM HA15, we observed that the cells recovered completely after 48 hours (**Figure 25**, grey columns). This clearly shows that the viability of cells were significantly influenced by the starvation condition and the drug had no effect under this condition. Beside the viability of the melanoma cells. This observation was opposite to the published data. In order to strengthen our observations of the effect of HA15 on melanoma cells, we ordered the HA15 drug from another company and repeated the experiments using two BRAFi sensitive melanoma cell lines (WM983A and WM983B) using both compounds. The first drug was originated from Selleck Chemicals and the second one from MedChemExpress. Cell viability was measured after 48 hours different concentrations of HA15 were added to the cell cultures in complete medium.

The viability of cells were measured as described before, data are summarized on **Figure 26**. We observed that the viability of WM983A cells did not decrease significantly after 10 µM HA15 treatment for 48 hours but that WM983B cells were sensitive to both compounds, as we detected before.

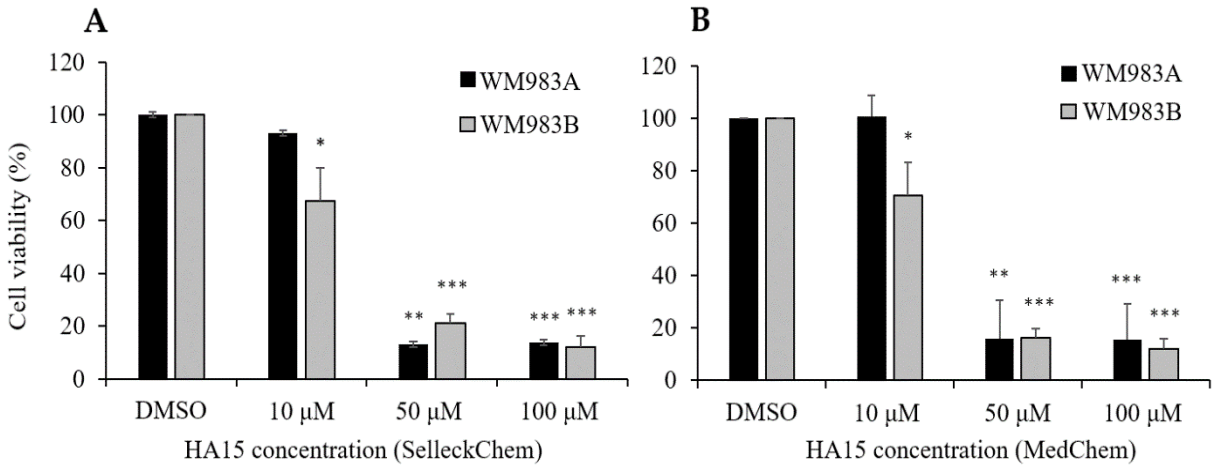

Figure 26. Viability of WM983A and WM983B cell lines after treatment with different concentrations of the drug. *Cells were cultured in complete medium and the viability was measured after 48 hours of drug treatment. HA15 was obtained from two different companies:* ***(A)*** *Sellect Chemicals* ***(B)*** *MedChemExpress. Data represent the mean viability of three independent experiments ± SD and expressed as percentages of the control. Asterisks indicate significant differences (*p < 0.05; **p < 0.01; ***p < 0.001).*

In summary, we observed the same effect for both compounds from different companies. A dramatic decrease in cell viability was observed only at 50 µM and 100 µM of HA15 independently from where the HA15 compound was originated from (**Figure 26 A and B**).

Effect of long-term starvation on A375 melanoma cell line viability

To investigate the effect of long-term starvation on cell viability (similar to the published cell culture conditions), A375 melanoma cells were cultures without FBS for 14 hours and then cultured with and without FBS for more 48 hours as well as with 10 µM HA15. Although the morphology of the cells was not influenced by drug treatment (**Figure 27a** and **27b**) under normal culture conditions, after 62 (14 hours + 48 hours starvation; grey column) hours of starvation, cell viability decreased significantly (**Figure 27c**). In contrast, 10 µM HA15 treatment of the starved A375 cells resulted in a tremendous decrease in cell viability, similar to the published data (Cerezo et al.) indicating that long-term starvation and HA15 treatment have synergistic effects on cell viability (**Figure 27d**).

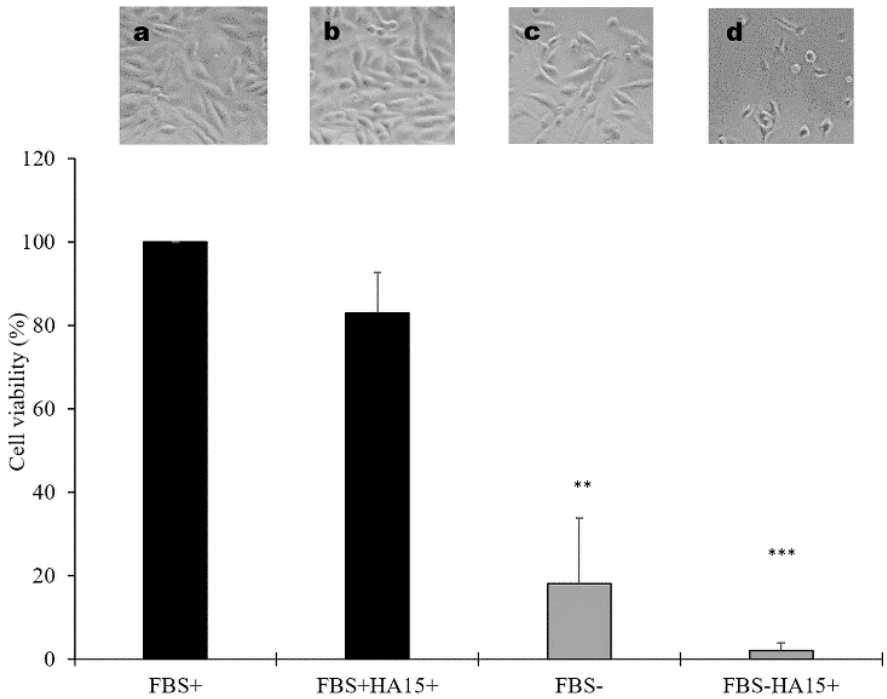

Figure 27. Viability of A375 cells under different cell culture conditions. *Before drug treatment, cells were cultured without FBS for 14 hours. Then, the cells were treated with 10 µM HA15 with (FBS+HA15+) or without FBS (FBS-HA15+) for 48 hours, and cell viability was determined. Images above the columns show the morphological changes in A375 melanoma cells under different cell culture conditions: (a) FBS+: cells grown in complete medium; (b) FBS+HA15+ complete medium and 10 µM HA15; (c) FBS- cells grown without FBS; (d) FBS-HA15+-starved cells treated with 10 µM HA15. Data are presented as the mean ± SD of three independent experiments. Significant differences are indicated by asterisks (**p < 0.01; ***p < 0.001).*

Effect of HA15 treatment on apoptosis induction in the WM983A melanoma cell line

Because HA15 concomitant induce apoptosis and autophagy [13], we determined the rate of the viable, apoptotic, dead and necrotic cells after HA15 treatment using the Annexin V-FITC apoptosis kit. The experimental conditions were as follows: WM983A melanoma cells were starved for 14 hours and then treated with various concentrations of HA15 (10 μM, 50 μM and 100 μM) for 48 hours. DMSO (control (0.5%)) was used as a control. Flow cytometric data are summarized in **Figure 28.** Based on the flow cytometric data, it is clear that HA15 treatment did not influence either cell viability nor the rate of apoptosis at 10 μM compared to DMSO-treated control cells. These data show that HA15 did not induce apoptosis at a concentration of 10 μM HA15 and did not affect viability. At the same time, higher concentrations of the drug clearly decreased viability (**Figure 26 and Table 6**).

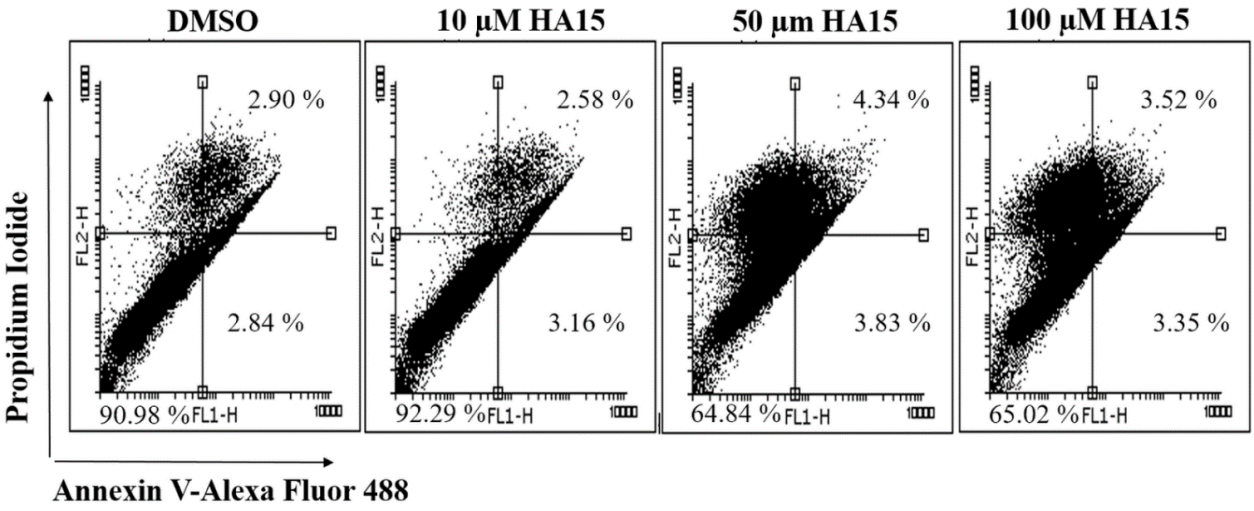

Figure 28. Scatter plots of WM983A melanoma cells after HA15 treatment using the Annexin V FITC/propidium iodide assay. *First, cells were starved for 14 hours, and the medium was replaced with complete medium containing 10 μM, 50 μM and 100 μM HA15. The cells were then incubated for 48 hours followed by staining with Annexin V-FITC/propidium iodide. The Annexin V-FITC-positive/PI-negative cells located in the lower right quadrant of the histogram represent early apoptotic cells; the Annexin V-FITC-positive/PI-positive cells in the upper right quadrant represent late apoptotic cells.*

Table 6. Summary of flow cytometric data of HA15 treated WM983A melanoma cells

	% of early and late apoptotic cells	% of viable cells
DMSO	5.74%;	90.98%
10 μM HA15	5.74 %	92.29%
50 μM **HA15**	8,17 %	64,84 %
100 μM **HA15**	6,87 %	65,02 %

Effect of serum withdrawal and HA15 treatment on stress marker expression in the A375 melanoma cell line

We also aimed to investigate the HA15 treatment induced ER stress under different experimental conditions at different time points in the A375 cell line, determining the gene expression level of three main stress markers (*CHOP*, *XBP1* and *BIP*) by qRT-PCR. First, the cells were starved for 14 hours and then, similar to the published data i.) further cultured without FBS, treated ii.) without FBS + 10 μM HA15 and iii.) with FBS + 10 μM HA15 for 24 and 48 hours [13]. The cells were harvested, and gene expressions of the three stress markers were determined (**Figure 29**).

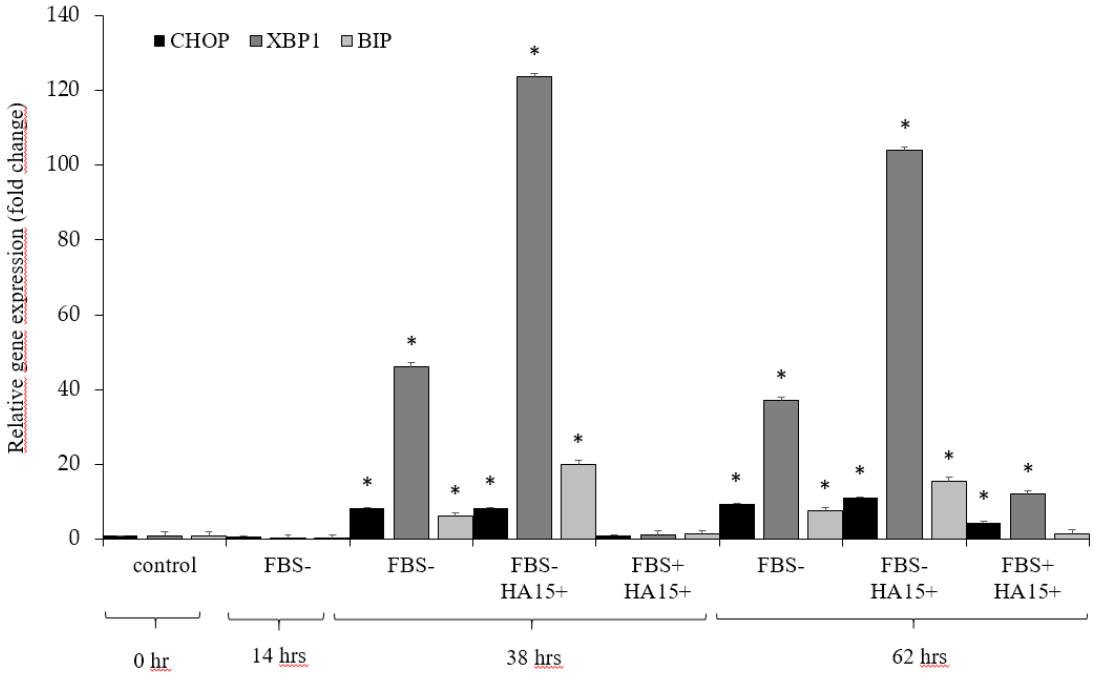

Figure 29. Relative gene expression patterns of stress markers in A375 melanoma cells under different culture conditions. *Cells were starved for 14 hours and then incubated as follows: without FBS (FBS-); without FBS or with 10 μM HA15 (FBS-HA15+); or with FBS and with 10 μM HA15 (FBS+HA15+) for 24 hours (14+24=38 hours) and 48 hours (14+48=62 hours). Significant differences are indicated by asterisks (*p ≤ 0.05).*

The relative gene expression of the three stress markers were similar to the control after 14 hours of drug withdrawal. However, after 38 hours, expression of the markers increased in the starved cells (without or with HA15 treatment: (FBS- and FBS-HA15+); in contrast to the cells grown under normal cell culture conditions (FBS+HA15+), only a slight increase was

observed at the end of the experiment (FBS+HA15+: 62 hours incubation). The highest relative expressions were observed for the XBP1 gene in the starved cells (almost 50x fold change: FBS-), and expression increased significantly after 38 hours in the presence of 10 μM HA15 (fold change ≥120x: FBS-HA15+) and was high at the endpoint.

Effect of serum withdrawal and HA15 treatment on gene expression of autophagy markers in the A375 melanoma cell line

To follow whether HA15 induces autophagy we choose four autophagy associated markers (*DRAM1, P62, ATG5* and *ATG7* [117]) and determined the gene expression levels after HA15 treatment under normal and starved cell culture conditions. We found that pre-starvation (FBS- for 14 hours) did not induce significant expression changes in these genes (**Figure 30**). After 38 hours of starvation, the expression level of all four genes increased (**Figure 30** FBS, 38 hours), the highest relative expression was measured for the *DRAM1* gene. When incubating the starved cells with 10 μM HA15 (FBS- and +10 μM HA15), the expression of two genes (*p62* and *ATG5*) increased significantly, at the same time notable expression changes of autophagy markers were not observed in cells grown in complete medium even after 48 hours of drug treatment. (**Figure 30:** last four columns).

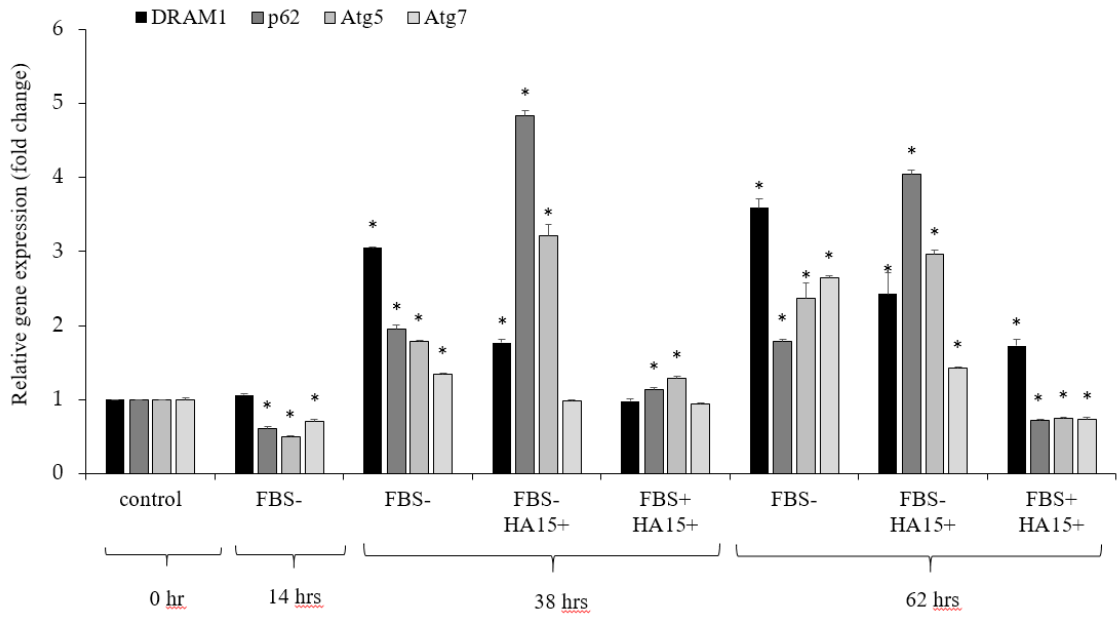

Figure 30. Relative gene expression patterns of autophagy markers in A375 cells. *Cells were starved for 14 hours and then incubated without FBS (FBS-), without FBS, with 10 μM HA15 (FBS-HA15+), with FBS or with 10 μM HA15 (FBS+HA15+) for an additional 48 hours. Gene expression was measured at the indicated time points. Significant differences are indicated by asterisks (*p ≤ 0.05).*

Overall, expression patterns of autophagy marker genes were similar in starved cells treated with HA15 at the time of 38 and 62 hours. In contrast, only *DRAM1* gene expression was elevated after HA15 treatment in cells growing in complete medium (FBS+HA15+, 62 hours).

Development and characterization of HA15-resistant melanoma cell lines

Because 10 μM HA15 treatment did not influenced the viability of melanoma cells significantly, we selected the most HA15-sensitive cell line (WM983B) to develop this drug resistant cell line and treated the cells continuously with 20 μM and 30 μM HA15 under normal cell culture conditions. After ~10 weeks, two resistant cell lines were developed: one resistant to 20 μM HA15 ($WM983B^{HA15RES20\mu M}$) and another was resistant to 30 μM HA15 ($WM983B^{HA15RES30\mu M}$) treatment. The viability of the resistant cells ($WM983B^{HA15RES30\mu M}$) was not affected by continuous HA15 treatment (30 μM HA15), except when concentration was increased to 50 μM. On the contrary, the parental WM983B cell line showed a significant decrease in viability at both concentrations (**Figure 31**).

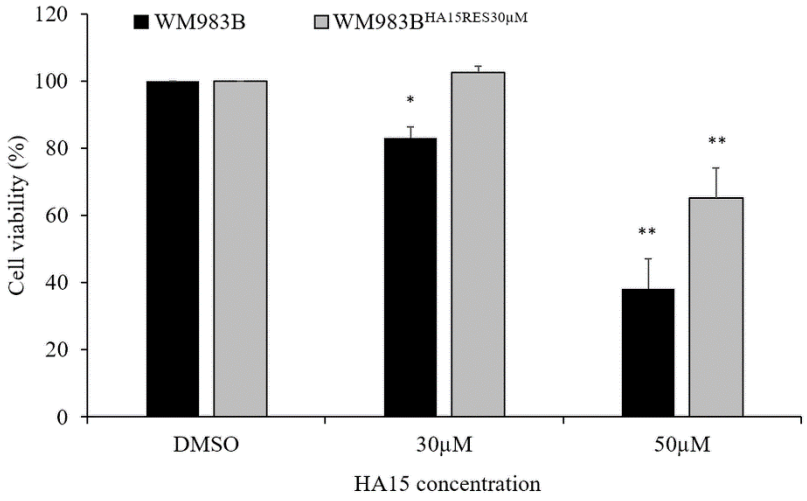

Figure 31. Viability of WM983B and WM983B$^{HA15RES30\mu M}$ melanoma cell lines.

*WM983B (black columns) and WM983B$^{HA15RES30\mu M}$ (grey columns) cell lines were treated with DMSO (0.5%), 30 μM and 50 μM HA15 under normal culture conditions. Cell viability was measured after 48 hours of drug treatment. Data are presented as the mean ± SD of three independent experiments. Significant differences are indicated by asterisks (*p ≤ 0.05; ** p ≤ 0.01).*

As HA15 targets the HSPA5/BiP protein (master regulator of the UPR), we determined the expression level of the *BiP* gene in the parental WM983B and in both resistant cell lines ($WM983B^{HA15RES20\mu M}$ and $WM983B^{HA15RES30\mu M}$). The HA15 resistant cell lines showed

significantly increased *BiP* gene expression compared to the parental WM983B cells (**Figure 32**).

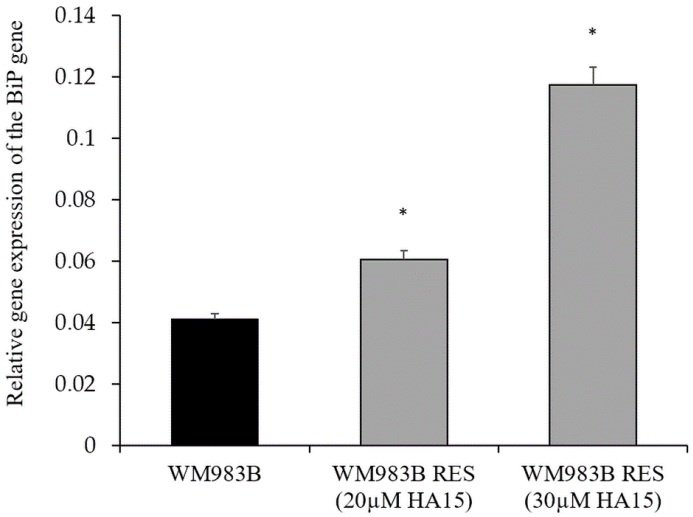

***Figure 32**. BIP gene expression of the WM983B^{HA15RES} cell line. Two HA15-resistant cell lines were developed by long-term HA15 treatment. The resistant cell lines (grey columns) showed increa-sed BiP gene expression compared to the parental cells (black column). Data are presented as the mean ± SD of three independent experiments. Asterisks indicate significant differences ($p \leq 0.05$).*

We also investigated how the resistant cells (WM983B^{HA15RES}) respond to the lack of HA15. During this experiment, we replaced the drug with DMSO and found that cell viability decreased and that the morphology of the cells changed (**Figure 33**). The morphological changes of the resistant cells indicates that the cells developed a drug-addiction phenotype, similar to BRAF inhibitor-resistant cell lines (**Figure 33. B and C**) [90].

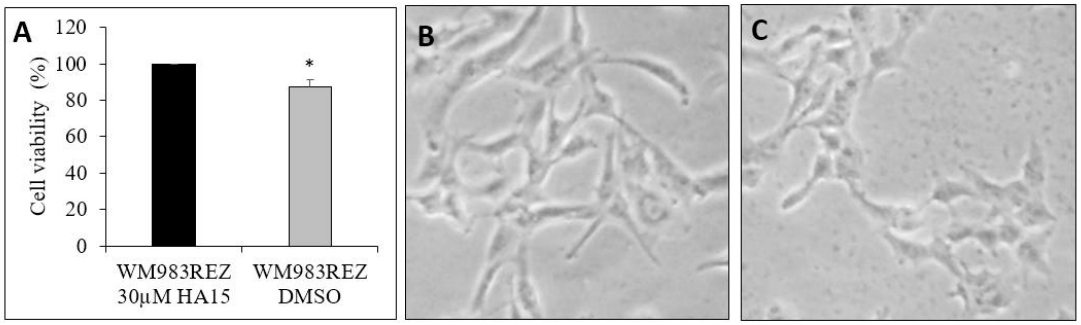

***Figure 33. The effect of HA15 withdrawal on the WM983B^{HA15RES}-resistant cell line. A.** Viability of the cells compared to cells grown in the presence of HA15 (black column) and after the withdrawal of the drug (grey column). The resistant cell lines were cultured in the presence of 30 µM HA15 or in the presence of the same volume of the solvent (DMSO (0.5%)). After 72 hours of drug withdrawal, the WM983B^{HA15RES} cells showed decreased cell proliferation. **B.** Photomicrographs of the WM983B^{HA15RES} cell line during continuous drug treatment and **C.** after 72 hours of drug withdrawal (100X magnification.). Significant differences are indicated by asterisks (*$p \leq 0.05$).*

Effect of starvation on gene expression in the WM983B melanoma cell line using RNA-Seq analysis

In the published manuscript during the characterization of the anti-cancer effect of HA15, Cerezo et al. used unusual experimental conditions, e.g., cells were starved for 14 hours before drug treatment [13] and we noticed during our study that the drug do not kill melanoma cells under normal cell culture condition, therefore we aimed to determine the gene expression signature of the starved cells and identify the differentially expressed genes of cells growing under normal culture conditions. Evaluating the RNA-Seq data, we found 6531 upregulated and 4890 downregulated transcripts in the WM983B melanoma cells growing under starved cell culture conditions. The highest expression difference was observed for the *RP11-134F2.8* gene (217-fold change), which encodes a novel DnaJ_C domain-containing protein. Another highly expressed gene was *RP11-618G20.1* (64-fold change), which encodes a long non-coding RNA associated with angiogenesis (http://angiogenes.unifrankfurt.de). Two starvation-related genes, *SLCO4C1* (32-fold change) and *PIK3IP1* (14-fold change), were also highly expressed in the starved WM983B cell population. We performed molecular functional characterization of the upregulated genes (at least 2-fold changes of 1807 genes), the genes were enriched in calcium ion binding, ion channel activity, and ion transmembrane transporter activity (**Table 7** and **Figure 34**).

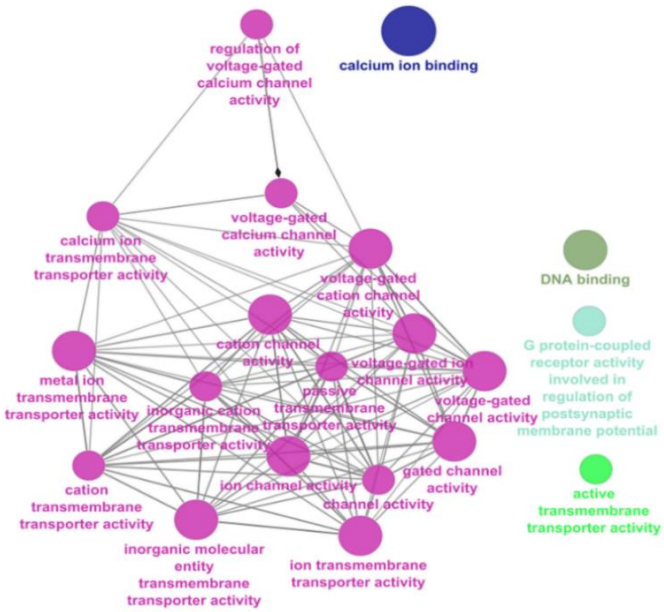

Figure 34. Upregulated genes in the WM983B melanoma cell line after 14 hours of starvation, as shown in a molecular functionally grouped network using the ClueGo (v. 2.3.5) tool kit of Cytoscape (www.cytoscape.org) software (v. 3.5.1).

Table 7: Molecular functional characterisation of the upregulated genes (6531 genes) in the WM983B melanoma cell line after 14 hours of FBS starvation

	Gene ID	Name	P-value	FDR B&H	FDR B&Y	Bonferroni	Genes from Input	Genes in Annotation
1.	GO:0005509	calcium ion binding	8.672E-12	1.383E-8	1.100E-7	1.383E-8	96	734
2.	GO:0005216	ion channel activity	4.644E-8	3.703E-5	2.945E-4	7.407E-5	77	641
3.	GO:0022857	transmembrane transporter activity	2.095E-7	8.968E-5	7.131E-4	3.342E-4	132	1340
4.	GO:0015318	inorganic molecular entity transmembrane transporter activity	2.249E-7	8.968E-5	7.131E-4	3.587E-4	112	1089
5.	GO:0022836	gated channel activity	3.733E-7	1.191E-4	9.469E-4	5.954E-4	61	491
6.	GO:0015075	ion transmembrane transporter activity	6.439E-7	1.712E-4	1.361E-3	1.027E-3	115	1150
7.	GO:0005261	cation channel activity	9.899E-7	2.050E-4	1.630E-3	1.579E-3	63	528
8.	GO:0015267	channel activity	1.095E-6	2.050E-4	1.630E-3	1.746E-3	78	705
9.	GO:0022803	passive transmembrane transporter activity	1.157E-6	2.050E-4	1.630E-3	1.845E-3	78	706
10.	GO:0022839	ion gated channel activity	1.554E-6	2.479E-4	1.971E-3	2.479E-3	58	478
11.	GO:0022832	voltage-gated channel activity	1.809E-6	2.623E-4	2.086E-3	2.885E-3	42	305
12.	GO:0005215	transporter activity	2.259E-6	3.002E-4	2.388E-3	3.603E-3	140	1505
13.	GO:0005244	voltage-gated ion channel activity	4.059E-6	4.980E-4	3.960E-3	6.474E-3	41	304
14.	GO:0022890	inorganic cation transmembrane transporter activity	5.608E-6	6.267E-4	4.984E-3	8.944E-3	87	847
15.	GO:0008324	cation transmembrane transporter activity	5.894E-6	6.267E-4	4.984E-3	9.401E-3	91	898
16.	GO:0046873	metal ion transmembrane transporter activity	1.225E-5	1.221E-3	9.710E-3	1.954E-2	68	630
17.	GO:0022843	voltage-gated cation channel activity	1.434E-5	1.346E-3	1.070E-2	2.288E-2	34	245

Pathways significantly associated with candidate genes in the WM983B melanoma cell line after 14 hours of FBS starvation are associated with plasma membrane structures and pathways

involved in cholesterol and steroid biosynthesis, calcium signalling pathways and activation of gene expression by SREBF pathways (ToppFun GO), as listed in **Table 8**.

Table 8: The significantly altered pathways in the WM983B melanoma cell line after 14 hours of FBS starvation

	ID	Name	Source	P-value	FDR B&H	FDR B&Y	Bonferroni	Genes from Input	Genes in Annotati
7.	M5889	Ensemble of genes encoding extracellular matrix and extracellular matrix-associated proteins	MSigDB C2 BIOCARTA (v7.1)	9.965E-8	1.390E-5	1.168E-4	2.501E-4	107	1026
24.	1270001	Metabolism of lipids and lipoproteins	BioSystems: REACTOME	8.309E-6	5.959E-4	5.008E-3	2.086E-2	83	816
21.	1269903	Transmembrane transport of small molecules	BioSystems: REACTOME	1.236E-6	9.697E-5	8.151E-4	3.103E-3	75	680
23.	M5884	Ensemble of genes encoding core extracellular matrix including ECM glycoproteins, collagens and proteoglycans	MSigDB C2 BIOCARTA (v7.1)	4.049E-6	2.989E-4	2.513E-3	1.016E-2	38	275
25.	83053	Neuroactive ligand-receptor interaction	BioSystems: KEGG	1.289E-5	8.988E-4	7.555E-3	3.236E-2	37	278
27.	M13380	Neuroactive ligand-receptor interaction	MSigDB C2 BIOCARTA (v7.1)	1.905E-5	1.258E-3	1.057E-2	4.781E-2	36	272
14.	83050	Calcium signaling pathway	BioSystems: KEGG	3.587E-7	3.547E-5	2.981E-4	9.002E-4	31	182
18.	M2890	Calcium signaling pathway	MSigDB C2 BIOCARTA (v7.1)	6.165E-7	5.336E-5	4.485E-4	1.547E-3	30	177
1.	1270037	Cholesterol biosynthesis	BioSystems: REACTOME	6.809E-13	1.709E-9	1.436E-8	1.709E-9	15	24
2.	142269	Superpathway of cholesterol biosynthesis	BioSystems: BIOCYC	1.603E-12	2.012E-9	1.691E-8	4.024E-9	15	25
19.	1270038	Regulation of cholesterol biosynthesis by SREBP (SREBF)	BioSystems: REACTOME	9.761E-7	8.166E-5	6.864E-4	2.450E-3	15	55
9.	1270039	Activation of gene expression by SREBF (SREBP)	BioSystems: REACTOME	1.435E-7	1.801E-5	1.514E-4	3.602E-4	14	42
3.	SMP00023	Steroid Biosynthesis	SMPDB	2.925E-11	2.447E-8	2.057E-7	7.341E-8	13	21
4.	PW:0000454	Cholesterol biosynthetic	Pathway Ontology	1.257E-9	4.732E-7	3.978E-6	3.155E-6	11	18
6.	82937	Steroid biosynthesis	BioSystems: KEGG	9.853E-8	1.390E-5	1.168E-4	2.473E-4	10	20
10.	M5872	Steroid biosynthesis	MSigDB C2 BIOCARTA (v7.1)	2.342E-7	2.473E-5	2.079E-4	5.878E-4	9	17
5.	P00014	Cholesterol biosynthesis	PantherDB	3.398E-8	5.331E-6	4.481E-5	8.529E-5	8	11
11.	142266	Cholesterol biosynthesis II (via 24,25-dihydrolanosterol)	BioSystems: BIOCYC	2.365E-7	2.473E-5	2.079E-4	5.935E-4	8	13
12.	142267	Cholesterol biosynthesis I	BioSystems: BIOCYC	2.365E-7	2.473E-5	2.079E-4	5.935E-4	8	13
13.	142268	Cholesterol biosynthesis III (via desmosterol)	BioSystems: BIOCYC	2.365E-7	2.473E-5	2.079E-4	5.935E-4	8	13
8.	PW:0000248	Steroid biosynthetic	Pathway Ontology	1.256E-7	1.659E-5	1.394E-4	3.152E-4	7	9
15.	MAP00100 Sterol biosynthesis	MAP00100 Sterol biosynthesis	GenMAPP	3.957E-7	3.547E-5	2.981E-4	9.931E-4	7	10
16.	413387	C5 isoprenoid biosynthesis, mevalonate pathway	BioSystems: KEGG	3.957E-7	3.547E-5	2.981E-4	9.931E-4	7	10
17.	142207	Mevalonate pathway	BioSystems: BIOCYC	3.957E-7	3.547E-5	2.981E-4	9.931E-4	7	10
20.	413390	Cholesterol biosynthesis, squalene 2,3-epoxide => cholesterol	BioSystems: KEGG	1.029E-6	8.328E-5	7.000E-4	2.582E-3	7	11

Identification of differentially expressed genes in HA15-resistant melanoma cell lines using RNA-Seq analysis

We are the first to successfully establish HA15 drug resistant melanoma cell lines (*WM983B*^{HA15RES}), which was not particularly difficult because the cell lines were not very sensitive to 10 μM HA15 treatment under normal cell culture conditions. However, when the drug concentration was increased to 20 M and 30 μM the viability of cells decreased, but after a few weeks, the cells were able to cope with the increased amount of HA15 and became a stable resistant cell line. To define gene expression alterations associated with the HA15-resistant phenotype, we performed RNA-Seq analysis on the newly developed resistant melanoma cell line and compared the gene expression signature to that of the original WM983 cell line. Gene Ontology analysis revealed that 2,964 of the upregulated genes in the resistant cells are mainly involved in DNA binding, transcription factor activity, and ion channel/transporter activities (**Table 9**).Table 9: Groups of the upregulated genes by molecular function in the WM983BHA15RES melanoma cell line using ToppFun Gene Ontology

	ID	Name	P-value	FDR B&H	FDR B&Y	Bonferroni	Genes from Input	Genes in Annotation
1.	GO:0000981	DNA-binding transcription factor activity, RNA polymerase II-specific	2.425E-7	2.581E-4	2.119E-3	5.002E-4	245	1615
2.	GO:0004713	protein tyrosine kinase activity	2.502E-7	2.581E-4	2.119E-3	5.161E-4	54	237
3.	GO:0046873	metal ion transmembrane transporter activity	4.297E-7	2.909E-4	2.388E-3	8.864E-4	112	630
4.	GO:0005261	cation channel activity	5.640E-7	2.909E-4	2.388E-3	1.164E-3	97	528
5.	GO:0022890	inorganic cation transmembrane transporter activity	2.034E-6	8.394E-4	6.891E-3	4.197E-3	139	847
6.	GO:0005216	ion channel activity	3.080E-6	1.059E-3	8.695E-3	6.355E-3	110	641
7.	GO:0022836	gated channel activity	5.259E-6	1.550E-3	1.272E-2	1.085E-2	88	491
8.	GO:0008324	cation transmembrane transporter activity	7.606E-6	1.961E-3	1.610E-2	1.569E-2	143	898
9.	GO:0022839	ion gated channel activity	1.031E-5	2.322E-3	1.906E-2	2.127E-2	85	478
10.	GO:0015318	inorganic molecular entity transmembrane transporter activity	1.231E-5	2.322E-3	1.906E-2	2.540E-2	167	1089
11.	GO:0015267	channel activity	1.265E-5	2.322E-3	1.906E-2	2.609E-2	116	705
12.	GO:0022803	passive transmembrane transporter activity	1.351E-5	2.322E-3	1.906E-2	2.786E-2	116	706
13.	GO:0005244	voltage-gated ion channel activity	1.718E-5	2.726E-3	2.238E-2	3.543E-2	59	304
14.	GO:0022832	voltage-gated channel activity	1.901E-5	2.802E-3	2.300E-2	3.922E-2	59	305

The 2,802 downregulated genes are related to the extracellular matrix, integrin, collagen, microtubule, DNA replication origin binding and DNA helicase activity and are involved in the cell cycle, mitotic prometaphase, resolution of sister chromatid cohesion and DNA strand elongation pathways (**Table 10**).

Table 10: Groups of the downregulated genes by molecular functions in the WM983BHA15RES melanoma cell line using ToppFun Gene Ontology.

	ID	Name	P-value	FDR B&H	FDR B&Y	Bonferroni	Genes from Input	Genes in Annotation
1.	GO:0005201	extracellular matrix structural constituent	5.652E-9	1.195E-5	9.843E-5	1.195E-5	47	178
2.	GO:0050840	extracellular matrix binding	8.101E-8	8.566E-5	7.054E-4	1.713E-4	23	63
3.	GO:0008301	DNA binding, bending	5.514E-7	2.796E-4	2.303E-3	1.166E-3	52	236
4.	GO:0005178	integrin binding	6.930E-7	2.796E-4	2.303E-3	1.466E-3	37	146
5.	GO:0005518	collagen binding	7.053E-7	2.796E-4	2.303E-3	1.492E-3	25	80
6.	GO:0003688	DNA replication origin binding	7.933E-7	2.796E-4	2.303E-3	1.678E-3	13	26
7.	GO:0008092	cytoskeletal protein binding	3.162E-6	9.553E-4	7.866E-3	6.687E-3	163	1061
8.	GO:0042802	identical protein binding	4.334E-6	1.146E-3	9.435E-3	9.166E-3	279	1997
9.	GO:0005539	glycosaminoglycan binding	1.020E-5	2.398E-3	1.974E-2	2.158E-2	50	246
10.	GO:0008017	microtubule binding	1.234E-5	2.516E-3	2.072E-2	2.609E-2	56	288
11.	GO:0003678	DNA helicase activity	1.309E-5	2.516E-3	2.072E-2	2.768E-2	24	87
12.	GO:0008094	DNA-dependent ATPase activity	2.021E-5	3.562E-3	2.933E-2	4.274E-2	30	124

We summarized the top 50 overexpressed genes in the HA15 resistant *WM983B^{HA15RES}* melanoma cell line in **Supplementary Table 4**. The highest expression was detected for the protein-coding gene *PAPPA2 (*Pappalysin 2*),* and several highly expressed genes on the list are specifically linked to drug resistance, such as *ABCC9* and *IL13RA2*.

Using ***gene set enrichment analysis*** (GSEA) depicting the hallmark gene set, we found that INTERFERON_ALPHA_RESPONSE, HYPOXIA, GLYCOLYSIS, KRAS_SIGNALING_UP, TNFA_SIGNALING_VIA_NFKB, and P53_PATHWAY gene sets correlated positively with the HA15-resistant phenotype (**Supplementary Figure 2**).

Discussion

Cutaneous melanoma is an aggressive, therapy-resistant skin cancer that develops from melanocytes originating from a highly migratory embryonic cell population [23] In addition, it has been observed as having one of the highest metastatic potentials among human cancers [118].

The discovery of mutations of the *BRAF* in different types of human malignancies has given fast improvement to the development of targeted therapies [35]. The highest frequency of *BRAF* mutations (especially $BRAF^{V600E}$) is found in malignant melanoma, this mutation constitutes a therapeutic target for patients with advanced and metastatic tumours [35]. Since the discovery of the $BRAF^{V600E}$ mutation the number of new drugs has expanded dramatically, including effective inhibitors of the MAPK pathway and antibodies targeting immune checkpoint inhibitor molecules, including cytotoxic T-lymphocyte-associated antigen 4 (CTLA-4), programmed cell death (PD)-1, and PD-ligand1 (PD-L1) [119]. These improvements have greatly increased the prognosis of patients with advanced melanoma; unfortunately, resistance to most of the drugs limits the number of patients with long-lasting responses. A large number of investigations have focused on identifying the molecular background of resistance, but regrettably, the leading mechanisms of resistance remain unclear [120]. Identification of a common vulnerability target in melanoma cells is an urgent need and will help to discover more effective treatments of melanoma [13], therefore, to test all promising treatment options is crucial.

Targeted inhibition of the mutant BRAF (BRAFmt) protein is one of the most promising therapeutic approaches for patients with unresectable or metastatic melanoma since 2011 [121]. Despite the 6-8 month median progression-free survival, unfortunately most patients develop resistance and the tumor re-growth [122]. Even though the mechanism of resistance has been extensively studied, the molecular mechanism of acquired resistance remains unclear. Acquired resistance has been found to be driven by hyperactivated signal transduction pathways, such as reactivated IGF1R/PI3K/AKT and MAPK pathways and pathways involving mutation of *PTEN* and *NRAS*, amplification of $BRAF^{V600E}$ and aberrant splicing of $BRAF^{V600E}$ [46][54,55].

The novelty of our study is that we developed BRAFi-resistant primary and BRAFi-resistant metastatic melanoma cell lines originated from the same patients and analysed the alterations

that arose during the development of drug resistance. Using a Proteome Profiler Human XL Oncology Array, we detected distinct protein signatures associated with acquired BRAFi resistance. During our aCGH experiment, we detected new BRAFi resistance-associated CNAs that were characteristic of all resistant cell lines. We also observed that in addition to developing drug resistance, melanoma cells developed BRAFi dependence. During the establishment of the resistant cells, we observed that the morphology of the cells was different from that of the parental cells. Three of the four resistant cell lines were more invasive than the original, sensitive cell lines. Melanoma and other types of tumour cells are known to display the EMT phenotype, which is adopted by cancer cells and is associated with increased invasiveness, increased production of ECM components and metastasis formation [93,94]. We demonstrated that all sensitive (parental) cell lines and one non-invasive resistant cell line ($WM1617^{RES}$) had increased *LEF1* and decreased *TCF4* expression, while the three PLX4720-resistant cell lines displayed opposite gene expression patterns for both genes. From a clinical perspective, drug dependency is an extremely important feature to consider during treatment. Das Thakur et al. observed that the cessation of drug administration leads to a regression of established drug-resistant tumours [123]. Additionally, several clinical observations suggest that intermittent BRAFi treatment might be associated with prolonged survival in $BRAF^{V600E}$ mutant melanoma patients [124,125]. In our study, withdrawal of PLX4720 resulted in decreased cell proliferation in resistant cell lines, except for the WM278RES cell line. On the one hand, this finding is consistent with the hypothesis that resistant cells can develop drug dependency, which has high clinical relevance [126]. In a recent research it was tested whether intermittent combination therapy using BRAF and MEK inhibitors (dabrafenib+ trametinib) significantly improved progression free survival (PFS) compared to standard continuous dosing of these agents. Unfortunately it was found that - contrary to the initial hypothesis-, continuous dosing yielded a statistically significant increase in PFS compared to intermittent dosing (9.0 months vs 5.5 months ;$p = 0.064$, pre-specified two-sided $\alpha = 0.2$) [127]. This means that more research is needed to clarify the use of the different dosing methods.

Using aCGH we found new genomic alterations altered in all resistant cell lines on chromosomes 8q24.11-q24.12 (*EXT1* and *SAMD12*) and 8q21.2 (*REXO1L2P* gene), and all three genes exhibited elevated CNs.

Transcriptome analysis of the resistant cell lines revealed well-known markers of drug resistance, including *PDGFRβ*, *EGFR* and *WNT5A* [46,128], consistent with the data reported by Shaffer et al. [106]. Based on our gene expression results, most genes upregulated in the resistant cell lines were involved in cell motility and angiogenesis and were enriched in the ECM, Syndecan-4 and TNF signalling pathways. In contrast, the downregulated genes were not related to any pathways; however, these genes (e.g. *MLANA*, *PMEL* and *TYRP1*) were responsible for pigmentation and melanocyte differentiation other specific features of the resistant cell lines [106,129].

To identify specific protein expression patterns in cancer-related proteins associated with acquired BRAFi resistance, we used a Proteome Profiler Human XL Oncology Array to enable analysis of the relative expression of 84 cancer-related proteins in all the cell lines. We found several differentially expressed proteins between the resistant and sensitive cell lines; however, more importantly, we observed that eight proteins (ANGPTL4, EGFR, ENDOGLIN, FGF2, SERPINE1, VCAM-1, Survivin and OPN) were differentially expressed in all resistant cell lines compared to the parental/sensitive lines. The increased expression of several genes, including *EGFR, ANGPTL4* and *ENDOGLIN* (*CD105*), has been reported to be associated with hyperactivation of the TGF-β signalling pathway in resistant cell lines [104,126,130].

Beside the encouraging results which were obtained by different BRAF (vemurafenib, dabrafenib, encorafenib etc.) and MEK/ERK inhibitors other drugs were also developed in order to avoid the development of drug resistance. Therefore it is very important to test all promising treatment options in melanoma cells. Cerezo et al. developed and tested a family of molecules (thiazolidinedione) and described the one of the compound, named HA15, which has high anti-cancer effect. They described that target of HA15 is the chaperone BiP/GRP78/HSPA5 and described that the interaction increases ER stress, leading to melanoma cell death by concomitant induction of autophagic and apoptotic mechanisms [13](Cerezo and manag cikk).

HA15 was effective in melanoma cells regardless of whether the cells were sensitive or resistant to BRAF inhibitors, whereas no toxicity was observed in normal cells. HA15-induced cancer cell death is mediated by concomitant induction of autophagy and apoptosis, both of which are the consequence of a rapid initiation of ER stress [13]. Although the anti-cancerous effects of HA15 was well detailed by Cerezo et al., we noticed that the drug treatment conditions for the

melanoma cell lines were not optimal [13]. To investigate the effect and to define the molecular target of HA15, during each experiment, Cerezo et al kept the cells under starvation conditions (cell culture without serum) for 14 hours before drug stimulation [13]. Because this is not truly a physiological condition, our aim was to investigate the effect of HA15 under normal (complete medium) and starvation culture conditions at different drug concentrations. In addition, we determined the expression of stress (*CHOP, XBP1* and *BIP*) and autophagy (*DRAM1, P62, ATG5* and *ATG7*) marker genes; furthermore, we successfully developed an HA15-resistant melanoma cell line. We found that under normal culture conditions, 10 μM HA15 had only a moderate effect on two of the 10 cell lines, including the A375 melanoma cell line used by Cerezo et al. [13]. Eight of our cell lines (including 4 BRAF inhibitor-resistant lines) were not sensitive to 10 μM HA15 treatment at all. In contrast, if cells were cultured without FBS, their viability decreased significantly after 14 hours of starvation. Under this condition, the cell lines responded differently to HA15: some detached from the surface, and others had rounded shapes; whereas the morphology of other cell lines was unaffected. In fact, we observed the cancer cell killing effect on melanoma cells referred by Cerezo et al. only if we used starvation conditions during the whole experiment [13]. Serum starvation is widely used for mammalian cell synchronization because serum deprivation arrests cells in G0/G1 phase [131-134], but after ~ 24 hours (depending on cell lines), the morphology of cells starts to change, as described above. It is well known that starvation results in deleterious effects on cell viability and massive DNA fragmentation [133,135-138] as a hallmark of apoptosis [139,140]. As FBS is essential for cellular growth and normal metabolism [141], a lack of serum stops cells from proliferating, and their viability decreases due to mitochondrial dysfunction and cytochrome C release, resulting in apoptosis [142-144]. How this circumstance affects cell viability, proliferation, and morphology can vary due to the methods used for FBS deprivation and for measuring cell viability [145].

Autophagy is another mechanism that has evolved to provide amino acids and fatty acids during starvation to maintain cell homeostasis; it is compatible with survival and helps cells to cope with stress. Therefore, serum starvation is an easy way to induce autophagy. Many publications have reported that 12 hours of starvation is sufficient to increase the number of autophagic vacuoles in cells [146-150]. FBS deprivation causes cell stress in many ways and is the most commonly used method of inducing cell stress [151,152]. For example, it has been reported that

HA15 treatment induces ER stress and leads to cancer cell death via concomitant autophagic and apoptotic mechanisms [13]. Nevertheless, the effectiveness of HA15 was determined after 14 hours of serum starvation, which would obviously alter the behavior of cells and induce autophagy and apoptotic mechanisms; hence, it is not an ideal experimental background to prove that these mechanisms are induced solely by HA15. To determine the effect of 14 hours of starvation on gene expression, we performed RNA-Seq experiments and compared the gene expression patterns in WM983B cells growing in normal growth medium and after 14 hours of FBS starvation. The highest difference in expression was detected for the *RP11-134F2.8* gene (217-fold change). This gene encodes a novel DnaJ_C domain-containing protein of the ER that is involved in unfolded protein binding and is an important paralogue of DNAJB11 and a co-chaperone for BiP, which is a master regulator of ER function. BiP is required for proper folding, trafficking and protein degradation and stimulates BiP ATPase activity [153-155]. Another highly expressed gene was *RP11-618G20.1* (64-fold change), which encodes a long non-coding RNA associated with angiogenesis (http://angiogenes.unifrankfurt.de) and has potential clinical implications in ovarian cancer [156]. Two starvation-related genes, *SLCO4C1* (32-fold change) and *PIK3IP1* (14-fold change), were also highly expressed in the starved WM983B cell population. Overexpression of the *SLCO4C1* gene has recently been described in endometrial cancer tissue, and it was shown that downregulation of this gene can promote apoptosis in endometrial cancer cell lines [157]. Furthermore, overexpression PIK3IP1 suppresses the activity of the PI3K/AKT/mTOR pathway as a critical regulator of autophagy [158,159].

Recent data support the existence of crosstalk between lipid metabolism and autophagy, as lipid metabolism is possibly involved in the formation of membrane structures related to autophagy (e.g., phagophores and autophagosomes) during stress [160]. SREBP is an ER-associated integral membrane protein complex that transcriptionally controls expression of the genes coding for a number of enzymes involved in cholesterol biosynthesis [161]. Similarly, it is well documented that Ca^{2+} ions have a clear and complex role in autophagy regulation [162,163] Finally, the active nuclear form of SREBP1 has been found to amplify ER stress and autophagy via regulation of PERK [164].

Cerezo et al. published that the duration of starvation can be interpreted in different ways, whereby 14 or 62 hours of starvation may have been imposed if the condition applies to the

entire duration of the experiment [13]. If we use cell line models in cancer biology, we must simulate *in vivo* conditions as "close as possible" to the "biological reality" to obtain useful and reliable information. In contrast to the published data under normal cell culture conditions, we were not able to detect the reported selective, harmful cell killing effect of HA15 at 10 μM. Interestingly, cell viability decreased significantly after starvation, but if the drug was added to the complete medium, the cells recovered after 62 hours of treatment. In summary, we found that at a small dose, HA15 had no significant effect on cell viability but that the viability of cells decreased significantly at high doses, even under normal culture conditions without starvation.

Finally, yet importantly, contrary to the original publication, we were able to generate HA15-resistant cells, which Cerezo et al. did not [13]. The failure to develop an HA15-resistant cell line was interpreted as “it is not surprising since HA15 affects a global cellular mechanism (like ER stress), rather than one specific protein, as the BRAF inhibitors do” [13]. Interestingly, the HA15-resistant cell line shows characteristics similar to those of BRAFi-resistant cell lines [90]. First, after withdrawal of the drug, the cells responded with decreased proliferation, probably because they developed not only resistance to HA15 but also drug addiction. Second, one of the resistance mechanisms to BRAF inhibitors is overexpression of the target *BRAF* gene [90]. Similar to our previous results, we observed increased expression of the HA15 target gene BiP in a dose-dependent manner in HA15-resistant cell lines. It was recently published that the resistance of cell lines to ER stress inducers is associated with elevation of GRP78/BiP at the mRNA and protein levels in all resistant cells, suggesting that overexpression of the *BiP* gene might be responsible for HA15 resistance [165].

Moreover, our RNA-Seq data highlight many genes that might contribute to the resistant phenotype. The highest expression was detected for the *PAPPA2* gene (more than 900-fold change) in the HA15-resistant cell line. While the role of this gene in drug resistance is not yet known, it is likely to exert its effects along the insulin-like growth factor (IGF) axis. Nevertheless, several of the other genes identified can be specifically linked to drug resistance. For example, the *ABCC9* gene is a member of the ABC transporter MRP subfamily and is involved in multi-drug resistance, including *IL13RA2* in resistance to sunitinib [166] and *ZEB1* in resistance to histone deacetylase inhibitors [167]. The overexpressed genes in the HA15-

resistant cell line are involved in ion channel/transporter activities, and these genes appear to be new actors in chemotherapeutic resistance [168,169].

In summary, we developed BRAFi (PLX4720)-resistant *BRAF*^{V600E} mutant, matched primary and metastatic melanoma model systems to characterize the molecular background of BRAFi resistance. We found new genomic alterations and characterized the protein expression patterns associated with the resistant phenotype.

Furthermore, in contrast to the published data, we conclude that the new drug HA15 is not effective at 10 μM concentration as it was published, it has only a moderate effect on melanoma cell lines, independent of whether the cells are BRAFi resistant under normal culture conditions. We showed that the drug-induced anti-melanoma effect is due in part to the starvation applied during the experiments and not exclusively linked to the effect of the drug. Furthermore, we were unable to confirm the selectivity of the HA15; i.e., it similarly influences the viability of normal melanocytes and different melanoma cell lines. In contrast with the published data, melanoma cells are able to develop resistance against the "anti-melanoma" HA15 drug. Finally, we hope our findings can assist in obtaining a more thorough understanding of the complex mechanisms of BRAFi resistance, and helps clarify that HA15 may have a place in future therapy for melanoma.

Summary

To clarify the molecular background of BRAF inhibitor (BRAFi) resistance, we generated four drug-resistant melanoma cell lines from paired primary/metastatic cell lines using a vemurafenib analogue PLX4720. No such a comparison was reported before.

By array CGH we detected new copy number alterations in all resistant cell lines (*EXT1* and *SAMD12* genes and *REXO1L2P*). Recently it was suggested that that *EXT1* could be a promising novel target to overcome cancer cell stemness in anthracycline-based therapeutic resistance. In addition, we observed that beside the development of drug resistance, one melanoma cell line was able to develop BRAFi dependence. This is in a very good agreement with a recent report that some BRAF or MEK inhibitor-resistant melanoma patients may regain sensitivity to these drugs after a 'drug holiday'. This might create a promising therapeutic opportunity for selected patients. Using Proteome Profiler Oncology Array we detected the expression of 84 cancer-related proteins in BRAFi sensitive and resistant melanoma cell lines. We could identify distinct protein signatures associated with acquired BRAFi resistance. Increased expression of six proteins (ANGPLT4, EGFR, Endoglin, FGF2, Serpin E1, and VCAM-1) and decreased expression of two (OPN and Survivin) were consistently observed in all resistant cell lines. Downregulation of the OPN in association with acquired drug resistance was first observed by us.

In parallel, we have investigated the effect a recently synthesized drug (HA15) that triggers endoplasmic reticulum (ER) stress and causes deleterious effects on melanoma cell viability due to autophagy and apoptosis, regardless of driver mutations or drug resistance. In contrast to the published data, we did not detect significant melanoma cell death under normal culture conditions using HA15 treatment. Indeed, only cells that were cultured under long-term starvation conditions were sensitive to the drug. Quantitative measurements of ER stress and autophagy markers showed that the compound HA15 does not trigger stress alone but synergistically enhances ER stress under starvation conditions. Importantly, we observed that the viability of normal melanocytes decreased significantly with treatment, even at low HA15 concentrations. Finally yet importantly, we were able to generate HA15-resistant cell lines, which failed by Cerezo et al. Taken together, HA15 only influences the viability of cells that are starved for several hours before and during treatment. In summary, further studies are needed to prove that HA15 is an effective anti-cancer agent.

Összefoglalás

Vizsgálataink célja melanomák BRAF inhibitorral (BRAFi, PLX4720: vemurafenib analóg) szemben létrejött rezisztencia hátterében álló molekuláris mechanizmusok részletes felderítése volt. Kísérleteink során BRAF inhibitor rezisztens primer és metasztázis eredetű melanoma sejvonalakat hoztunk létre és vizsgáltuk a sejtvonalak közötti molekuláris eltéréseket. ArrayCGH elemzéseink során új, a rezisztenciával összefüggésbe hozható kópiaszám eltéréseket találtunk az *EXT1*, *SAMD12* és a *REXO1L2P* géneknél. Irodalmi adatok alapján az *EXT1* gén ígéretes új célpont lehet egyes daganatok antraciklin terápiával szemben kialakuló rezisztencia leküzdésében. Megfigyeltük, hogy rezisztencia kialakulását követően egy sejtvonalnál BRAF-inhibitor "függőség" jött létre, ami teljes összhangban van mások megfigyelésével. Ezek szerint egyes BRAF- vagy MEK-inhibitorral szemben rezisztens melanomás betegek képesek ismét érzékennyé válni a gyógyszeres kezelésre, ami ígéretes terápiás lehetőséget jelenthet a kiválasztott betegek számára. Proteome Profiler Oncology Array vizsgálataink során megfigyeltük, hogy 84 daganat specifikus fehérje közül hat fehérje (ANGPLT4, EGFR, Endoglin, FGF2, Serpin E1, és VCAM-1) az összes rezisztens sejtvonalban növekedett expresszióval jellemezhető, ugyanakkor az OPN és a Survivin fehérjék expressziója csökken. Ezeknek a fehérjéknek a megváltozott expressziója egyértelműen arra utal, hogy a rezisztencia kialakulása több jelátviteli útvonalat érint, melyek megismerése további vizsgálatokat sürget a sikeres, több targetet célzó terápiák kidolgozásához.

Párhuzamosan a BRAF inhibitorral szemben kialakult rezisztencia molekuláris hátterének feltárása mellett, vizsgáltuk egy nemrégiben szintetizált gyógyszer (HA15) hatását $BRAF^{V600E}$ mutáns melanoma sejteken. Az eredeti közlemény szerint a HA15 ER stresszt indukálva olyan hatásokat vált ki, melyek autofágián és apoptózison keresztül, jelentősen csökkentik a melanoma sejtek életképességét, ami független a melanoma sejtek mutációs státuszától és a rezisztencia kialakulásától. A publikált adatokkal ellentétben az *in vivo* állapotot közelítő sejttenyésztési körülmények között nem mutattunk ki szignifikáns melanoma sejtpusztulást HA15 kezelés során, csak azok a sejtek voltak érzékenyek a HA15-re, melyek előzőleg tápanyag megvonásban részesültek. Stressz és autofágia markerek kvantitatív analízise szerint a HA15 önmagában nem vált ki ER stresszt, de azt szinergikusan fokozza a tápanyag megvonással kezelt sejtekben. Ellentétben a közölt adatokkal HA15 rezisztens melanoma sejtvonalak is létrehozhatók. Összefoglalva, további vizsgálatokra van szükség annak bizonyítására, hogy a HA15 hatékony a melanoma ellenes gyógyszernek tekinthető.

Main findings and results

The major focus of our study were to investigate the effect of two drugs targeting melanoma cells, with different molecular mechanisms.

Characterization of the molecular background of a BRAF inhibitor, PLX4720 (vemurafenib analogue) targeting the *BRAF^{V600E}* mutated melanomas:

- We successfully developed BRAFi-resistant primary and metastatic melanoma cell lines originated from the same patients. Withdrawal of PLX4720 from the cell cultures reduced cell proliferation in the resistant cell lines.
- We found new copy number gains altered in all resistant cell lines on chromosomes 8q24.11-q24.12 (*EXT1* and *SAMD12*) and 8q21.2 (*REXO1L2P* gene). High-level amplification of the BRAF gene was detected in in one resistant cell line, which already been shown to contribute to BRAFi resistance.

Analyses of the invasion properties of BRAFi sensitive melanoma cells

- The invasive properties of the BRAFi sensitive cell lines were limited. In contrast, 3 of the four resistant cell lines (WM983A^{RES} WM983B^{RES} WM278^{RES}) the average number of the invasive cells were significantly higher.

Gene expression patterns of BRAFi sensitive and resistant cell lines

- We found that the number of unique genes with a > 2 fold change was 437, among these, 204 genes were upregulated and 233 downregulated in the resistant cell lines.
- The overexpressed genes are associated with growth factors, growth factor receptors, extra cellular matrix (ECM), integrins and cell adhesion molecules.
- The significantly altered pathways included e.g. genes encoding ECM-associated proteins; involved in non-integrin membrane ECM interactions; genes involved in the TNF signalling pathway.
- Downregulated genes were not involved in any pathways or molecular functions, except for biological processes including developmental pigmentation, cellular lipid metabolic processes, melanocyte differentiation and lipid metabolic processes.

Protein array analysis of the BRAFi sensitive and resistant melanoma cell lines

- Importantly we found the increased expression of six proteins (ANGPLT4, EGFR, Endoglin, FGF2, Serpin E1, and VCAM-1) and decreased expression of two proteins (OPN and Survivin) were consistently detected in all resistant cell lines.

Investigation the effect of HA15 on *BRAF^{V600E}* mutated BRAFi sensitive and resistant melanoma cell lines

Is HA15 a selective anti-melanoma drug?

In contrast to the published data, we did not detected significant melanoma cell death under normal cell culture conditions using HA15 treatment. The drug-induced anti-melanoma effect is due in part to the starvation and not exclusively linked to the effect of the drug.

- Long-term starvation and HA15 treatment have synergistic effects on cell viability. We could not confirm the selectivity of the HA15; i.e., it similarly influences the viability of normal melanocytes and different melanoma cell lines

Effect of serum withdrawal and HA15 treatment on stress marker expression in melanoma cell line

- By quantitative measurements of ER stress and autophagy markers we found that HA15 does not trigger stress alone but synergistically enhances ER stress under starvation conditions.
- We observed increased expression of the HA15 target gene *BiP* in a dose-dependent manner in HA15-resistant cell lines, suggesting that overexpression of the *BiP* gene might be involved to the development of HA15 resistance.
- After withdrawal of the drug, cells responded with decreased proliferation, probably because they developed not only resistance to HA15 but also drug addiction.

Are melanoma cells resistant for HA15 treatment?

- We were able to generate HA15-resistant cell line and found that the HA15-resistant cells show similar features to BRAFi-resistant cell lines.
- We found very high expression for the *PAPPA2* gene (more than 900-fold change) in the HA15-resistant cell line by RNA-Seq. While the role of this gene in drug resistance is not yet known, it is likely to exert its effects along the insulin-like growth fa234ctor (IGF) axis.

References

1. Leiter, U.; Keim, U.; Garbe, C. Epidemiology of Skin Cancer: Update 2019. *Advances in experimental medicine and biology* **2020**, *1268*, 123-139, doi:10.1007/978-3-030-46227-7_6.
2. Whiteman, D.C.; Whiteman, C.A.; Green, A.C. Childhood sun exposure as a risk factor for melanoma: a systematic review of epidemiologic studies. *Cancer causes & control : CCC* **2001**, *12*, 69-82, doi:10.1023/a:1008980919928.
3. Elwood, J.M.; Jopson, J. Melanoma and sun exposure: an overview of published studies. *International journal of cancer* **1997**, *73*, 198-203, doi:10.1002/(sici)1097-0215(19971009)73:2<198::aid-ijc6>3.0.co;2-r.
4. Miller, K.D.; Fidler-Benaoudia, M.; Keegan, T.H.; Hipp, H.S.; Jemal, A.; Siegel, R.L. Cancer statistics for adolescents and young adults, 2020. *CA: a cancer journal for clinicians* **2020**, 10.3322/caac.21637, doi:10.3322/caac.21637.
5. Svedman, F.C.; Pillas, D.; Taylor, A.; Kaur, M.; Linder, R.; Hansson, J. Stage-specific survival and recurrence in patients with cutaneous malignant melanoma in Europe - a systematic review of the literature. *Clinical epidemiology* **2016**, *8*, 109-122, doi:10.2147/CLEP.S99021.
6. Rozeman, E.A.; Dekker, T.J.A.; Haanen, J.; Blank, C.U. Advanced Melanoma: Current Treatment Options, Biomarkers, and Future Perspectives. *American journal of clinical dermatology* **2018**, *19*, 303-317, doi:10.1007/s40257-017-0325-6.
7. Chapman, P.B.; Hauschild, A.; Robert, C.; Haanen, J.B.; Ascierto, P.; Larkin, J.; Dummer, R.; Garbe, C.; Testori, A.; Maio, M., et al. Improved survival with vemurafenib in melanoma with BRAF V600E mutation. *The New England journal of medicine* **2011**, *364*, 2507-2516, doi:10.1056/NEJMoa1103782.
8. Balch, C.M.; Gershenwald, J.E.; Soong, S.J.; Thompson, J.F.; Atkins, M.B.; Byrd, D.R.; Buzaid, A.C.; Cochran, A.J.; Coit, D.G.; Ding, S., et al. Final version of 2009 AJCC melanoma staging and classification. *Journal of clinical oncology : official journal of the American Society of Clinical Oncology* **2009**, *27*, 6199-6206, doi:10.1200/JCO.2009.23.4799.
9. Hodi, F.S.; O'Day, S.J.; McDermott, D.F.; Weber, R.W.; Sosman, J.A.; Haanen, J.B.; Gonzalez, R.; Robert, C.; Schadendorf, D.; Hassel, J.C., et al. Improved survival with ipilimumab in patients with metastatic melanoma. *The New England journal of medicine* **2010**, *363*, 711-723, doi:10.1056/NEJMoa1003466.
10. Griewank, K.G. Biomarkers in melanoma. *Scandinavian journal of clinical and laboratory investigation. Supplementum* **2016**, *245*, S104-112, doi:10.1080/00365513.2016.1210336.
11. Topalian, S.L.; Sznol, M.; McDermott, D.F.; Kluger, H.M.; Carvajal, R.D.; Sharfman, W.H.; Brahmer, J.R.; Lawrence, D.P.; Atkins, M.B.; Powderly, J.D., et al. Survival, durable tumor remission, and long-term safety in patients with advanced melanoma receiving nivolumab. *Journal of clinical oncology : official journal of the American Society of Clinical Oncology* **2014**, *32*, 1020-1030, doi:10.1200/JCO.2013.53.0105.
12. Dummer, R.; Ascierto, P.A.; Gogas, H.J.; Arance, A.; Mandala, M.; Liszkay, G.; Garbe, C.; Schadendorf, D.; Krajsova, I.; Gutzmer, R., et al. Overall survival in patients with BRAF-mutant melanoma receiving encorafenib plus binimetinib versus vemurafenib or encorafenib (COLUMBUS): a multicentre, open-label, randomised,

phase 3 trial. *The Lancet. Oncology* **2018**, *19*, 1315-1327, doi:10.1016/S1470-2045(18)30497-2.

13. Cerezo, M.; Lehraiki, A.; Millet, A.; Rouaud, F.; Plaisant, M.; Jaune, E.; Botton, T.; Ronco, C.; Abbe, P.; Amdouni, H., et al. Compounds Triggering ER Stress Exert Anti-Melanoma Effects and Overcome BRAF Inhibitor Resistance. *Cancer cell* **2016**, *29*, 805-819, doi:10.1016/j.ccell.2016.04.013.
14. Potrony, M.; Badenas, C.; Aguilera, P.; Puig-Butille, J.A.; Carrera, C.; Malvehy, J.; Puig, S. Update in genetic susceptibility in melanoma. *Annals of translational medicine* **2015**, *3*, 210, doi:10.3978/j.issn.2305-5839.2015.08.11.
15. Primiero, C.A.; Yanes, T.; Finnane, A.; Soyer, H.P.; McInerney-Leo, A.M. A Systematic Review on the Impact of Genetic Testing for Familial Melanoma II: Psychosocial Outcomes and Attitudes. *Dermatology* **2021**, 10.1159/000513576, 1-11, doi:10.1159/000513576.
16. Shain, A.H.; Bastian, B.C. From melanocytes to melanomas. *Nature reviews. Cancer* **2016**, *16*, 345-358, doi:10.1038/nrc.2016.37.
17. Wang, L.; Rao, M.; Fang, Y.; Hameed, M.; Viale, A.; Busam, K.; Jhanwar, S.C. A genome-wide high-resolution array-CGH analysis of cutaneous melanoma and comparison of array-CGH to FISH in diagnostic evaluation. *The Journal of molecular diagnostics : JMD* **2013**, *15*, 581-591, doi:10.1016/j.jmoldx.2013.04.001.
18. Curtin, J.A.; Fridlyand, J.; Kageshita, T.; Patel, H.N.; Busam, K.J.; Kutzner, H.; Cho, K.H.; Aiba, S.; Brocker, E.B.; LeBoit, P.E., et al. Distinct sets of genetic alterations in melanoma. *The New England journal of medicine* **2005**, *353*, 2135-2147, doi:10.1056/NEJMoa050092.
19. Gupta, R.; Janostiak, R.; Wajapeyee, N. Transcriptional regulators and alterations that drive melanoma initiation and progression. *Oncogene* **2020**, *39*, 7093-7105, doi:10.1038/s41388-020-01490-x.
20. Armstrong, B.K.; Cust, A.E. Sun exposure and skin cancer, and the puzzle of cutaneous melanoma: A perspective on Fears et al. Mathematical models of age and ultraviolet effects on the incidence of skin cancer among whites in the United States. American Journal of Epidemiology 1977; 105: 420-427. *Cancer epidemiology* **2017**, *48*, 147-156, doi:10.1016/j.canep.2017.04.004.
21. Rabbie, R.; Ferguson, P.; Molina-Aguilar, C.; Adams, D.J.; Robles-Espinoza, C.D. Melanoma subtypes: genomic profiles, prognostic molecular markers and therapeutic possibilities. *The Journal of pathology* **2019**, *247*, 539-551, doi:10.1002/path.5213.
22. Hodis, E.; Watson, I.R.; Kryukov, G.V.; Arold, S.T.; Imielinski, M.; Theurillat, J.P.; Nickerson, E.; Auclair, D.; Li, L.; Place, C., et al. A landscape of driver mutations in melanoma. *Cell* **2012**, *150*, 251-263, doi:10.1016/j.cell.2012.06.024.
23. Paluncic, J.; Kovacevic, Z.; Jansson, P.J.; Kalinowski, D.; Merlot, A.M.; Huang, M.L.; Lok, H.C.; Sahni, S.; Lane, D.J.; Richardson, D.R. Roads to melanoma: Key pathways and emerging players in melanoma progression and oncogenic signaling. *Biochimica et biophysica acta* **2016**, *1863*, 770-784, doi:10.1016/j.bbamcr.2016.01.025.
24. Balmanno, K.; Cook, S.J. Tumour cell survival signalling by the ERK1/2 pathway. *Cell death and differentiation* **2009**, *16*, 368-377, doi:10.1038/cdd.2008.148.
25. Davies, H.; Bignell, G.R.; Cox, C.; Stephens, P.; Edkins, S.; Clegg, S.; Teague, J.; Woffendin, H.; Garnett, M.J.; Bottomley, W., et al. Mutations of the BRAF gene in human cancer. *Nature* **2002**, *417*, 949-954, doi:10.1038/nature00766.

26. Philpott, C.; Tovell, H.; Frayling, I.M.; Cooper, D.N.; Upadhyaya, M. The NF1 somatic mutational landscape in sporadic human cancers. *Human genomics* **2017**, *11*, 13, doi:10.1186/s40246-017-0109-3.
27. Arafeh, R.; Qutob, N.; Emmanuel, R.; Keren-Paz, A.; Madore, J.; Elkahloun, A.; Wilmott, J.S.; Gartner, J.J.; Di Pizio, A.; Winograd-Katz, S., et al. Recurrent inactivating RASA2 mutations in melanoma. *Nature genetics* **2015**, *47*, 1408-1410, doi:10.1038/ng.3427.
28. Kong, B.Y.; Carlino, M.S.; Menzies, A.M. Biology and treatment of BRAF mutant metastatic melanoma. *Melanoma management* **2016**, *3*, 33-45, doi:10.2217/mmt.15.38.
29. Yao, Z.; Torres, N.M.; Tao, A.; Gao, Y.; Luo, L.; Li, Q.; de Stanchina, E.; Abdel-Wahab, O.; Solit, D.B.; Poulikakos, P.I., et al. BRAF Mutants Evade ERK-Dependent Feedback by Different Mechanisms that Determine Their Sensitivity to Pharmacologic Inhibition. *Cancer cell* **2015**, *28*, 370-383, doi:10.1016/j.ccell.2015.08.001.
30. Yao, Z.; Yaeger, R.; Rodrik-Outmezguine, V.S.; Tao, A.; Torres, N.M.; Chang, M.T.; Drosten, M.; Zhao, H.; Cecchi, F.; Hembrough, T., et al. Tumours with class 3 BRAF mutants are sensitive to the inhibition of activated RAS. *Nature* **2017**, *548*, 234-238, doi:10.1038/nature23291.
31. Wan, P.T.; Garnett, M.J.; Roe, S.M.; Lee, S.; Niculescu-Duvaz, D.; Good, V.M.; Jones, C.M.; Marshall, C.J.; Springer, C.J.; Barford, D., et al. Mechanism of activation of the RAF-ERK signaling pathway by oncogenic mutations of B-RAF. *Cell* **2004**, *116*, 855-867, doi:10.1016/s0092-8674(04)00215-6.
32. Bollag, G.; Freeman, S.; Lyons, J.F.; Post, L.E. Raf pathway inhibitors in oncology. *Current opinion in investigational drugs* **2003**, *4*, 1436-1441.
33. Wilhelm, S.; Carter, C.; Lynch, M.; Lowinger, T.; Dumas, J.; Smith, R.A.; Schwartz, B.; Simantov, R.; Kelley, S. Discovery and development of sorafenib: a multikinase inhibitor for treating cancer. *Nature reviews. Drug discovery* **2006**, *5*, 835-844, doi:10.1038/nrd2130.
34. White, P.T.; Cohen, M.S. The discovery and development of sorafenib for the treatment of thyroid cancer. *Expert opinion on drug discovery* **2015**, *10*, 427-439, doi:10.1517/17460441.2015.1006194.
35. Bollag, G.; Tsai, J.; Zhang, J.; Zhang, C.; Ibrahim, P.; Nolop, K.; Hirth, P. Vemurafenib: the first drug approved for BRAF-mutant cancer. *Nature reviews. Drug discovery* **2012**, *11*, 873-886, doi:10.1038/nrd3847.
36. King, A.J.; Arnone, M.R.; Bleam, M.R.; Moss, K.G.; Yang, J.; Fedorowicz, K.E.; Smitheman, K.N.; Erhardt, J.A.; Hughes-Earle, A.; Kane-Carson, L.S., et al. Dabrafenib; preclinical characterization, increased efficacy when combined with trametinib, while BRAF/MEK tool combination reduced skin lesions. *PloS one* **2013**, *8*, e67583, doi:10.1371/journal.pone.0067583.
37. Kortum, R.L.; Morrison, D.K. Path Forward for RAF Therapies: Inhibition of Monomers and Dimers. *Cancer cell* **2015**, *28*, 279-281, doi:10.1016/j.ccell.2015.08.006.
38. Tse, A.; Verkhivker, G.M. Exploring Molecular Mechanisms of Paradoxical Activation in the BRAF Kinase Dimers: Atomistic Simulations of Conformational Dynamics and Modeling of Allosteric Communication Networks and Signaling Pathways. *PloS one* **2016**, *11*, e0166583, doi:10.1371/journal.pone.0166583.

39. Hall-Jackson, C.A.; Eyers, P.A.; Cohen, P.; Goedert, M.; Boyle, F.T.; Hewitt, N.; Plant, H.; Hedge, P. Paradoxical activation of Raf by a novel Raf inhibitor. *Chemistry & biology* **1999**, *6*, 559-568, doi:10.1016/s1074-5521(99)80088-x.
40. Su, F.; Viros, A.; Milagre, C.; Trunzer, K.; Bollag, G.; Spleiss, O.; Reis-Filho, J.S.; Kong, X.; Koya, R.C.; Flaherty, K.T., et al. RAS mutations in cutaneous squamous-cell carcinomas in patients treated with BRAF inhibitors. *The New England journal of medicine* **2012**, *366*, 207-215, doi:10.1056/NEJMoa1105358.
41. Zhang, C.; Spevak, W.; Zhang, Y.; Burton, E.A.; Ma, Y.; Habets, G.; Zhang, J.; Lin, J.; Ewing, T.; Matusow, B., et al. RAF inhibitors that evade paradoxical MAPK pathway activation. *Nature* **2015**, *526*, 583-586, doi:10.1038/nature14982.
42. Pratilas, C.A.; Solit, D.B. Targeting the mitogen-activated protein kinase pathway: physiological feedback and drug response. *Clinical cancer research : an official journal of the American Association for Cancer Research* **2010**, *16*, 3329-3334, doi:10.1158/1078-0432.CCR-09-3064.
43. Sharma, S.V.; Lee, D.Y.; Li, B.; Quinlan, M.P.; Takahashi, F.; Maheswaran, S.; McDermott, U.; Azizian, N.; Zou, L.; Fischbach, M.A., et al. A chromatin-mediated reversible drug-tolerant state in cancer cell subpopulations. *Cell* **2010**, *141*, 69-80, doi:10.1016/j.cell.2010.02.027.
44. Konieczkowski, D.J.; Johannessen, C.M.; Abudayyeh, O.; Kim, J.W.; Cooper, Z.A.; Piris, A.; Frederick, D.T.; Barzily-Rokni, M.; Straussman, R.; Haq, R., et al. A melanoma cell state distinction influences sensitivity to MAPK pathway inhibitors. *Cancer discovery* **2014**, *4*, 816-827, doi:10.1158/2159-8290.CD-13-0424.
45. Shi, H.; Hugo, W.; Kong, X.; Hong, A.; Koya, R.C.; Moriceau, G.; Chodon, T.; Guo, R.; Johnson, D.B.; Dahlman, K.B., et al. Acquired resistance and clonal evolution in melanoma during BRAF inhibitor therapy. *Cancer discovery* **2014**, *4*, 80-93, doi:10.1158/2159-8290.CD-13-0642.
46. Nazarian, R.; Shi, H.; Wang, Q.; Kong, X.; Koya, R.C.; Lee, H.; Chen, Z.; Lee, M.K.; Attar, N.; Sazegar, H., et al. Melanomas acquire resistance to B-RAF(V600E) inhibition by RTK or N-RAS upregulation. *Nature* **2010**, *468*, 973-977, doi:10.1038/nature09626.
47. Johannessen, C.M.; Boehm, J.S.; Kim, S.Y.; Thomas, S.R.; Wardwell, L.; Johnson, L.A.; Emery, C.M.; Stransky, N.; Cogdill, A.P.; Barretina, J., et al. COT drives resistance to RAF inhibition through MAP kinase pathway reactivation. *Nature* **2010**, *468*, 968-972, doi:10.1038/nature09627.
48. Villanueva, J.; Vultur, A.; Lee, J.T.; Somasundaram, R.; Fukunaga-Kalabis, M.; Cipolla, A.K.; Wubbenhorst, B.; Xu, X.; Gimotty, P.A.; Kee, D., et al. Acquired resistance to BRAF inhibitors mediated by a RAF kinase switch in melanoma can be overcome by cotargeting MEK and IGF-1R/PI3K. *Cancer cell* **2010**, *18*, 683-695, doi:10.1016/j.ccr.2010.11.023.
49. Sullivan, R.J.; Flaherty, K.T. Resistance to BRAF-targeted therapy in melanoma. *European journal of cancer* **2013**, *49*, 1297-1304, doi:10.1016/j.ejca.2012.11.019.
50. Atefi, M.; von Euw, E.; Attar, N.; Ng, C.; Chu, C.; Guo, D.; Nazarian, R.; Chmielowski, B.; Glaspy, J.A.; Comin-Anduix, B., et al. Reversing melanoma cross-resistance to BRAF and MEK inhibitors by co-targeting the AKT/mTOR pathway. *PloS one* **2011**, *6*, e28973, doi:10.1371/journal.pone.0028973.

51. Poulikakos, P.I.; Zhang, C.; Bollag, G.; Shokat, K.M.; Rosen, N. RAF inhibitors transactivate RAF dimers and ERK signalling in cells with wild-type BRAF. *Nature* **2010**, *464*, 427-430, doi:10.1038/nature08902.
52. Heidorn, S.J.; Milagre, C.; Whittaker, S.; Nourry, A.; Niculescu-Duvas, I.; Dhomen, N.; Hussain, J.; Reis-Filho, J.S.; Springer, C.J.; Pritchard, C., et al. Kinase-dead BRAF and oncogenic RAS cooperate to drive tumor progression through CRAF. *Cell* **2010**, *140*, 209-221, doi:10.1016/j.cell.2009.12.040.
53. Tap, W.D.; Gong, K.W.; Dering, J.; Tseng, Y.; Ginther, C.; Pauletti, G.; Glaspy, J.A.; Essner, R.; Bollag, G.; Hirth, P., et al. Pharmacodynamic characterization of the efficacy signals due to selective BRAF inhibition with PLX4032 in malignant melanoma. *Neoplasia* **2010**, *12*, 637-649, doi:10.1593/neo.10414.
54. Poulikakos, P.I.; Persaud, Y.; Janakiraman, M.; Kong, X.; Ng, C.; Moriceau, G.; Shi, H.; Atefi, M.; Titz, B.; Gabay, M.T., et al. RAF inhibitor resistance is mediated by dimerization of aberrantly spliced BRAF(V600E). *Nature* **2011**, *480*, 387-390, doi:10.1038/nature10662.
55. Shi, H.; Moriceau, G.; Kong, X.; Lee, M.K.; Lee, H.; Koya, R.C.; Ng, C.; Chodon, T.; Scolyer, R.A.; Dahlman, K.B., et al. Melanoma whole-exome sequencing identifies (V600E)B-RAF amplification-mediated acquired B-RAF inhibitor resistance. *Nature communications* **2012**, *3*, 724, doi:10.1038/ncomms1727.
56. Emery, C.M.; Vijayendran, K.G.; Zipser, M.C.; Sawyer, A.M.; Niu, L.; Kim, J.J.; Hatton, C.; Chopra, R.; Oberholzer, P.A.; Karpova, M.B., et al. MEK1 mutations confer resistance to MEK and B-RAF inhibition. *Proceedings of the National Academy of Sciences of the United States of America* **2009**, *106*, 20411-20416, doi:10.1073/pnas.0905833106.
57. Wagle, N.; Emery, C.; Berger, M.F.; Davis, M.J.; Sawyer, A.; Pochanard, P.; Kehoe, S.M.; Johannessen, C.M.; Macconaill, L.E.; Hahn, W.C., et al. Dissecting therapeutic resistance to RAF inhibition in melanoma by tumor genomic profiling. *Journal of clinical oncology : official journal of the American Society of Clinical Oncology* **2011**, *29*, 3085-3096, doi:10.1200/JCO.2010.33.2312.
58. Moreira, A.; Heinzerling, L.; Bhardwaj, N.; Friedlander, P. Current Melanoma Treatments: Where Do We Stand? *Cancers* **2021**, *13*, doi:10.3390/cancers13020221.
59. Bhatia, S.; Tykodi, S.S.; Thompson, J.A. Treatment of metastatic melanoma: an overview. *Oncology* **2009**, *23*, 488-496.
60. Knuth, A.; Danowski, B.; Oettgen, H.F.; Old, L.J. T-cell-mediated cytotoxicity against autologous malignant melanoma: analysis with interleukin 2-dependent T-cell cultures. *Proceedings of the National Academy of Sciences of the United States of America* **1984**, *81*, 3511-3515, doi:10.1073/pnas.81.11.3511.
61. Rosenberg, S.A.; Packard, B.S.; Aebersold, P.M.; Solomon, D.; Topalian, S.L.; Toy, S.T.; Simon, P.; Lotze, M.T.; Yang, J.C.; Seipp, C.A., et al. Use of tumor-infiltrating lymphocytes and interleukin-2 in the immunotherapy of patients with metastatic melanoma. A preliminary report. *The New England journal of medicine* **1988**, *319*, 1676-1680, doi:10.1056/NEJM198812223192527.
62. Sparano, J.A.; Fisher, R.I.; Sunderland, M.; Margolin, K.; Ernest, M.L.; Sznol, M.; Atkins, M.B.; Dutcher, J.P.; Micetich, K.C.; Weiss, G.R., et al. Randomized phase III trial of treatment with high-dose interleukin-2 either alone or in combination with interferon alfa-2a in patients with advanced melanoma. *Journal of clinical oncology :*

official journal of the American Society of Clinical Oncology **1993**, *11*, 1969-1977, doi:10.1200/JCO.1993.11.10.1969.
63. Wrobel, S.; Przybylo, M.; Stepien, E. The Clinical Trial Landscape for Melanoma Therapies. *Journal of clinical medicine* **2019**, *8*, doi:10.3390/jcm8030368.
64. Larkin, J.; Chiarion-Sileni, V.; Gonzalez, R.; Grob, J.J.; Cowey, C.L.; Lao, C.D.; Schadendorf, D.; Dummer, R.; Smylie, M.; Rutkowski, P., et al. Combined Nivolumab and Ipilimumab or Monotherapy in Untreated Melanoma. *The New England journal of medicine* **2015**, *373*, 23-34, doi:10.1056/NEJMoa1504030.
65. Hetz, C.; Chevet, E.; Oakes, S.A. Proteostasis control by the unfolded protein response. *Nature cell biology* **2015**, *17*, 829-838, doi:10.1038/ncb3184.
66. Chevet, E.; Hetz, C.; Samali, A. Endoplasmic reticulum stress-activated cell reprogramming in oncogenesis. *Cancer discovery* **2015**, *5*, 586-597, doi:10.1158/2159-8290.CD-14-1490.
67. Dejeans, N.; Barroso, K.; Fernandez-Zapico, M.E.; Samali, A.; Chevet, E. Novel roles of the unfolded protein response in the control of tumor development and aggressiveness. *Seminars in cancer biology* **2015**, *33*, 67-73, doi:10.1016/j.semcancer.2015.04.007.
68. Hetz, C. The unfolded protein response: controlling cell fate decisions under ER stress and beyond. *Nature reviews. Molecular cell biology* **2012**, *13*, 89-102, doi:10.1038/nrm3270.
69. Mann, M.J.; Hendershot, L.M. UPR activation alters chemosensitivity of tumor cells. *Cancer biology & therapy* **2006**, *5*, 736-740.
70. Urra, H.; Dufey, E.; Lisbona, F.; Rojas-Rivera, D.; Hetz, C. When ER stress reaches a dead end. *Biochimica et biophysica acta* **2013**, *1833*, 3507-3517, doi:10.1016/j.bbamcr.2013.07.024.
71. Avril, T.; Vauleon, E.; Chevet, E. Endoplasmic reticulum stress signaling and chemotherapy resistance in solid cancers. *Oncogenesis* **2017**, *6*, e373, doi:10.1038/oncsis.2017.72.
72. Hitomi, J.; Katayama, T.; Eguchi, Y.; Kudo, T.; Taniguchi, M.; Koyama, Y.; Manabe, T.; Yamagishi, S.; Bando, Y.; Imaizumi, K., et al. Involvement of caspase-4 in endoplasmic reticulum stress-induced apoptosis and Abeta-induced cell death. *The Journal of cell biology* **2004**, *165*, 347-356, doi:10.1083/jcb.200310015.
73. Ma, Y.; Hendershot, L.M. The role of the unfolded protein response in tumour development: friend or foe? *Nature reviews. Cancer* **2004**, *4*, 966-977, doi:10.1038/nrc1505.
74. Cubillos-Ruiz, J.R.; Bettigole, S.E.; Glimcher, L.H. Tumorigenic and Immunosuppressive Effects of Endoplasmic Reticulum Stress in Cancer. *Cell* **2017**, *168*, 692-706, doi:10.1016/j.cell.2016.12.004.
75. Hill, D.S.; Lovat, P.E.; Haass, N.K. Induction of endoplasmic reticulum stress as a strategy for melanoma therapy: is there a future? *Melanoma management* **2014**, *1*, 127-137, doi:10.2217/mmt.14.16.
76. Ojha, R.; Amaravadi, R.K. Targeting the unfolded protein response in cancer. *Pharmacological research* **2017**, *120*, 258-266, doi:10.1016/j.phrs.2017.04.003.
77. Denoyelle, C.; Abou-Rjaily, G.; Bezrookove, V.; Verhaegen, M.; Johnson, T.M.; Fullen, D.R.; Pointer, J.N.; Gruber, S.B.; Su, L.D.; Nikiforov, M.A., et al. Anti-oncogenic role of the endoplasmic reticulum differentially activated by mutations in the MAPK pathway. *Nature cell biology* **2006**, *8*, 1053-1063, doi:10.1038/ncb1471.

78. Beck, D.; Niessner, H.; Smalley, K.S.; Flaherty, K.; Paraiso, K.H.; Busch, C.; Sinnberg, T.; Vasseur, S.; Iovanna, J.L.; Driessen, S., et al. Vemurafenib potently induces endoplasmic reticulum stress-mediated apoptosis in BRAFV600E melanoma cells. *Science signaling* **2013**, *6*, ra7, doi:10.1126/scisignal.2003057.
79. Darling, N.J.; Cook, S.J. The role of MAPK signalling pathways in the response to endoplasmic reticulum stress. *Biochimica et biophysica acta* **2014**, *1843*, 2150-2163, doi:10.1016/j.bbamcr.2014.01.009.
80. Martin, S.; Hill, D.S.; Paton, J.C.; Paton, A.W.; Birch-Machin, M.A.; Lovat, P.E.; Redfern, C.P. Targeting GRP78 to enhance melanoma cell death. *Pigment cell & melanoma research* **2010**, *23*, 675-682, doi:10.1111/j.1755-148X.2010.00731.x.
81. Lovat, P.E.; Corazzari, M.; Armstrong, J.L.; Martin, S.; Pagliarini, V.; Hill, D.; Brown, A.M.; Piacentini, M.; Birch-Machin, M.A.; Redfern, C.P. Increasing melanoma cell death using inhibitors of protein disulfide isomerases to abrogate survival responses to endoplasmic reticulum stress. *Cancer research* **2008**, *68*, 5363-5369, doi:10.1158/0008-5472.CAN-08-0035.
82. Lee, H.K.; Xiang, C.; Cazacu, S.; Finniss, S.; Kazimirsky, G.; Lemke, N.; Lehman, N.L.; Rempel, S.A.; Mikkelsen, T.; Brodie, C. GRP78 is overexpressed in glioblastomas and regulates glioma cell growth and apoptosis. *Neuro-oncology* **2008**, *10*, 236-243, doi:10.1215/15228517-2008-006.
83. Mhaidat, N.M.; Alzoubi, K.H.; Khabour, O.F.; Banihani, M.N.; Al-Balas, Q.A.; Swaidan, S. GRP78 regulates sensitivity of human colorectal cancer cells to DNA targeting agents. *Cytotechnology* **2016**, *68*, 459-467, doi:10.1007/s10616-014-9799-8.
84. Fu, W.; Wu, X.; Li, J.; Mo, Z.; Yang, Z.; Huang, W.; Ding, Q. Upregulation of GRP78 in renal cell carcinoma and its significance. *Urology* **2010**, *75*, 603-607, doi:10.1016/j.urology.2009.05.007.
85. Shuda, M.; Kondoh, N.; Imazeki, N.; Tanaka, K.; Okada, T.; Mori, K.; Hada, A.; Arai, M.; Wakatsuki, T.; Matsubara, O., et al. Activation of the ATF6, XBP1 and grp78 genes in human hepatocellular carcinoma: a possible involvement of the ER stress pathway in hepatocarcinogenesis. *Journal of hepatology* **2003**, *38*, 605-614.
86. Niu, Z.; Wang, M.; Zhou, L.; Yao, L.; Liao, Q.; Zhao, Y. Elevated GRP78 expression is associated with poor prognosis in patients with pancreatic cancer. *Scientific reports* **2015**, *5*, 16067, doi:10.1038/srep16067.
87. Wolfson, J.J.; May, K.L.; Thorpe, C.M.; Jandhyala, D.M.; Paton, J.C.; Paton, A.W. Subtilase cytotoxin activates PERK, IRE1 and ATF6 endoplasmic reticulum stress-signalling pathways. *Cellular microbiology* **2008**, *10*, 1775-1786, doi:10.1111/j.1462-5822.2008.01164.x.
88. Martin, S.; Lamb, H.K.; Brady, C.; Lefkove, B.; Bonner, M.Y.; Thompson, P.; Lovat, P.E.; Arbiser, J.L.; Hawkins, A.R.; Redfern, C.P. Inducing apoptosis of cancer cells using small-molecule plant compounds that bind to GRP78. *British journal of cancer* **2013**, *109*, 433-443, doi:10.1038/bjc.2013.325.
89. Cerezo, M.; Lehraiki, A.; Millet, A.; Rouaud, F.; Plaisant, M.; Jaune, E.; Botton, T.; Ronco, C.; Abbe, P.; Amdouni, H., et al. Compounds Triggering ER Stress Exert Anti-Melanoma Effects and Overcome BRAF Inhibitor Resistance. *Cancer cell* **2016**, *30*, 183, doi:10.1016/j.ccell.2016.06.007.
90. Szasz, I.; Koroknai, V.; Kiss, T.; Vizkeleti, L.; Adany, R.; Balazs, M. Molecular alterations associated with acquired resistance to BRAFV600E targeted therapy in

melanoma cells. *Melanoma research* **2019**, 10.1097/CMR.0000000000000588, doi:10.1097/CMR.0000000000000588.

91. Koroknai, V.; Ecsedi, S.; Vizkeleti, L.; Kiss, T.; Szasz, I.; Lukacs, A.; Papp, O.; Adany, R.; Balazs, M. Genomic profiling of invasive melanoma cell lines by array comparative genomic hybridization. *Melanoma research* **2016**, *26*, 100-107, doi:10.1097/CMR.0000000000000227.
92. Vizkeleti, L.; Kiss, T.; Koroknai, V.; Ecsedi, S.; Papp, O.; Szasz, I.; Adany, R.; Balazs, M. Altered integrin expression patterns shown by microarray in human cutaneous melanoma. *Melanoma research* **2017**, *27*, 180-188, doi:10.1097/CMR.0000000000000322.
93. Wang, J.; Huang, S.K.; Marzese, D.M.; Hsu, S.C.; Kawas, N.P.; Chong, K.K.; Long, G.V.; Menzies, A.M.; Scolyer, R.A.; Izraely, S., et al. Epigenetic Changes of EGFR Have an Important Role in BRAF Inhibitor-Resistant Cutaneous Melanomas. *The Journal of investigative dermatology* **2015**, *135*, 532-541, doi:10.1038/jid.2014.418.
94. Sandri, S.; Faiao-Flores, F.; Tiago, M.; Pennacchi, P.C.; Massaro, R.R.; Alves-Fernandes, D.K.; Berardinelli, G.N.; Evangelista, A.F.; Vazquez, V.D.; Reis, R.M., et al. Vemurafenib resistance increases melanoma invasiveness and modulates the tumor microenvironment by MMP-2 upregulation. *Pharmacol Res* **2016**, *111*, 523-533, doi:10.1016/j.phrs.2016.07.017.
95. Eichhoff, O.M.; Weeraratna, A.; Zipser, M.C.; Denat, L.; Widmer, D.S.; Xu, M.; Kriegl, L.; Kirchner, T.; Larue, L.; Dummer, R., et al. Differential LEF1 and TCF4 expression is involved in melanoma cell phenotype switching. *Pigment cell & melanoma research* **2011**, *24*, 631-642, doi:10.1111/j.1755-148X.2011.00871.x.
96. Busse, M.; Feta, A.; Presto, J.; Wilen, M.; Gronning, M.; Kjellen, L.; Kusche-Gullberg, M. Contribution of EXT1, EXT2, and EXTL3 to heparan sulfate chain elongation. *The Journal of biological chemistry* **2007**, *282*, 32802-32810, doi:10.1074/jbc.M703560200.
97. Lind, T.; Tufaro, F.; McCormick, C.; Lindahl, U.; Lidholt, K. The putative tumor suppressors EXT1 and EXT2 are glycosyltransferases required for the biosynthesis of heparan sulfate. *The Journal of biological chemistry* **1998**, *273*, 26265-26268.
98. Khoontawad, J.; Hongsrichan, N.; Chamgramol, Y.; Pinlaor, P.; Wongkham, C.; Yongvanit, P.; Pairojkul, C.; Khuntikeo, N.; Roytrakul, S.; Boonmars, T., et al. Increase of exostosin 1 in plasma as a potential biomarker for opisthorchiasis-associated cholangiocarcinoma. *Tumour biology : the journal of the International Society for Oncodevelopmental Biology and Medicine* **2014**, *35*, 1029-1039, doi:10.1007/s13277-013-1137-9.
99. Reijmers, R.M.; Groen, R.W.; Rozemuller, H.; Kuil, A.; de Haan-Kramer, A.; Csikos, T.; Martens, A.C.; Spaargaren, M.; Pals, S.T. Targeting EXT1 reveals a crucial role for heparan sulfate in the growth of multiple myeloma. *Blood* **2010**, *115*, 601-604, doi:10.1182/blood-2009-02-204396.
100. Kanamori, M.; Sano, A.; Yasuda, T.; Hori, T.; Suzuki, K. Array-based comparative genomic hybridization for genomic-wide screening of DNA copy number alterations in aggressive bone tumors. *Journal of experimental & clinical cancer research : CR* **2012**, *31*, 100, doi:10.1186/1756-9966-31-100.
101. Manandhar, S.; Kim, C.G.; Lee, S.H.; Kang, S.H.; Basnet, N.; Lee, Y.M. Exostosin 1 regulates cancer cell stemness in doxorubicin-resistant breast cancer cells. *Oncotarget* **2017**, *8*, 70521-70537, doi:10.18632/oncotarget.19737.

102. Krepler, C.; Xiao, M.; Sproesser, K.; Brafford, P.A.; Shannan, B.; Beqiri, M.; Liu, Q.; Xu, W.; Garman, B.; Nathanson, K.L., et al. Personalized Preclinical Trials in BRAF Inhibitor-Resistant Patient-Derived Xenograft Models Identify Second-Line Combination Therapies. *Clinical cancer research : an official journal of the American Association for Cancer Research* **2016**, *22*, 1592-1602, doi:10.1158/1078-0432.CCR-15-1762.
103. Sun, Y.; Long, J.; Zhou, Y. Angiopoietin-like 4 promotes melanoma cell invasion and survival through aldolase A. *Oncology letters* **2014**, *8*, 211-217, doi:10.3892/ol.2014.2071.
104. Liao, Y.H.; Chiang, K.H.; Shieh, J.M.; Huang, C.R.; Shen, C.J.; Huang, W.C.; Chen, B.K. Epidermal growth factor-induced ANGPTL4 enhances anoikis resistance and tumour metastasis in head and neck squamous cell carcinoma. *Oncogene* **2017**, *36*, 2228-2242, doi:10.1038/onc.2016.371.
105. Liu, F.; Cao, J.; Wu, J.; Sullivan, K.; Shen, J.; Ryu, B.; Xu, Z.; Wei, W.; Cui, R. Stat3-targeted therapies overcome the acquired resistance to vemurafenib in melanomas. *The Journal of investigative dermatology* **2013**, *133*, 2041-2049, doi:10.1038/jid.2013.32.
106. Shaffer, S.M.; Dunagin, M.C.; Torborg, S.R.; Torre, E.A.; Emert, B.; Krepler, C.; Beqiri, M.; Sproesser, K.; Brafford, P.A.; Xiao, M., et al. Rare cell variability and drug-induced reprogramming as a mode of cancer drug resistance. *Nature* **2017**, *546*, 431-435, doi:10.1038/nature22794.
107. Chalkiadaki, G.; Nikitovic, D.; Berdiaki, A.; Sifaki, M.; Krasagakis, K.; Katonis, P.; Karamanos, N.K.; Tzanakakis, G.N. Fibroblast growth factor-2 modulates melanoma adhesion and migration through a syndecan-4-dependent mechanism. *The international journal of biochemistry & cell biology* **2009**, *41*, 1323-1331, doi:10.1016/j.biocel.2008.11.008.
108. Ji, Z.; Kumar, R.; Taylor, M.; Rajadurai, A.; Marzuka-Alcala, A.; Chen, Y.E.; Njauw, C.N.; Flaherty, K.; Jonsson, G.; Tsao, H. Vemurafenib synergizes with nutlin-3 to deplete survivin and suppresses melanoma viability and tumor growth. *Clinical cancer research : an official journal of the American Association for Cancer Research* **2013**, *19*, 4383-4391, doi:10.1158/1078-0432.CCR-13-0074.
109. Kiss, T.; Ecsedi, S.; Vizkeleti, L.; Koroknai, V.; Emri, G.; Kovacs, N.; Adany, R.; Balazs, M. The role of osteopontin expression in melanoma progression. *Tumour biology : the journal of the International Society for Oncodevelopmental Biology and Medicine* **2015**, *36*, 7841-7847, doi:10.1007/s13277-015-3495-y.
110. Craig, A.M.; Bowden, G.T.; Chambers, A.F.; Spearman, M.A.; Greenberg, A.H.; Wright, J.A.; McLeod, M.; Denhardt, D.T. Secreted phosphoprotein mRNA is induced during multi-stage carcinogenesis in mouse skin and correlates with the metastatic potential of murine fibroblasts. *International journal of cancer. Journal international du cancer* **1990**, *46*, 133-137.
111. Oates, A.J.; Barraclough, R.; Rudland, P.S. The identification of osteopontin as a metastasis-related gene product in a rodent mammary tumour model. *Oncogene* **1996**, *13*, 97-104.
112. Rakosy, Z.; Ecsedi, S.; Toth, R.; Vizkeleti, L.; Hernandez-Vargas, H.; Lazar, V.; Emri, G.; Szatmari, I.; Herceg, Z.; Adany, R., et al. Integrative genomics identifies gene signature associated with melanoma ulceration. *PloS one* **2013**, *8*, e54958, doi:10.1371/journal.pone.0054958.

113. Haga, Y.; Kanda, T.; Nakamura, M.; Nakamoto, S.; Sasaki, R.; Takahashi, K.; Wu, S.; Yokosuka, O. Overexpression of c-Jun contributes to sorafenib resistance in human hepatoma cell lines. *PloS one* **2017**, *12*, e0174153, doi:10.1371/journal.pone.0174153.
114. Mirzaei, A.; Mohammadi, S.; Ghaffari, S.H.; Nikbakht, M.; Bashash, D.; Alimoghaddam, K.; Ghavamzadeh, A. Osteopontin b and c isoforms: Molecular Candidates Associated with Leukemic Stem Cell Chemoresistance in Acute Myeloid Leukemia. *Asian Pacific journal of cancer prevention : APJCP* **2017**, *18*, 1707-1715, doi:10.22034/APJCP.2017.18.6.1707.
115. Qian, C.; Li, P.; Yan, W.; Shi, L.; Zhang, J.; Wang, Y.; Liu, H.; You, Y. Downregulation of osteopontin enhances the sensitivity of glioma U251 cells to temozolomide and cisplatin by targeting the NF-kappaB/Bcl2 pathway. *Molecular medicine reports* **2015**, *11*, 1951-1955, doi:10.3892/mmr.2014.2951.
116. Shurin, M.R. Osteopontin controls immunosuppression in the tumor microenvironment. *The Journal of clinical investigation* **2018**, *128*, 5209-5212, doi:10.1172/JCI124918.
117. Klionsky, D.J.; Abdelmohsen, K.; Abe, A.; Abedin, M.J.; Abeliovich, H.; Acevedo Arozena, A.; Adachi, H.; Adams, C.M.; Adams, P.D.; Adeli, K., et al. Guidelines for the use and interpretation of assays for monitoring autophagy (3rd edition). *Autophagy* **2016**, *12*, 1-222, doi:10.1080/15548627.2015.1100356.
118. Whiteman, D.C.; Pavan, W.J.; Bastian, B.C. The melanomas: a synthesis of epidemiological, clinical, histopathological, genetic, and biological aspects, supporting distinct subtypes, causal pathways, and cells of origin. *Pigment Cell Melanoma Res* **2011**, *24*, 879-897, doi:10.1111/j.1755-148X.2011.00880.x.
119. Winder, M.; Viros, A. Mechanisms of Drug Resistance in Melanoma. *Handbook of experimental pharmacology* **2018**, *249*, 91-108, doi:10.1007/164_2017_17.
120. Bai, X.; Fisher, D.E.; Flaherty, K.T. Cell-state dynamics and therapeutic resistance in melanoma from the perspective of MITF and IFNgamma pathways. *Nature reviews. Clinical oncology* **2019**, *16*, 549-562, doi:10.1038/s41571-019-0204-6.
121. Garber, K. Cancer research. Melanoma drug vindicates targeted approach. *Science* **2009**, *326*, 1619, doi:10.1126/science.326.5960.1619.
122. Manzano, J.L.; Layos, L.; Buges, C.; de Los Llanos Gil, M.; Vila, L.; Martinez-Balibrea, E.; Martinez-Cardus, A. Resistant mechanisms to BRAF inhibitors in melanoma. *Annals of translational medicine* **2016**, *4*, 237, doi:10.21037/atm.2016.06.07.
123. Das Thakur, M.; Salangsang, F.; Landman, A.S.; Sellers, W.R.; Pryer, N.K.; Levesque, M.P.; Dummer, R.; McMahon, M.; Stuart, D.D. Modelling vemurafenib resistance in melanoma reveals a strategy to forestall drug resistance. *Nature* **2013**, *494*, 251-255, doi:10.1038/nature11814.
124. Jain, T.; Bryce, A. Intermittent BRAF Inhibition Can Achieve Prolonged Disease Control in BRAF Mutant Melanoma. *Cureus* **2015**, *7*, e410, doi:10.7759/cureus.410.
125. Dooley, A.J.; Gupta, A.; Middleton, M.R. Ongoing Response in BRAF V600E-Mutant Melanoma After Cessation of Intermittent Vemurafenib Therapy: A Case Report. *Targeted oncology* **2016**, *11*, 557-563, doi:10.1007/s11523-015-0410-9.
126. Sun, C.; Wang, L.; Huang, S.; Heynen, G.J.; Prahallad, A.; Robert, C.; Haanen, J.; Blank, C.; Wesseling, J.; Willems, S.M., et al. Reversible and adaptive resistance to BRAF(V600E) inhibition in melanoma. *Nature* **2014**, *508*, 118-122, doi:10.1038/nature13121.

127. Algazi, A.P.; Othus, M.; Daud, A.I.; Lo, R.S.; Mehnert, J.M.; Truong, T.G.; Conry, R.; Kendra, K.; Doolittle, G.C.; Clark, J.I., et al. Continuous versus intermittent BRAF and MEK inhibition in patients with BRAF-mutated melanoma: a randomized phase 2 trial. *Nature medicine* **2020**, *26*, 1564-1568, doi:10.1038/s41591-020-1060-8.
128. Webster, M.R.; Weeraratna, A.T. A Wnt-er migration: the confusing role of beta-catenin in melanoma metastasis. *Science signaling* **2013**, *6*, pe11, doi:10.1126/scisignal.2004114.
129. Jenkins, M.H.; Steinberg, S.M.; Alexander, M.P.; Fisher, J.L.; Ernstoff, M.S.; Turk, M.J.; Mullins, D.W.; Brinckerhoff, C.E. Multiple murine BRaf(V600E) melanoma cell lines with sensitivity to PLX4032. *Pigment cell & melanoma research* **2014**, *27*, 495-501, doi:10.1111/pcmr.12220.
130. Izraely, S.; Ben-Menachem, S.; Sagi-Assif, O.; Meshel, T.; Marzese, D.M.; Ohe, S.; Zubrilov, I.; Pasmanik-Chor, M.; Hoon, D.S.B.; Witz, I.P. ANGPTL4 promotes the progression of cutaneous melanoma to brain metastasis. *Oncotarget* **2017**, *8*, 75778-75796, doi:10.18632/oncotarget.19018.
131. Khammanit, R.; Chantakru, S.; Kitiyanant, Y.; Saikhun, J. Effect of serum starvation and chemical inhibitors on cell cycle synchronization of canine dermal fibroblasts. *Theriogenology* **2008**, *70*, 27-34, doi:10.1016/j.theriogenology.2008.02.015.
132. Caamano, J.N.; Rodriguez, A.; Salas, A.; Munoz, M.; Diez, C.; Prather, R.S.; Gomez, E. Flow cytometric cell cycle analysis of cultured brown bear fibroblast cells. *Cell biology international* **2008**, *32*, 855-859, doi:10.1016/j.cellbi.2008.02.005.
133. Schorl, C.; Sedivy, J.M. Analysis of cell cycle phases and progression in cultured mammalian cells. *Methods* **2007**, *41*, 143-150, doi:10.1016/j.ymeth.2006.07.022.
134. Langan, T.J.; Chou, R.C. Synchronization of mammalian cell cultures by serum deprivation. *Methods in molecular biology* **2011**, *761*, 75-83, doi:10.1007/978-1-61779-182-6_5.
135. Shichiri, M.; Hanson, K.D.; Sedivy, J.M. Effects of c-myc expression on proliferation, quiescence, and the G0 to G1 transition in nontransformed cells. *Cell growth & differentiation : the molecular biology journal of the American Association for Cancer Research* **1993**, *4*, 93-104.
136. Kues, W.A.; Anger, M.; Carnwath, J.W.; Paul, D.; Motlik, J.; Niemann, H. Cell cycle synchronization of porcine fetal fibroblasts: effects of serum deprivation and reversible cell cycle inhibitors. *Biology of reproduction* **2000**, *62*, 412-419, doi:10.1095/biolreprod62.2.412.
137. Mengual Gomez, D.L.; Belaich, M.N.; Rodriguez, V.A.; Ghiringhelli, P.D. Effects of fetal bovine serum deprivation in cell cultures on the production of Anticarsia gemmatalis multinucleopolyhedrovirus. *BMC biotechnology* **2010**, *10*, 68, doi:10.1186/1472-6750-10-68.
138. Rodriguez-Ayerbe, C.; Smith-Zubiaga, I. Effect of serum withdrawal on the proliferation of B16F10 melanoma cells. *Cell biology international* **2000**, *24*, 279-283, doi:10.1006/cbir.1999.0502.
139. Wyllie, A.H. Glucocorticoid-induced thymocyte apoptosis is associated with endogenous endonuclease activation. *Nature* **1980**, *284*, 555-556, doi:10.1038/284555a0.
140. Gavrieli, Y.; Sherman, Y.; Ben-Sasson, S.A. Identification of programmed cell death in situ via specific labeling of nuclear DNA fragmentation. *The Journal of cell biology* **1992**, *119*, 493-501, doi:10.1083/jcb.119.3.493.

141. Bieback, K.; Hecker, A.; Kocaomer, A.; Lannert, H.; Schallmoser, K.; Strunk, D.; Kluter, H. Human alternatives to fetal bovine serum for the expansion of mesenchymal stromal cells from bone marrow. *Stem cells* **2009**, *27*, 2331-2341, doi:10.1002/stem.139.
142. Zhu, W.; Chen, J.; Cong, X.; Hu, S.; Chen, X. Hypoxia and serum deprivation-induced apoptosis in mesenchymal stem cells. *Stem cells* **2006**, *24*, 416-425, doi:10.1634/stemcells.2005-0121.
143. Potier, E.; Ferreira, E.; Meunier, A.; Sedel, L.; Logeart-Avramoglou, D.; Petite, H. Prolonged hypoxia concomitant with serum deprivation induces massive human mesenchymal stem cell death. *Tissue engineering* **2007**, *13*, 1325-1331, doi:10.1089/ten.2006.0325.
144. Wang, F.; Zhou, H.; Du, Z.; Chen, X.; Zhu, F.; Wang, Z.; Zhang, Y.; Lin, L.; Qian, M.; Zhang, X., et al. Cytoprotective effect of melatonin against hypoxia/serum deprivation-induced cell death of bone marrow mesenchymal stem cells in vitro. *European journal of pharmacology* **2015**, *748*, 157-165, doi:10.1016/j.ejphar.2014.09.033.
145. Amiri, F.; Halabian, R.; Salimian, M.; Shokrgozar, M.A.; Soleimani, M.; Jahanian-Najafabadi, A.; Roudkenar, M.H. Induction of multipotency in umbilical cord-derived mesenchymal stem cells cultivated under suspension conditions. *Cell stress & chaperones* **2014**, *19*, 657-666, doi:10.1007/s12192-014-0491-x.
146. Zhao, S.; Li, L.; Wang, S.; Yu, C.; Xiao, B.; Lin, L.; Cong, W.; Cheng, J.; Yang, W.; Sun, W., et al. H2O2 treatment or serum deprivation induces autophagy and apoptosis in naked mole-rat skin fibroblasts by inhibiting the PI3K/Akt signaling pathway. *Oncotarget* **2016**, *7*, 84839-84850, doi:10.18632/oncotarget.13321.
147. Shang, L.; Chen, S.; Du, F.; Li, S.; Zhao, L.; Wang, X. Nutrient starvation elicits an acute autophagic response mediated by Ulk1 dephosphorylation and its subsequent dissociation from AMPK. *Proceedings of the National Academy of Sciences of the United States of America* **2011**, *108*, 4788-4793, doi:10.1073/pnas.1100844108.
148. Abounit, K.; Scarabelli, T.M.; McCauley, R.B. Autophagy in mammalian cells. *World journal of biological chemistry* **2012**, *3*, 1-6, doi:10.4331/wjbc.v3.i1.1.
149. Mizushima, N.; Yoshimori, T.; Levine, B. Methods in mammalian autophagy research. *Cell* **2010**, *140*, 313-326, doi:10.1016/j.cell.2010.01.028.
150. Mehrpour, M.; Esclatine, A.; Beau, I.; Codogno, P. Overview of macroautophagy regulation in mammalian cells. *Cell research* **2010**, *20*, 748-762, doi:10.1038/cr.2010.82.
151. Witwer, K.W.; Buzas, E.I.; Bemis, L.T.; Bora, A.; Lasser, C.; Lotvall, J.; Nolte-'t Hoen, E.N.; Piper, M.G.; Sivaraman, S.; Skog, J., et al. Standardization of sample collection, isolation and analysis methods in extracellular vesicle research. *Journal of extracellular vesicles* **2013**, *2*, doi:10.3402/jev.v2i0.20360.
152. de Castro, L.L.; Xisto, D.G.; Kitoko, J.Z.; Cruz, F.F.; Olsen, P.C.; Redondo, P.A.G.; Ferreira, T.P.T.; Weiss, D.J.; Martins, M.A.; Morales, M.M., et al. Human adipose tissue mesenchymal stromal cells and their extracellular vesicles act differentially on lung mechanics and inflammation in experimental allergic asthma. *Stem cell research & therapy* **2017**, *8*, 151, doi:10.1186/s13287-017-0600-8.
153. Yu, M.; Haslam, R.H.; Haslam, D.B. HEDJ, an Hsp40 co-chaperone localized to the endoplasmic reticulum of human cells. *The Journal of biological chemistry* **2000**, *275*, 24984-24992, doi:10.1074/jbc.M000739200.

154. Shen, Y.; Hendershot, L.M. ERdj3, a stress-inducible endoplasmic reticulum DnaJ homologue, serves as a cofactor for BiP's interactions with unfolded substrates. *Molecular biology of the cell* **2005**, *16*, 40-50, doi:10.1091/mbc.e04-05-0434.
155. Cornec-Le Gall, E.; Olson, R.J.; Besse, W.; Heyer, C.M.; Gainullin, V.G.; Smith, J.M.; Audrezet, M.P.; Hopp, K.; Porath, B.; Shi, B., et al. Monoallelic Mutations to DNAJB11 Cause Atypical Autosomal-Dominant Polycystic Kidney Disease. *American journal of human genetics* **2018**, *102*, 832-844, doi:10.1016/j.ajhg.2018.03.013.
156. Zhan, L.; Li, J.; Wei, B. Long non-coding RNAs in ovarian cancer. *Journal of experimental & clinical cancer research : CR* **2018**, *37*, 120, doi:10.1186/s13046-018-0793-4.
157. Hu, X.; Han, T.; Bian, Y.; Tong, H.; Wen, X.; Li, Y.; Wan, X. Knockdown of SLCO4C1 inhibits cell proliferation and metastasis in endometrial cancer through inactivating the PI3K/Akt signaling pathway. *Oncology reports* **2020**, *43*, 919-929, doi:10.3892/or.2020.7478.
158. Heras-Sandoval, D.; Perez-Rojas, J.M.; Hernandez-Damian, J.; Pedraza-Chaverri, J. The role of PI3K/AKT/mTOR pathway in the modulation of autophagy and the clearance of protein aggregates in neurodegeneration. *Cellular signalling* **2014**, *26*, 2694-2701, doi:10.1016/j.cellsig.2014.08.019.
159. Xu, Z.; Han, X.; Ou, D.; Liu, T.; Li, Z.; Jiang, G.; Liu, J.; Zhang, J. Targeting PI3K/AKT/mTOR-mediated autophagy for tumor therapy. *Applied microbiology and biotechnology* **2020**, *104*, 575-587, doi:10.1007/s00253-019-10257-8.
160. Xie, Y.; Li, J.; Kang, R.; Tang, D. Interplay Between Lipid Metabolism and Autophagy. *Frontiers in cell and developmental biology* **2020**, *8*, 431, doi:10.3389/fcell.2020.00431.
161. Hu, J.; Zhang, Z.; Shen, W.J.; Azhar, S. Cellular cholesterol delivery, intracellular processing and utilization for biosynthesis of steroid hormones. *Nutrition & metabolism* **2010**, *7*, 47, doi:10.1186/1743-7075-7-47.
162. Liu, B.; Oltvai, Z.N.; Bayir, H.; Silverman, G.A.; Pak, S.C.; Perlmutter, D.H.; Bahar, I. Quantitative assessment of cell fate decision between autophagy and apoptosis. *Scientific reports* **2017**, *7*, 17605, doi:10.1038/s41598-017-18001-w.
163. Decuypere, J.P.; Bultynck, G.; Parys, J.B. A dual role for Ca(2+) in autophagy regulation. *Cell calcium* **2011**, *50*, 242-250, doi:10.1016/j.ceca.2011.04.001.
164. Hu, Q.; Mao, Y.; Liu, M.; Luo, R.; Jiang, R.; Guo, F. The active nuclear form of SREBP1 amplifies ER stress and autophagy via regulation of PERK. *The FEBS journal* **2020**, *287*, 2348-2366, doi:10.1111/febs.15144.
165. Cagala, M.; Pavlikova, L.; Seres, M.; Kadlecikova, K.; Breier, A.; Sulova, Z. Development of Resistance to Endoplasmic Reticulum Stress-Inducing Agents in Mouse Leukemic L1210 Cells. *Molecules* **2020**, *25*, doi:10.3390/molecules25112517.
166. Shibasaki, N.; Yamasaki, T.; Kanno, T.; Arakaki, R.; Sakamoto, H.; Utsunomiya, N.; Inoue, T.; Tsuruyama, T.; Nakamura, E.; Ogawa, O., et al. Role of IL13RA2 in Sunitinib Resistance in Clear Cell Renal Cell Carcinoma. *PloS one* **2015**, *10*, e0130980, doi:10.1371/journal.pone.0130980.
167. Lazarova, D.; Bordonaro, M. ZEB1 Mediates Drug Resistance and EMT in p300-Deficient CRC. *Journal of Cancer* **2017**, *8*, 1453-1459, doi:10.7150/jca.18762.
168. Kischel, P.; Girault, A.; Rodat-Despoix, L.; Chamlali, M.; Radoslavova, S.; Abou Daya, H.; Lefebvre, T.; Foulon, A.; Rybarczyk, P.; Hague, F., et al. Ion Channels:

New Actors Playing in Chemotherapeutic Resistance. *Cancers* **2019**, *11*, doi:10.3390/cancers11030376.

169. Hoffmann, E.K.; Lambert, I.H. Ion channels and transporters in the development of drug resistance in cancer cells. *Philosophical transactions of the Royal Society of London. Series B, Biological sciences* **2014**, *369*, 20130109, doi:10.1098/rstb.2013.0109.

Publications related to the dissertation

UNIVERSITY of DEBRECEN

UNIVERSITY AND NATIONAL LIBRARY
UNIVERSITY OF DEBRECEN
H-4002 Egyetem tér 1, Debrecen
Phone: +3652/410-443, email: publikaciok@lib.unideb.hu

Registry number: DEENK/42/2021.PL
Subject: PhD Publication List

Candidate: István Szász
Doctoral School: Doctoral School of Health Sciences

List of publications related to the dissertation

1. **Szász, I.**, Koroknai, V., Patel, V., Hajdú, T., Kiss, T., Ádány, R., Balázs, M.: Cell Proliferation Is Strongly Associated with the Treatment Conditions of an ER Stress Inducer New Anti-Melanoma Drug in Melanoma Cell Lines.
   Biomedicines. 9 (2), 1-19, 2021.
   DOI: http://dx.doi.org/10.3390/biomedicines9020096
   IF: 4.717 (2019)
2. **Szász, I.**, Koroknai, V., Kiss, T., Vízkeleti, L., Ádány, R., Balázs, M.: Molecular alterations associated with acquired resistance to BRAFV600E targeted therapy in melanoma cells.
   Melanoma Res. 29 (4), 390-400, 2019.
   DOI: http://dx.doi.org/10.1097/CMR.0000000000000588
   IF: 2.75

List of other publications

3. Koroknai, V., **Szász, I.**, Hernandez, V. H., Fernandez, J. N., Cuenin, C., Herceg, Z., Vízkeleti, L., Ádány, R., Ecsedi, S., Balázs, M.: DNA hypermethylation is associated with invasive phenotype of malignant melanoma.
   Exp. Dermatol. 29 (1), 39-50, 2020.
   DOI: http://dx.doi.org/10.1111/exd.14047
   IF: 3.368 (2019)
4. Koroknai, V., Patel, V., **Szász, I.**, Ádány, R., Balázs, M.: Gene Expression Signature of BRAF Inhibitor Resistant Melanoma Spheroids.
   Pathol. Oncol. Res. 26 (4), 2557-2566, 2020.
   DOI: http://dx.doi.org/10.1007/s12253-020-00837-9
   IF: 2.826 (2019)

UNIVERSITY of DEBRECEN

UNIVERSITY AND NATIONAL LIBRARY
UNIVERSITY OF DEBRECEN
H-4002 Egyetem tér 1, Debrecen
Phone: +3652/410-443, email: publikaciok@lib.unideb.hu

5. Balázs, M., Koroknai, V., **Szász, I.**, Ecsedi, S.: Detection of CCND1 Locus Amplification by Fluorescence In Situ Hybridization.
In: The Retinoblastoma Protein. Ed.: Pedro G. Santiago-Cardona, Springer Science+Business Media, New York, NY, 85-100, 2018.

6. Vízkeleti, L., Kiss, T., Koroknai, V., Ecsedi, S., Papp, O., **Szász, I.**, Ádány, R., Balázs, M.: Altered integrin expression patterns revealed by microarray in human cutaneous melanoma.
Melanoma Res. 27 (3), 180-188, 2017.
IF: 3.135

7. Koroknai, V., Ecsedi, S., Vízkeleti, L., Kiss, T., **Szász, I.**, Lukács, A., Papp, O., Ádány, R., Balázs, M.: Genomic profiling of invasive melanoma cell lines by array comparative genomic hybridization.
Melanoma Res. 2, 100-107, 2016.
DOI: http://dx.doi.org/10.1097/CMR.0000000000000227
IF: 2.615

Total IF of journals (all publications): 19,411
Total IF of journals (publications related to the dissertation): 7,467

The Candidate's publication data submitted to the iDEa Tudóstér have been validated by DEENK on the basis of the Journal Citation Report (Impact Factor) database.

02 February, 2021

DEBRECENI EGYETEM * Egyetemi és Nemzeti Könyvtár *

Keywords

cutaneous melanoma, *BRAFV600E* mutation, BRAF inhibitors, MAPK pathway, drug resistance, development of resistant cell lines, copy number alteration, ER stress, autophagy, apoptosis, HA15 anti-melanoma drug, RNA-Seq

Kulcsszavak

malignus melanoma, *BRAFV600E* mutáció, BRAF inhibitorok, MAPK jelátviteli útvonal, gyógyszerrezisztencia, rezisztens sejtvonalak létrehozása, kópiaszám eltérések, ER stressz, autofágia, apoptózis, HA15 anti-melanoma drug, RNA-Seq

Acknowledgements

My deep gratitude goes first to my supervisor Professor Margit Balázs, who expertly guided me through my graduate education and who shared the excitement of melanoma research. Her unwavering enthusiasm for science kept me constantly engaged with my research, and her personal generosity helped make my time at "MOI" enjoyable.

My appreciation also extends to Professor Róza Ádány for providing me the opportunity to work in the MTA-DE Public Health Research Group, as well as for all of her support during my PhD study.

I would like to express my thankfulness to my colleagues Viktória Koroknai, Tímea Kiss, Krisztina Jámbor and Vikas Patel for their always generous help and their critique during my experiments.

I would like to acknowledge my colleagues of the Department of Public Health and Epidemiology, Faculty of Medicine for their help during my experiments, especially to Györgyné Kovács for her assistance.

Finally, I would like to say special thanks to my family for their support and patient.

Financial supports

This research was supported by the Hungarian National Research Fund (OTKA K112327) and the TÁMOP-4.2.2.A-11/1/KONV-2012–0031 project; the TÁMOP project is co-financed by the European Union and the European Social Fund. The work was co-financed by the European Union under the European Social Fund and European Regional Development Fund (GINOP-2.3.2-15-2016-00005). This research was also supported by ÚNKP-18-3 and ÚNKP-19-3 New National Excellence Programs of the Ministry of Human Capacities and by the IARC Postdoctoral Fellowship and Marie Curie Actions-People-COFUND.

Appendix

Supplementary Table 1

Primer sequences used in RT-qPCR experiments used during the BRAF resitence experiments

Gene	Primer sequence (5'-3')[1]	Amplicon size (bp)[2]
LOXL2	F: CTATGACCTGCTGAACCTCAAT	100
	R: ATTCTTCTGGATGTCTCCTTCAC	
PMEL	F: GTCAGCACCCAGCTTATCAT	118
	R: CAAGGACCACAGCCATCAA	
TCF4	F: CCATGGAGGTACAGACAAAGAA	127
	R: GCTGGTTTGGAGGAAGGATAG	
SERPINE1	F: GCTTTTGTGTGCCTGGTAGAAA	69
	R: TGGCAGGCAGTACAAGAGTGA	
EPHA2	F: GGAGGGATCTGGCAACTTGG	103
	R: CTTCCTCCTGCGGTGGATAA	
LEF1	F: CCGAAGAGGAAGGCGATTTAG	111
	R: CCTGAGAGGTTTGTGCTTGT	
WNT5A	F: CACCAGAGCAGACAACCTAT	99
	R: CCAGCATCACATCACAACAC	
BRAF	F: TCAGCTCCCAATGTGCATATAA	88
	R: ATCCTCCATCACCACGAAATC	
OPN	F: AGTTTCGCAGACCTGACATCCAGT	161
	R: TTCATAACTGTCCTTCCCACGGCT	
GAPDH	F: AGCCACATCGCTCAGACAC	66
	R: GCCCAATACGACCAAATCC	
EXT1	F: GACCAGTTGTCACCTCAGTATG	113
	R: GGCCAAGTGCCGGAATATAA	
SAMD12	F: CTATCTAAACCGGTGGCTCTATG	117
	R: CCCAGTTATGTCATGCTGTTTG	

Primer sequences used in RT-qPCR experiments.during the ER stress experiments

Gene	Primer sequence (5'-3')[1]	Amplicon size (bp)[2]
XBP1_spliced	F: TGCTGAGTCCGCAGCAGGTG	169
	R: GCTGGCAGGCTCTGGGGAAG	
CHOP	F:GCACCTCCCAGAGCCCTCACTCTCC	422
	R:GTCTACTCCAAGCCTTCCCCCTGCG	
BiP	F: CGAGGAGGAGGACAAGAAGG	304
	R: CACCTTGAACGGCAAGAACT	
Atg5	F: AAAGATGTGCTTCGAGATGTGT	144
	R: CACTTTGTCAGTTACCAACGTCA	
Atg7	F: CAGTTTGCCCCTTTTAGTAGTGC	82
	R: CCAGCCGATACTCGTTCAGC	
p62	F: GCACCCCAATGTGATCTGC	92
	R: CGCTACACAAGTCGTAGTCTGG	
DRAM1	F: CGTCAGCCGCCTTCATTATCT	245
	R: TCCAAGCACTAAAGACACCAAG	
GAPDH	F: AGCCACATCGCTCAGACAC	66
	R: GCCCAATACGACCAAATCC	

[1]F: forward, R: reverse; [2]bp: base pair

Supplementary Table 2 Significantly upregulated genes in resistant cell lines grouped by biological processes. The first twenty cellular processes from 151 are presented in the table.

ID	Name	P-value	Bonferroni	Genes included
GO:0048514	blood vessel morphogenesis	1.61E-17	7.48E-14	*ARHGAP24, DDAH1, MYLK, PDGFRB, RRAS, ITGA5, PRDM1, SLIT2, FAP, HEG1, SRPX2, FGF2, C3, CCL5, MMP9, VEGFC, HSPG2, TCF4, WNT5A, ESM1, CCDC80, CAV1, EDN1, THBS1, CYR61, CCBE1, LOXL2, EPHA2, ANGPTL4, SERPINE1, LRP1, PRKCA, ENG, IL6, EPAS1*
GO:0072358	cardiovascular system development	1.96E-16	9.11E-13	*NRG1, ARHGAP24, DDAH1, MYLK, PDGFRB, RRAS, ITGA5, PRDM1, SLIT2, FAP, HEG1, SRPX2, FBN1, BASP1, FGF2, C3, CCL5, MMP9, BICC1, VCAM1, VEGFC, HSPG2, TCF4, RARB, WNT5A, ESM1, CCDC80, CAV1, EDN1, TGFB1, THBS1, DKK1, CYR61, MICAL2, CCBE1, LOX, LOXL2,EPHA2,ANKRD1, ANGPTL4, SERPINE1, LRP1, PRKCA, ENG, IL6, EPAS1*
GO:0072359	circulatory system development	1.96E-16	9.11E-13	*NRG1, ARHGAP24, DDAH1, MYLK, PDGFRB, RRAS, ITGA5, PRDM1, SLIT2, FAP, HEG1, SRPX2, FBN1, BASP1, FGF2, C3, CCL5, MMP9, BICC1, VCAM1, VEGFC, HSPG2, TCF4, RARB, WNT5A, ESM1, CCDC80, CAV1, EDN1, TGFB1, THBS1, DKK1, CYR61, MICAL2, CCBE1, LOX, LOXL2,EPHA2,ANKRD1, ANGPTL4, SERPINE1, LRP1, PRKCA, ENG, IL6, EPAS1*
GO:0001525	angiogenesis	3.38E-16	1.57E-12	*ARHGAP24, DDAH1, PDGFRB, RRAS, ITGA5, SLIT2, FAP, SRPX2, FGF2, C3, CCL5, MMP9, VEGFC, HSPG2, TCF4, WNT5A, ESM1, CCDC80, CAV1, EDN1, THBS1, CYR61, CCBE1, LOXL2, EPHA2, ANGPTL4, SERPINE1, PRKCA, ENG, IL6, EPAS1*
GO:0001568	blood vessel development	4.24E-16	1.97E-12	*ARHGAP24, DDAH1, MYLK, PDGFRB, RRAS, ITGA5, PRDM1, SLIT2, FAP, HEG1, SRPX2, FGF2, C3, CCL5, MMP9, VEGFC, HSPG2, TCF4, WNT5A, ESM1, CCDC80, CAV1, EDN1, THBS1, CYR61, CCBE1, LOX, LOXL2, EPHA2, ANGPTL4, SERPINE1, LRP1, PRKCA, ENG, IL6, EPAS1*
GO:0001944	vasculature development	1.43E-15	6.66E-12	*ARHGAP24, DDAH1, MYLK, PDGFRB, RRAS, ITGA5, PRDM1, SLIT2, FAP, HEG1, SRPX2, FGF2, C3, CCL5, MMP9, VEGFC, HSPG2, TCF4, WNT5A, ESM1, CCDC80, CAV1, EDN1, THBS1, CYR61, CCBE1, LOX, LOXL2, EPHA2, ANGPTL4, SERPINE1, LRP1, PRKCA, ENG, IL6, EPAS1*
GO:0051094	positive regulation of developmental process	1.72E-13	8.01E-10	*IL34, BCL9L, NRG1, MYADM, DDAH1, PDGFRB, INHBA, PDLIM7, IRF1, RRAS, ITGA5, ADA, PLXNB2, BDNF, PRDM1, SLIT2, SRPX2, BASP1, FGF2, C3, CCL5, MMP9, VEGFC, TCF4, RARB, WNT5A, TMEM119, RUNX2, LPAR1, AR, EDN1, TGFB1, TRIM16, THBS1, CSF2, DKK1, CYR61, CCBE1, LOXL2, ANKRD1, ANGPTL4, SERPINE1, PRKCA, LYN, ENG, IL6, TPBG*
GO:0042060	wound healing	5.65E-13	2.63E-09	*NRG1, ARHGAP24, MYLK, PDGFRB, DGKA, IRF1, ITGA5, SLC7A11, FAP, FGF2, C3, PDGFC, VCL, RAC2, PROCR, WNT5A, CAV1, PAPSS2, EDN1, TFPI, TGFB1, THBS1, CYR61, LOX, SERPINE1, SERPINB2, PRKCA, LYN, ENG, IL6*
GO:2000026	regulation of multicellular organismal development	9.47E-13	4.4E-09	*IL34, BCL9L, NRG1, MYADM, DDAH1, FSTL3, PDGFRB, INHBA, IRF1, RRAS, ITGA5, NREP, ADA, PLXNB2, BDNF, PRDM1 SLIT2, SRPX2, BASP1, NFKBIA, FGF2, C3, CCL5, MMP9, VEGFC, TCF4, RARB, WNT5A, LAMA3, TMEM119, CAV1, RUNX2, LPAR1, AR, EDN1, TGFB1, TRIM16, NTN4, THBS1, DKK1, CYR61, CCBE1, SRGN, LOXL2, EPHA2,*

APPENDIX

ID	Name	P-value	Bonferroni	Genes included
				ANKRD1, ANGPTL4, SLIT3, SERPINE1, LRP1, PRKCA, SNAP25, LYN, ENG, IL6, TPBG
GO:0045766	positive regulation of angiogenesis	1.02E-12	4.74E-09	*DDAH1, RRAS, ITGA5, SRPX2, FGF2, C3, CCL5, MMP9, VEGFC, WNT5A, THBS1, CCBE1, ANGPTL4, SERPINE1, PRKCA, ENG*
GO:0051240	positive regulation of multicellular organismal process	1.04E-12	4.85E-09	*IL34, BCL9L, NRG1, DDAH1, PDGFRB, INHBA, PDLIM7, IRF1, BCL3, RRAS, ITGA5, ADA, PLXNB2, BDNF, PRDM1, SLIT2, HEG1, SRPX2, CADM1, BASP1, FGF2, C3, CCL5, MMP9, VEGFC, TCF4, RARB, WNT5A, TMEM119, CAV1, RUNX2, LPAR1, AR, EDN1, TGFB1, TRIM16, THBS1, CSF2, DKK1, CYR61, CCBE1, LOXL2, ANKRD1, ANGPTL4, SERPINE1, PRKCA, LYN, ENG, IL6, LRRFIP1, TPBG*
GO:0030334	regulation of cell migration	3.57E-12	1.66E-08	*NRG1, MYADM, MYLK, PDGFRB, RRAS, ITGA5, ADA, PLXNB2, SLIT2, SRPX2, FGF2, CCL5, MMP9, PDGFC, VCL, RAC2, VEGFC, ABCC1, WNT5A, LAMA3, LPAR1, EDN1, TGFB1, THBS1, CYR61, CCBE1, EPHA2, SERPINE1, LRP1, PRKCA, LYN, ENG, IL6*
GO:1904018	positive regulation of vasculature development	6E-12	2.79E-08	*DDAH1, RRAS, ITGA5, SRPX2, FGF2, C3, CCL5, MMP9, VEGFC, WNT5A, THBS1, CCBE1, ANGPTL4, SERPINE1, PRKCA, ENG*
GO:0016477	cell migration	6.24E-12	2.9E-08	*NRG1, MYADM, ARHGAP24, MYLK, PDGFRB, RRAS, ITGA5, ADA, PLXNB2, SLC7A11, SLIT2, FAP, SRPX2, FGF2, CCL5, MMP9, PDGFC, FMNL1, VCAM1, VCL, TNS3, RAC2, VEGFC, ABCC1, PROCR, WNT5A, APBB2, LAMA3, CAV1, LPAR1, EDN1, TGFB1, THBS1, CYR61, CCBE1, LOXL2, EPHA2, SLIT3, SERPINE1, LRP1, PRKCA, LYN, ENG, IL6*
GO:0040012	regulation of locomotion	1.08E-11	5.02E-08	*NRG1, MYADM, MYLK, PDGFRB, RRAS, ITGA5, ADA, PLXNB2, SLIT2, SRPX2, PTX3, FGF2, CCL5, MMP9, PDGFC, VCL, RAC2, VEGFC, ABCC1, WNT5A, LAMA3, CAV1, LPAR1, EDN1, TGFB1, THBS1, CYR61, CCBE1, EPHA2, SERPINE1, LRP1, PRKCA, LYN, ENG, IL6*
GO:0045765	regulation of angiogenesis	1.27E-11	5.92E-08	*DDAH1, RRAS, ITGA5, SRPX2, FGF2, C3, CCL5, MMP9, VEGFC, TCF4, WNT5A, THBS1, CCBE1, EPHA2, ANGPTL4, SERPINE1, PRKCA, ENG, IL6*
GO:2000145	regulation of cell motility	2.12E-11	9.83E-08	*NRG1, MYADM, MYLK, PDGFRB, RRAS, ITGA5, ADA, PLXNB2, SLIT2, SRPX2, FGF2, CCL5, MMP9, PDGFC, VCL, RAC2, VEGFC, ABCC1, WNT5A, LAMA3, LPAR1, EDN1, TGFB1, THBS1, CYR61, CCBE1, EPHA2, SERPINE1, LRP1, PRKCA, LYN, ENG, IL6*
GO:0030198	extracellular matrix organization	3.73E-11	1.73E-07	*MATN3, BCL3, ITGA5, FAP, FBN1, FGF2, MMP9, VCAM1, HSPG2, COL6A1, COL6A2, OLFML2B, APBB2, LAMA3, CCDC80, TGFB1, THBS1, CYR61, LOX, LOXL2, SERPINE1, ENG*
GO:0051674	localization of cell	3.76E-11	1.75E-07	*NRG1, MYADM, ARHGAP24, MYLK, PDGFRB, RRAS, ITGA5, ADA, PLXNB2, SLC7A11, SLIT2, FAP, SRPX2, FGF2, CCL5, MMP9, PDGFC, FMNL1, VCAM1, VCL, TNS3, RAC2, VEGFC, ABCC1, PROCR, WNT5A, APBB2, LAMA3, CCDC80, CAV1, LPAR1, EDN1, TGFB1, THBS1, CYR61, CCBE1, LOXL2, EPHA2, SLIT3, SERPINE1, LRP1, PRKCA, LYN, ENG, IL6*
GO:0048870	cell motility	3.76E-11	1.75E-07	*NRG1, MYADM, ARHGAP24, MYLK, PDGFRB, RRAS, ITGA5, ADA, PLXNB2, SLC7A11, SLIT2, FAP, SRPX2, FGF2, CCL5, MMP9, PDGFC, FMNL1, VCAM1, VCL, TNS3, RAC2, VEGFC, ABCC1, PROCR, WNT5A, APBB2, LAMA3, CCDC80, CAV1, LPAR1, EDN1, TGFB1, THBS1, CYR61, CCBE1, LOXL2, EPHA2, SLIT3, SERPINE1, LRP1, PRKCA, LYN, ENG, IL6*

Supplemetary Figure 1 Relative protein expression changes in the parental and PLX4720 resistant cell lines (WM983A-WM983A^{RES}, WM983B-WM983B^{RES}, WM278-WM278^{RES}, WM1617-WM1617^{RES}) obtaine by Proteome Profiler Human XL Oncology Array

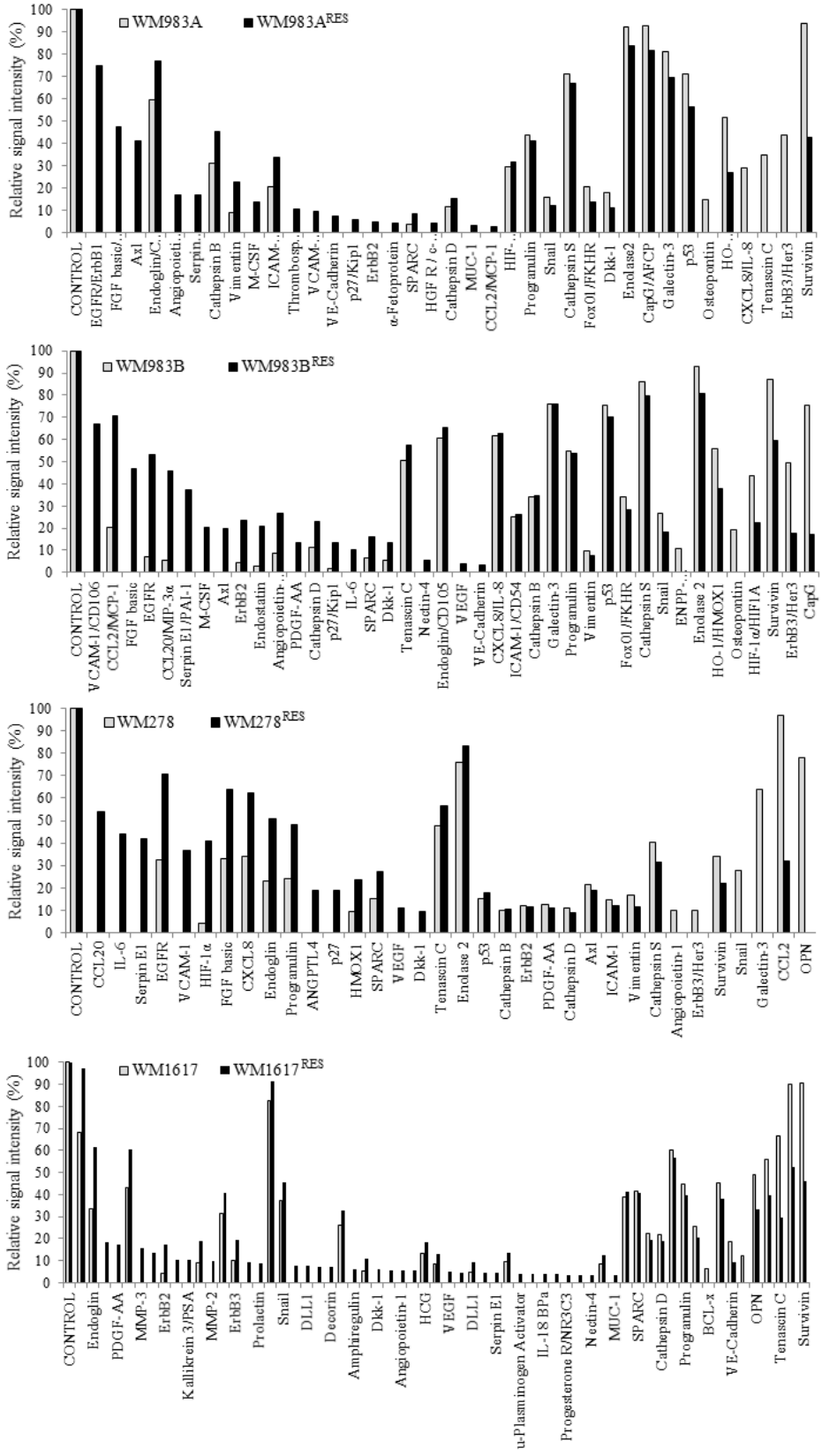

Supplementary Table 3:
List of proteins with membrane coordinates of the Proteome Profiler Human XL Oncology Array

Coordinate	Analyte/Control	Entrez Gene ID	Alternate Nomenclature
A1, A2	Reference Spots	N/A	———
A3, A4	α-Fetoprotein	174	AFP, DSCAM2
A5, A6	Amphiregulin	374	AREG
A7, A8	Angiopoietin-1	284	ANGPT1
A9, A10	Angiopoietin-like 4	51129	ANGPTL4
A11, A12	ENPP-2/Autotaxin	5168	ATX, Lysophosphatidic Acid, NPP2, PDNP2
A13, A14	Axl	558	Ark, Ufo
A15, A16	BCL-x	598	BCL2L1
A17, A18	CA125/MUC16	94025	MUC16
A19, A20	E-Cadherin	999	Arc-1, CAD1, Cadherin-1, CD324, CDH1, Cell-CAM120/80, ECAD, L-CAM
A21, A22	VE-Cadherin	1003	Cadherin-5, CD144, CDH5
A23, A24	Reference Spots	N/A	———
B3, B4	CapG	822	AFCP
B5, B6	Carbonic Anhydrase IX	768	CA9, G250, MN, RCC
B7, B8	Cathepsin B	1508	CTSB
B9, B10	Cathepsin D	1509	CTSD
B11, B12	Cathepsin S	1520	CTSS
B13, B14	CEACAM-5	1048	CD66e, CEA
B15, B16	Decorin	1634	DCN, DSPG2, PG-II, PSG2, SLRR1B
B17, B18	Dkk-1	22943	Dickkopf-1
B19, B20	DLL1	28514	Delta 1
B21, B22	EGF R/ErbB1	1956	ErbB, ErbB1, HER-1
C3, C4	Endoglin/CD105	2022	CD105, ENG
C5, C6	Endostatin	80781	COL18A1
C7, C8	Enolase 2	2026	ENO2; γ-Enolase; NSE
C9, C10	eNOS	4846	NOS3
C11, C12	EpCAM/TROP1	4072	17-1A, CD326, GA733-2, gp40, KS1/4, M4S1, TACSTD1
C13, C14	ERα/NR3A1	2099	ESR1, NR3A1
C15, C16	ErbB2	2064	CD340, HER2, Neu Oncogene, NGL, TKR1
C17, C18	ErbB3/Her3	2065	HER3
C19, C20	ErbB4	2066	HER4
C21, C22	FGF basic	2247	FGF2, FGF-2, FGF2AS, GFG1, HBGH-2, NUDT6, Prostatropin
D1, D2	FoxC2	2303	Fkh14, LD, MFH1
D3, D4	FoxO1/FKHR	2308	FKH1, FKHR
D5, D6	Galectin-3	3958	AGE-R3, CBP35, GAL3, L29, LGALS3, Mac-2
D7, D8	GM-CSF	1437	CSF2
D9, D10	CG α/β (HCG)	1081 (α)/1082 (β)	CGB, CGB3, Choriogonadotropin
D11, D12	HGF R/c-Met	4233	MET

Coordinate	Analyte/Control	Entrez Gene ID	Alternate Nomenclature
D13, D14	HIF-1α	3091	HIF1A
D15, D16	HNF-3β	3170	FoxA2
D17, D18	HO-1/HMOX1	3162	HSP32
D19, D20	ICAM-1/CD54	3383	———
D21, D22	IL-2 Rα	3559	CD25, IL2RA
D23, D24	IL-6	3569	BSF-2, IFN-β2, MGI-2A
E1, E2	CXCL8/IL-8	3576	GCP1, IL8, LAI, MDNCF, NAP1, NCF, TCF, TSG1
E3, E4	IL-18 BPa	10068	IL18BP
E5, E6	Kallikrein 3/PSA	354	KLK3
E7, E8	Kallikrein 5	25818	KLK5, KLK-L2, SCTE
E9, E10	Kallikrien 6	5653	KLK6, Neurosin, Protease M, PRSS18, PRSS9, SP59, Zyme
E11, E12	Leptin	3952	LEP, OB
E13, E14	Lumican	4060	LDC, LUM, SLRR2D
E15, E16	CCL2/MCP-1	6347	MCAF
E17, E18	CCL8/MCP-2	6355	———
E19, E20	CCL7/MCP-3	6354	MARC
E21, E22	M-CSF	1435	CSF1, CSF-1
E23, E24	Mesothelin	10232	CAK1, MPF, MSLN, SMR
F1, F2	CCL3/MIP-1α	6348/6351	LD78a; MIP-1 alpha
F3, F4	CCL20/MIP-3α	6364	exodus-1; LARC; MIP-3 alpha
F5, F6	MMP-2	4313	Gelatinase A
F7, F8	MMP-3	4314	Stromelysin-1
F9, F10	MMP-9	4318	CLG4B, Gelatinase B, GELB
F11, F12	MSP/MST1	4485	HGFL, MST1, SF2
F13, F14	MUC-1	4582	CD227, Episialin, H23AG, KL-6, Mucin-1, PEM, PEMT
F15, F16	Nectin-4	81607	LNIR, PRR4, PVRL4
F17, F18	Osteopontin (OPN)	6696	Eta-1, Spp1
F19, F20	p27/Kip1	1027	CDKN1B
F21, F22	p53	7157	BCC7, LFS1, TP53, TRP53
F23, F24	PDGF-AA	5154	———
G1, G2	CD31/PECAM-1	5175	PECAM1
G3, G4	Progesterone R/NR3C3	5241	———
G5, G6	Progranulin	2896	Acrogranin, GEP, GP88, GRN, PCDGF, PEPI, PGRN, Proepithelin
G7, G8	Prolactin	5617	PRL
G9, G10	Prostasin/Prss8	5652	———
G11, G12	E-Selectin/CD62E	6401	ELAM1, LECAM2, SELE
G13, G14	Serpin B5/Maspin	5268	PI5
G15, G16	Serpin E1/PAI-1	5054	Nexin, PLANH1

Coordinate	Analyte/Control	Entrez Gene ID	Alternate Nomenclature
G17, G18	Snail	6615	SLUGH2, SNAH, SNAI1
G19, G20	SPARC	6678	BM-40, Osteonectin
G21, G22	Survivin	332	API4, BIRC5
G23, G24	Tenascin C	3371	Cytotactin, HXB, Tenascin J1, TNC
H1, H2	Thrombospondin-1	7057	THBS1, TSP-1
H3, H4	Tie-2	7010	———
H5, H6	u-Plasminogen Activator/Urokinase	5328	PLAU, uPA
H7, H8	VCAM-1/CD106	7412	———
H9, H10	VEGF	7422	VAS, Vasculotropin, VEGFA, VPF
H11, H12	Vimentin	7431	VIM
I1, I2	Reference Spots	N/A	———
I23, I24	Negative Control	N/A	———

Supplementary Table 4:
Top 50 overexpressed gene in the WM983B^{HA15RES} melanoma cell line

	Gene ID	Fold Changes ([WM983B-^{HA15RES}] vs [WM983B])	Gene Symbol
1.	ENSG00000116183	946.29	PAPPA2
2.	ENSG00000069431	397.36	ABCC9
3.	ENSG00000125398	344.64	SOX9
4.	ENSG00000123496	328.15	IL13RA2
5.	ENSG00000163395	320.50	IGFN1
6.	ENSG00000128591	305.40	FLNC
7.	ENSG00000153976	305.34	HS3ST3A1
8.	ENSG00000148516	304.59	ZEB1
9.	ENSG00000183873	290.84	SCN5A
10.	ENSG00000121904	258.94	CSMD2
11.	ENSG00000128805	222.57	ARHGAP22
12.	ENSG00000224407	214.40	RP5-956O18.3
13.	ENSG00000164484	209.80	TMEM200A
14.	ENSG00000254741	196.14	RP11-661A12.7
15.	ENSG00000124496	192.52	TRERF1
16.	ENSG00000139970	191.95	RTN1
17.	ENSG00000160013	191.81	PTGIR
18.	ENSG00000259948	180.34	RP11-326A19.5
19.	ENSG00000283149	178.91	RP11-134F2.8
20.	ENSG00000076356	176.66	PLXNA2
21.	ENSG00000155093	173.21	PTPRN2
22.	ENSG00000111885	170.14	MAN1A1
23.	ENSG00000176788	167.50	BASP1
24.	ENSG00000258964	166.23	RP11-618G20.1
25.	ENSG00000221866	160.97	PLXNA4
26.	ENSG00000106366	156.16	SERPINE1
27.	ENSG00000273275	155.57	RP11-474G23.2
28.	ENSG00000196139	147.58	AKR1C3
29.	ENSG00000167971	146.16	CASKIN1
30.	ENSG00000256292	145.54	RP11-955H22.1
31.	ENSG00000077420	145.41	APBB1IP
32.	ENSG00000243742	140.31	RPLP0P2
33.	ENSG00000166446	139.95	CDYL2
34.	ENSG00000133216	138.53	EPHB2
35.	ENSG00000232044	135.27	LINC01105
36.	ENSG00000227051	131.58	C14orf132
37.	ENSG00000163285	131.01	GABRG1
38.	ENSG00000155269	129.44	GPR78
39.	ENSG00000187720	126.51	THSD4
40.	ENSG00000224982	119.93	TMEM233
41.	ENSG00000198768	119.14	APCDD1L
42.	ENSG00000109625	118.63	CPZ

	Gene ID	Fold Changes ([WM983B-^{HA15RES}] vs [WM983B])	Gene Symbol
43.	ENSG00000145107	117.14	TM4SF19
44.	ENSG00000022267	114.91	FHL1
45.	ENSG00000204161	111.66	C10orf128
46.	ENSG00000101188	110.13	NTSR1
47.	ENSG00000183671	106.81	GPR1
48.	ENSG00000089199	106.81	CHGB
49.	ENSG00000273812	105.84	WI2-87327B8.2
50.	ENSG00000245112	103.24	SMARCA5-AS1

Supplementary Figure 2: Gene set enrichment analysis (GSEA) of the WM983B^{HA15RES} melanoma cell line using the hallmark gene set.